AD/A-003 302

THE SHOCK AND VIBRATION BULLETIN. PART 1. SUMMARIES OF PRESENTED PAPERS

Naval Research Laboratory
Washington, D. C.
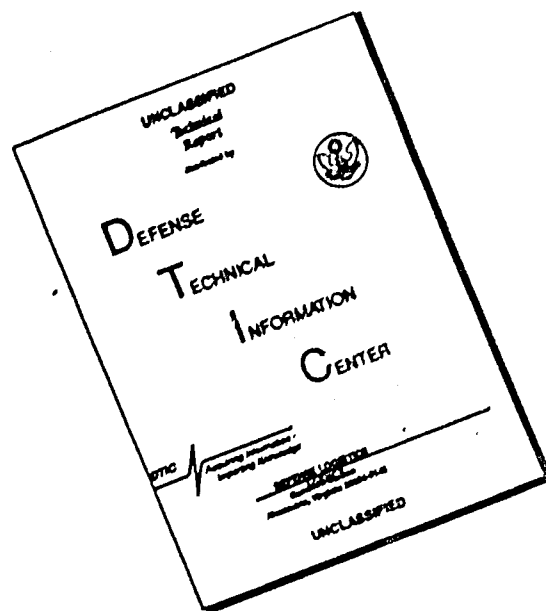
October 1973

AD/A-003 302

DISCLAIMER NOTICE

THIS DOCUMENT IS BEST
QUALITY AVAILABLE. THE COPY
FURNISHED TO DTIC CONTAINED
A SIGNIFICANT NUMBER OF
PAGES WHICH DO NOT
REPRODUCE LEGIBLY.

Bulletin 44
(Part 1)

THE SHOCK AND VIBRATION BULLETIN

Part 1
Summaries of Presented Papers

OCTOBER 1973

A Publication of
THE SHOCK AND VIBRATION
INFORMATION CENTER
Naval Research Laboratory, Washington, D.C.

ANNOUNCEMENT ONLY

D D C
JAN 21 1975
D

Office of
The Director of Defense
Research and Engineering

SYMPOSIUM MANAGEMENT

THE SHOCK AND VIBRATION INFORMATION CENTER

Robert O. Belsheim, Director
Henry C. Pusey, Coordinator
Edward H. Schell, Coordinator
Rudolph H. Volin, Coordinator

Bulletin Production

Graphic Arts Branch, Technical Information Division,
Naval Research Laboratory

THE
SHOCK AND VIBRATION
BULLETIN

OCTOBER 1973

A Publication of
**THE SHOCK AND VIBRATION
INFORMATION CENTER**
Naval Research Laboratory, Washington, D.C.

Office of
The Director of Defense
Research and Engineering

D D C

JAN 21 1975

D

i

FOREWORD

Part I of the 44th Shock and Vibration Bulletin is a new departure, in a sense, from previous practices. It is the first time that summaries of presented papers have been published as part of the Bulletin. And it is also the first time that part of the bulletin has been published prior to the corresponding Symposium.

Several reasons exist for so doing:

(1) The summaries in this part are delivered to registrants in advance of the meeting to enable them to choose more wisely the papers which they wish to hear.
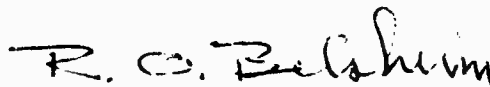
(2) It is our intent that these advance summaries be used to formulate pertinent questions and comments to be posed during the question and answer sessions at the meeting.

(3) Some of the papers to be presented are not offered for publication in the bulletin.

(4) Papers covering a very useful piece of work may fail to survive the refereeing procedure for reasons unrelated to the work itself.

In the latter two cases, the summaries provide information not otherwise available, and if one is interested in further details, he may contact the authors. Thus, it becomes important to publish this information where it may be referenced in other papers and becomes a part of the useful body of literature.

In particular, we request you to use these summaries to prepare questions for the discussion periods following the paper presentation. Nothing adds to a symposium quite as much as an interesting and informative question and answer session. In controversial areas, it is quite useful to have other views presented. We encourage you to prepare for an active participation in the discussions. Rest assured that your questions and comments will be appreciated.

R. O. Belsheim

CONTENTS

Part 1

Underwater Problems I

Environments and Measurements

Shock I

Structural Analysis

Shock II

Environments and Their Simulation

Isolation and Damping

Special Problems

Vibration Testing and Analysis

UNDERWATER PROBLEMS I

APPLICATION OF MECHANICAL IMPEDANCE CONCEPTS TO THE COUPLING PROBLEM OF STRUCTURES IN SHOCK ENVIRONMENT

Robert Aquilina and Lionel Gaudriot
Direction Des Constructions Et Armes Navales
Toulon, France

An important question in shock problems lies in the coupling between the test equipment and the supporting structure. This structure, considered as the source of shock motion, is, in our applications a shock test machine or a submarine hull excited by an underwater explosion. According to the shock spectrum concept, the problem is to set up a Design Shock Spectrum from Measured Shock Spectrum. As we possess at present a limited quantity of experimental information, the method consisting in tests of large number of oscillators, i.e. equipments modes, of various weights and frequencies seems to be too much time consuming. So we attempt to make use of the mechanical impedance concept for obtaining a practical solution of the problem.

From that point of view the problem can be considered under the three following aspects:

- Modal characterisation of equipment
- Modal characterisation of the supporting structure
- Mechanical coupling between the two connected systems.

The considered shock motions are limited to translation of the foundation base, and so the correlative modal parameters to define relates to fixed base conditions. These parameters, effective masses and natural frequencies, are obtained from sinusoidal excitation tests by an analytical treatment of mechanical impedance results. Experiments in submarine test section have confirmed that a limited number of lower modes is sufficient for properly describing the response of a complex equipment to the measured actual acceleration. Measurement techniques are described and some difficulties are discussed.

On an other hand, the submarine hull is analysed by single-point impedance measurements in order to get a sufficient knowledge of its dynamic behaviour. Electrodynamic shakers limit the study of the hull for the frequencies of rigidly mounted equipment. For the lower frequencies transient test techniques may be used, but the problem of elastic mounts is shown to be quite different. Analytical expressions of mechanical impedance for the equipment and structure are combined algebraically, using Fourier techniques, to give the effective acceleration signal.

The method is tested with two coupled oscillators mounted on a shock machine. A full scale verification, prepared on the submarine shock test section, with heavy single degree of freedom Systems, is presented. The difficulty which appeared in the designing

1

of such linear oscillators destined to withstand high severity shock raises questions abou the limits of validity of the linear behavior of actual equipments. Moreover limitations implied by the hypothesis of translation motion for the foundation base, equivalent to unicity of attachment point, is examined.

NEAR MISS SHOCK AND WHAT TO DO ABOUT IT

James R. Suhre
McDonnell Douglas Corp., St. Louis, Mo.

INTRODUCTION

Near Miss Shock is a subject fraught with emotion and controversy, mainly because it often breaks equipment, especially large, expensive, highly specialized equipment, such as missiles, antennas, and electronic equipment.

An enormous amount of literature has been written on near miss shock, but it is felt that a presentation of, what appears at this time, to be the most practical approach to this problem would be of interest to analysts and designers. It often happens that the preliminary analysis of a design will indicate peak accelerations on the order of 200 g's and stresses 2 or 3 times the yield strength of the structural material. At this point many otherwise brave designers will; (a) try to get the requirement deleted, (b) beef everything up and shock mount all equipment at the expense of other performance requirements, and (c) get a new shock analyst, or seek some data, method, or whatever to bring the calculated loads down.

Assuming that a reasonably good analysis was done at the beginning, any of the above will usually degrade the design, sometimes with sad results when compared with what could have been achieved. However, it takes a great deal of self-confidence and knowledge for an analyst or designer to defend as optimum, including the various performance criteria, a design having very high shock stresses and accelerations.

It is a basic premise of this paper that if well thought out near miss shock requirements are integrated into the design criteria from the beginning, with calculated risks taken where necessary to live within other constraints, but with prudent provisions made where needed, a high level of toughness can be obtained, even in the most difficult cases. Excuse the expression, but it appears that an ounce of prevention is worth a pound of cure. Perhaps our ancestors knew something after all.

BACKGROUND

A brief outline of the British experience during World War II will be presented, along with the derivation of the shock testing machines. Reference will be made to the tendency to backslide as new, more specialized and sensitive equipment is continually introduced.

IMPORTANCE OF NEAR MISS SHOCK

Many nations now have modern anti-ship weapons such as influence mines and missiles which would produce near miss shock in combat conditions. Also, the ability to locate ships anywhere in the world has increased vastly.

The assumption that we need only concern ourselves with a final nuclear holocost was always a bleak prospect, and is out of style after many years of non-nuclear warfare in S.E. Asia. Such an assumption leads to vulnerability to, and therefore likelihood of, conventional war. These factors, and others, have increased the likelihood of near miss shock if our navy becomes engaged in combat in the foreseeable future.

SHOCK LEVEL CRITERIA

The basic criterion for the equipment necessary for continued combat and ship maneuver is to remain usable up to the point where the ship structure begins to fail. Other equipment can fail, but must not break loose, explode or otherwise become dangerous.

It would be impractical to design for and test to the exact shock conditions at the beginning of hull failure on every ship which potentially would carry a particular equipment. Testing per MIL-S-901C has been developed as a standardized test which can be substituted for such a program. This test is checked for validity by occasional shock tests of fully equipped surface ships and submarines. It should be noted that a crucial instruction in MIL-S-901C calls for representative support structure to be placed between the test platform and the equipment, as if the platform were the ships hull. Further support for the validity for 901C testing will be presented, and the relative merit, of pulse and time histories will be discussed. Keel Shock Factor will be discussed and disposed of.

ANALYSIS METHODS

MIL-S-901C shock test data including special test setups have been evaluated on the basis of "what input shock spectrum would produce the measured structural loads and deflections"? These input spectra can be used for reasonably accurate calculations, per DDAM. However, non-linear structures are not strictly covered, and modal phasing is usually taken on a conservative basis. An example of such an analysis (Encapsulated Harpoon) will be presented in an appendix to the paper. Work is progressing at NAEC on a method which would alleviate these problems, at least for FSP testing. This method begins with the pressure wave in the water, and calculates the shock waves progress through the FSP and equipment structure.

ALLOWABLE STRESSES

It should be recognized that considerable yielding can be tolerated in ductile structures which can function afterward with a certain amount of misalignment. "Rules of thump" are available, but usable analysis awaits methods such as those being developed by NAEC. If full level 901C testing cannot be achieved, a trade-off must be made between shock hardness and the performance of the equipment. A full discussion of this trade-off will be presented.

EARLY TESTING

The case will be made for planned preliminary testing of representative hardware or whatever can be diverted.

NATO SEA SPARROW LAUNCHER SHOCK ANALYSES AND BARGE TESTS

Paul V. Roberts
Raytheon Company, Bedford, Mass.

This paper compares shock response of the NATO sea sparrow launcher and eight missile load, measured during complete barge shock tests at Arvonia, Va. with theoretical results using the DDAM procedure of Nav Ships 250-423-30.

The launcher successfully withstood the required underwater shock barge test conditions, with 60, 40, 30, 25 and 20 Ft. charge stand-off distances, and was fully operational after the tests. Shock acceleration, velocity and displacement data obtained during the tests are reported in the paper.

The analyses of launcher missile shock response, utilized a UNIVAC 1108 computer and an existing Raytheon program of the Nav Ships 250-423-30 method, see (1) below. Shock inputs used in the computer analyses were generally in accordance with (2) below. Velocity inputs were increased at frequencies under 10 Hz, based on information contained in (3), (4) and (5).

(1) Nav Ships 250-423-30, "Shock Design of Shipboard Equipment, Dynamic Design Analysis Method," May, 1961.

(2) G. O'Hara and R. Belsheim, "Interim Design Values for Shock Design of Shipboard Equipment," NRL Memorandum Report 1396, February 1963.

(3) G. O'Hara and P. Cuniff, "Elements of Normal Mode Theory," NRL Report 6002, November 1963.

(4) R. Belsheim, "Preliminary Shock Design Criteria for Floating Shock Platform," Enclosure (1) to NRL Ltr. 6260-7: ROB:kep SER 1722 of February 1964.

(5) R. Willem and R. Bort, "Measured Rigid-Body Motions of the Floating Shock Platform for Testing Heavy Weight Shipboard Equipment." Enclosure (1) to NRL Ltr 8440-114:ROB:kep.

Use of higher velocity shock inputs at low frequencies under 10 Hz, compared to the inputs of (2) above, was substantiated by velocity shock data measured on the barge and equipment.

The launcher was barge tested with a 10 Hz mounting platform designed to attenuate shock response below structural design limit loads of 15g vertical, 9g tranverse and 6g longitudinal to the ship. Design to these loads had been specified in order to limit weight and complexity and facilitate use aboard smaller ships.

The shock response analyses conducted during launcher design and development used several deck stiffnesses, to determine shock loads with the recommended 10 Hz deck and evaluate potential increases with stiffer decks. Analytical results are reported in the paper with 10 Hz, 15 Hz, 25 Hz and infinitely rigid decks.

Accelerations, with durations and frequencies, were measured at seventeen key locations on the launcher, missiles and barge deck, during each of the five barge test shots. Shock velocity with time on the barge deck and launcher base as well as relative displacement across the 10 Hz mounting platform, are also reported for each shot.

Successive shock inputs due to blast pressure bubble action were quite severe as verified by magnetic tape and oscillograph data and indicated in a short movie.

With respect to comparison of analytical results using the DDAM procedure of Nav Ships 250-423-30, and experimental data from the barge tests, good correlation was found between overall predicted shock loads and test results. Higher frequency missile response was less predictable than at lower frequencies, due to non linearities associated with free play at attachments and motion limiting devices.

MATHEMATICAL INVESTIGATIONS OF UNDERWATER EXPLOSIONS AND FLOATING SHOCK PLATFORM RESPONSE PHENOMENA

Robert P. Brooks
Naval Air Engineering Center, Philadelphia, Pa.

and

Brian C. McNaight
The M & T Co., Philadelphia, Pa.

INTRODUCTION

The analytic determination of ship structure response to non-contact underwater explosions has historically proven to be a difficult problem. Different theories of the physical mechanisms involved in shock wave/plating interaction, and gas globe phenomena, have been advanced. Two of these theories are due to G. I. Taylor (Ref. 1) and Mindlin-Bleich (Ref. 2). These different analyses are in common usage today.

In order to compare the response phenomena generated by the theories, the authors have refined their earlier mathematical model of the floating shock platform (FSP) (Ref. 3) to accept various shock wave loading functions, complete gas globe effects, and an improved cavitation model.

Accordingly, a series of FSP test simulations were computed to observe the response "signatures" caused by the different loading functions.

To gain a better understanding of the phenomena resulting from an underwater explosion, a unique, regional concept for the mathematical modeling of fluids has been evolved. This concept utilizes only the natural physical laws of fluid mechanics to obtain a deterministic description of the sequence of events.

THE FLOATING SHOCK PLATFORM MODEL

The FSP mathematical model used for the test simulations was an optimized version of the model reported on in Ref. 3. The analytic rational, construction, and finite difference technique employed was basically the same as for the earlier model.

During all the test simulations the FSP was considered clean (no test loads), but with the sheltering canopy in place.

THE UNDERWATER EXPLOSION MODEL

The underwater explosion model developed for Ref. 3 was expanded primarily to include gas globe effects, although modifications were made to the cavitation and water resistance logic.

The computer program of the model was tailored to accept three different shock wave/plating impingement functions: the function due to G. I. Taylor, the Mindlin-Bleich impingement function, and an impingement function derived from a direct application of rigid body, conservation-of-momentum laws.

THE REGIONAL FLUID MODEL

In order to obtain the natural sequence of events occurring during an underwater explosion from the physical laws governing fluid mechanics, a regional water model was defined. This unique concept was evolved by an analogous implementation of the same lumped parameter, finite difference technique used to model the FSP.

Basically, a control region of water is defined. This region is then partitioned into cubical sub-regions with individual identities and descriptors of their fluid properties. An explosion is introduced to the model by defining a particular sub-region as a gas at a very high pressure at time equal to zero. The mathematical process then starts and the sequence of events is seen by monitoring the histories of various regions, i.e. pressure, flow, etc.

Included in the model are: hydrostatic pressure distributions, a variable bottom boundary condition, a free surface boundary, and an inserted target vessel (actually the FSP model). Also included is the expansion, contraction, and migration of the gas globe.

The model has been made more efficient by the application of an infinite medium approximation at the control region vertical boundaries. This necessary effort has resulted in large savings in computer core size and overall running time.

SUMMARY AND CONCLUSIONS

Examination of the output data from the FSP test simulations has shown: that for the qualifying standoff distance of 20 ft for MIL-S-901C, there are no significant differences in the analytic dynamic loading of the FSP whether the Taylor or the Mindlin-Bleich theory is applied. At an increased standoff to 100 ft, the Mindlin-Bleich theory provided consistently higher response motions of the FSP model. At the same stand-off the Taylor theory created unrealistic motions in the 50 to 100 msec range.

6

The preliminary results of the regional fluid model have been very encouraging. The authors feel that this concept is needed to proceed further in the mathematical modeling of underwater explosion/ship structure response phenomena.

REFERENCES

1. Taylor, G.I., "The Pressure and Impulse of Submarine Explosive Waves on Plates," Ministry of Home Security Report, RC 235, 1941.

2. Mindlin, R.D. and H.H. Bleich, "Response of an Elastic Cylindrical Shell to a Transverse Step Shock Wave," Journal of Applied Mechanics, June, 1953.

3. Brooks, R.P. and B.C. McNaight, "Mathematical Model of a Typical Floating Shock Platform Subjected to Underwater Explosions," The Shock and Vibration Bulletin, No. 43, 1973.

THE NAVY LARGE FLOATING SHOCK PLATFORM
PART I—PHYSICAL DESCRIPTION AND CAPABILITIES

C. G. Schrader
Hunters Point Naval Shipyard
San Francisco, California

In 1969, the West Coast Shock Facility at Hunters Point Naval Shipyard was tasked by the Naval Research Laboratory to conduct a Conceptual Study for a Large Floating Shock Platform which would be capable of Shock Testing Loads up to 160 tons per specification, MIL-S-901. This study indicated that due to economic considerations, the physical design of the Large Platform would have to differ considerably from the existing Floating Shock Platforms which were being used to test loads up to 30 tons. The basic steel was changed from HY 80 to HTS and the closed deck was changed to open framing.

In 1971, we were tasked by Naval Ship Systems Command as part of Div-Under, Phase II, reference ( ), to provide contract plans and specifications which resulted in the Large Floating Shock Platform (LFSP) being delivered in February 1973.

A fourteen-shot calibration series was completed in May 1973.

As shown in Figure 1,* the LFSP is 30 feet by 50 feet and 18 feet deep. The bottom and wetted sides are made of 1-1/2 inch HTS steel. The bottom frames, Figure 2, are about four feet apart and three feet deep. The platform is covered with a three-piece canopy, Figure 3, which is 18 feet high and will allow the covered installation of objects approximately 32 feet high. Taller objects will require a custom cover. Side and end frames are protruding 2 feet inboard from the hullplates and therefore, objects up to 26 feet by 46 feet can be installed.

Figure 4 shows a regular Floating Shock Platform (16' X 28') inside the LFSP. This FSP was used as a test load for the calibration series. To allow access for the welders to install an interface foundation, the small FSP was mounted 18 inches above the main

---

*Figures have been eliminated to speed publication.

frames as shown by Figure 5. This interface foundation, Figure 6, must be designed to be of sufficient strength to withstand the shock loads.

We have bettered the original design total load capacity by approximately 50 tons so that if the CG of the load permits, 200 tons may be tested.

To inform all future users of all the details involved in the LFSP test, an Operations Manual, reference (2) has been prepared. A short movie of a LFSP test will follow.

REFERENCES

(1) NAVSHIPS TDP for Element 63714, Project S4815 of Operation Dive-Under 1 April 1971.

(2) Operation Manual for Large Floating Shock Platform (LFSP) NAVSHIPYD HUNTERS PT Technical Report 10-73 of July 1973.

THE NAVY LARGE FLOATING SHOCK PLATFORM
PART II—SHOCK CHARACTERISTICS

E. W. Clements
Naval Research Laboratory, Washington, D.C.

The Large Floating Shock Platform (LFSP) described in Part I of this paper was subjected to an eight-shot calibration test series in May 1973. The test series was conducted at the West Coast Shock Facility (WCSF), San Francisco, Ca. by personnel from WCSF and the Naval Research Laboratory (NRL), Washington, D.C.

Charges weighing 300 lb were detonated at a depth of 20 ft, with near-side standoffs of from 45 to 120 ft against the port side and of 45 ft against the aft end of the LFSP. A Floating Shock Platform (FSP) (a smaller version of the LFSP, 28 X 16 ft) was installed in the LFSP as a test load, adding a total weight of 112.6 klb. After four shots, the total added weight was increased to 176.9 klb by filling the FSP inner bottom with water.

Instrumentation was installed for measuring motions at the junction of the LFSP with the FSP mounting system (FSP inputs) and within the FSP (FSP responses), and also motions and strains at a few locations on the shell plating and stiffeners of the LFSP. Motions were measured as velocities in one or more of the three component directions, vertical, athwartship and fore-and-aft.

The points at which velocities were measured outline a considerable area of the LFSP, and the magnitudes of the velocities vary accordingly. In general, the peak velocity increases with the proximity of the point of measurement to the charge. This is most pronounced in the vertical direction, less in the horizontal direction parallel to the line of the charge (i.e., athwartship for a side shot) and negligible for the horizontal direction transverse to the line of the charge. For the FSP input velocities, the greatest vertical peak is 1.75 times the smallest; when velocities in a given direction are averaged over location, the

relative peak magnitudes are in the ratio 1:.7:.3 (vertical:horizontal-parallel:horizontal-transverse), with an average vertical peak of 10.7 ft/sec for a 45 ft standoff. This ratio is not significantly affected by charge standoff or test load weight, and the effect of charge orientation (end vs. side shots) is primarily to interchange the characters of the athwartship and fore-and-aft velocities.

The load (FSP response) velocities are higher than the corresponding input velocities and show similar relationships in exaggerated form. The variation in peak velocity with position is more pronounced, the vertical velocities are larger multiples of the horizontal velocities, and the peak velocities are more strongly influenced by charge standoff and load weight. Moreover, the response velocities in all three directions are predominantly sinusoidal, while the input waveforms are more steplike.

Design shock spectra have been derived from the shock spectra of the individual input velocity waveforms by the following procedure: reasonably good measurements of peak displacements in all three directions and shock spectra for the vertical direction are available, together with estimates of the peak accelerations in all three directions from the velocity slopes. From these, with the assumption that the shock spectrum values lie in the same ratio as the peak velocities, the cutoff frequencies can be calculated. With the additional assumption that 80% of the total load weight is in the first mode, the variation of shock spectrum value with modal weight can be derived. On this basis, the cutoff frequencies are: vertical, 9.5 and 117 Hz; horizontal-parallel, 31 and 154 Hz; horizontal-transverse, 59 and 171 Hz. The shock spectrum value for the vertical direction varies as V_0 (ips) = 156 − .38 × modal weight (klb), and the V_0's for the vertical, horizontal-parallel and horizontal-transverse directions have the ratio 1:.7:.3.

FLOW-INDUCED VIBRATIONS OF A
GLASS-REINFORCED PLASTIC SONAR DOME

Douglas A. King
Autonetics Div., Rockwell International, Anaheim, Ca.

A comparison is made between applicable theory and experimental results of dome wall vibrations and boundary layer pressure fluctuations measured in tests of a large buoyancy propelled underwater vehicle.

The configuration of the vehicle, a streamlined body stabilized by fins on a tail boom, is shown in the enclosed figure.* The body was a laminar-flow shaped body of revolution with a length to diameter ratio of 2.5, and a contour designated NACA 63040. The laminar flow shape allowed extensive laminar boundary layer flow to be developed at high Reynolds numbers, back to the maximum diameter station. In alternate runs, the boundary layer was artifically tripped at 10% body length.

The sonar dome comprised the forward half of the body, and was attached through vibration isolation mounts, which could be locked out to determine effects of isolation. The dome was an air-cured Fiber-glass-eopxy laminate 14 ft in maximum diameter, with

*Figures eliminated to speed publication.

9

thickness of 1/2 in. over the forward 40% of its length and graduating to 1.5 in. near the attachment ring. To attain the greatest extent of laminar flow, special care was taken to maintain small surface roughness and contour waviness.

Data taken during the tests were reduced to spectral power density form by a Fast Fourier Transform computer algorithm.

Where the boundary layer was laminar no pressure fluctuations were present, yet dome wall accelerations were measured there, coming from other portions excited by turbulent boundary layer further aft. The smaller extent of turbulence in the untripped runs resulted in smaller accelerations occurring than in the tripped runs. Isolating the dome also reduced the accelerations. Effects of these and other parameters are discussed.

The most pertinent theoretical work is that of Strawderman and Christman (J. Acous. Soc. Amer., v 52, p 1537. Nov. 1972), which is based on an unsupported infinite flat plate acted upon by uniform boundary layer pressure fluctuations, and vibrating in vacuo or in an acoustic fluid medium. Application to the dome is complicated by the stiffening effect of the body of revolution form, the varying thickness at various stations, the large lengthwise variation in boundary layer characteristics, and by the varying local velocity. A method of coping with the varying boundary layer and local velocity is described, essentially consisting of summing the incremental accelerations that result from the varying pressure fluctuations at various locations. Effects of tripping and dome isolation are calculated by including only pressure fluctuations from areas that are turbulent or structurally attached to the dome.

Experimental and calculated results are compared. There is general agreement in spectral distributions as functions of vehicle speed and frequency, indicating that the technique of summing incremental accelerations is valid. There is less agreement between tripped and untripped runs, perhaps because of simplifying assumptions in the calculations as to the location of boundary layer transition. The calculated results always indicate larger accelerations than experienced since they do not include the stiffening effects of the dome shape.

ENVIRONMENTS AND MEASUREMENTS

HARPOON MISSILE FLIGHT ENVIRONMENTAL MEASUREMENT PROGRAM

J. L. Gubser and V. S. Noonan
McDonnell Douglas Astronautics Company—East

With the award of the Harpoon Missile Program to McDonnell Douglas Astronautics Company—East (MDAC-E), an inflight environmental data acquisition program was implemented. Part of this program involved obtaining vibration, acoustic and shock data to substantiate the environmental predictions made for the Harpoon missile. The flight program to obtain the dynamic data covered four vehicle configurations during the overall Harpoon Missile Design Phase.

The first measurements were made on an Aerodynamic Test Vehicle (ATV) which was captive carried on a Navy Orion (P-3) type aircraft. The ATV was structurally a boilerplate vehicle with the correct mass, center of gravity and inertias of the Harpoon missile. Six external acoustic measurements with a frequency range of 10 to 2000 Hz were made. The acoustic sensors were located on top, bottom, and sides of the missile at forward, midpoint and aft stations to provide good overall coverage of the missile and to detect possible effects due to aerodynamic interference between missile and aircraft and adjacent stores.

The second set of dynamic measurements involved the Blast Test Vehicle (BTV) which were launched from ASROC launcher located at the Harpoon Integration Test Site at Naval Missile Center, Point Mugu, California. The BTV is again a boilerplate missile but utilized a production solid propellant booster. As in the case of the ATV's, the vehicle had the correct mass, center of gravity location and inertias. Two dynamic environmental measurements were made on each of four vehicles. These measurements included two external acoustic sensors on two vehicles and two vibration sensors on two vehicles. The frequency range of these sensors was 10 to 2000 Hz. The acoustic environment resulting from booster firing and the two vibration measurements were made to determine the shock environments resulting from booster ignition and booster separation and to quantitatively obtain some idea as to the severity of the vibrations induced into the missile as a result of booster burning. For the BTV's, the acoustic sensors were located on top in the forward and aft sections of the missile. The two vibration sensors were located at the missile/booster interface with the sensitive axis orientated along the longitudinal axis of the missile.

The final phases of this inflight data program involved the Control Test Vehicles (CTV) and the Guidance Test Vehicles (GTV). These missiles are functional missiles, basically identical with one exception. The GTV had a functional seeker while the CTV utilized a dummy seeker which is dynamically similar to the real seeker. The air launched and surface CTV's and GTV's utilized a jet engine during cruise flight and the surface launched vehicles used a solid propellant booster prior to jet engine start.

The CTV and GTV missiles had three dynamic environmental sensors with a frquency range of 10 to 2000 Hz installed for each missile flight. Vibration measurements have been made at the interface of the seeker, missile guidance unit, aircraft carry hooks, jet engine and control actuator with the vehicle primary structure. Both internal and external acoustic measurements were made at various locations.

The dynamic environmental data obtained to date in the Harpoon program will have a direct bearing on the Weapon System Development Phase of the program. Environmental predictions will be compared with measured data and these results may result in design changes on critical on-board components. The data that is presented in this paper will be in the form of power spectral density and shock spectra plots and selected time histories correlated with critical flight events.

In addition to the Harpoon application, the data presented in this paper is applicable to future tactical missile designs to aid in environmental predictions. The data will provide a good cross section of dynamic environments resulting from aircraft captive carry, solid propellant boost launched flight, jet engine flight, high and low altitude drops, maximum aerodynamic pressures and transient conditions resulting from aircraft launch, booster and jet sustainer engine ignition.

NARROW BAND TIME HISTORY ANALYSIS OF
TRANSPORT AIRCRAFT VIBRATION DATA

Roger E. Thaller and Jerome Pearson
Air Force Flight Dynamics Laboratory
Wright-Patterson AFB, Ohio

The Air Force requirment to transport fragile payloads in large aircraft has generated a need to accurately define the dynamics environment in aircraft such as the C-135, the C-141, and the C-5A. To determine the probability of occurrence of damaging accelerations during flight and ground operations of these large cargo aircraft, a special method was developed for analyzing and displaying the data, which may be both non-stationary and non-Guassian.

This method involves recording the complex vibration time history corresponding to each flight condition and filtering these data into time histories, each limited to a unique frequency band. For each band-limited time history, the values of acceleration of a_1, a_2 and a_3 were computed and plotted versus frequency band. The a_3 is the maximum acceleration observed in the band-limited time history. The a_1 and a_2 are the accelerations which exceed 84.135% and 97.725% of the data respectively. If the data are Gaussian, the a_1 and a_2 then correspond to σ and 2σ of the distribution, $a_2 = 2a_1$, and the probabilities of occurrence of higher accelerations can be easily computed. If $a_2 \neq 2a_1$, the data are non-Gaussian, and their ratio then gives an indication of how the probabilities of higher accelerations differ from the Gaussian case.

The method was applied to the analysis of cargo deck vibration data obtained during flight tests of a C-5A aircraft. The analysis was mainly concerned with low-frequency accelerations, because engineering knowledge from previous experiences indicated that some large cargoes to be carried in the C-5A are vulnerable to low frequency accelerations.

The flight tests included a full range of flight conditions. Data were taken during taxi, takeoff, climb, cruise in turbulence, descent, low-level terrain following, landing, and thrust reversal. During each flight condition the fuel and cargo loading were varied over a wide range. A complete analysis of variance can be performed to determine the extent of dependence of a_1, a_2, and a_3 on flight condition.

During each flight condition, accelerometers were located in the aircraft to provide measurement of vertical, lateral, and longitudinal vibration. The sensor placement provides the capability of using data from pairs of sensors to produce roll, pitch, and yaw accelerations.

Previously obtained engineering data provided an estimate of the natural frequencies of the cargo deck. In order to identify the mode responsible for a particular peak acceleration, it was desirable to filter the vibration data into frequency bands which were sufficiently narrow that each band-limited time history would show the response of only one mode. The frequency bands chosen were the twenty one-third octave bands with center frequencies of 0.4 to 31.5 Hz. Based on available prediction and measurements of C-5A natural frequencies, normally only one vertical, lateral, longitudinal, roll, pitch, or yaw natural frequency should be found in each of the one-third octave bands used.

After the data are filtered, the a_1, a_2, and a_3 are computed from band-limited time histories. The collection of a_1, a_2, and a_3 values for all flight conditions for each frequency band can be used to determine the probability of occurrence of given levels of acceleration. Thus the acceleration for which the payload must be qualified can be determined for a selected risk of failure. If the payload cannot be qualified at these levels, the values of a_1, a_2, and a_3 as functions of frequency band can be used to design isolators for cargo deck mounting.

PRELIMINARY MEASUREMENT AND ANALYSIS OF THE VIBRATION ENVIRONMENT OF COMMON MOTOR CARRIERS

W. N. Sharpe, T. J. Kusza, F. W. Sherman, and J. W. Goff
Michigan State University, East Lansing, Mich.

PURPOSE

The purpose of these measurements is to obtain and analyze data on the vibration environment in commercial trucks for ultimate use in the testing of packages before shipment. Published truck vibration data is quite limited and has not been obtained on common carriers. Research of the kind described can lead to a sounder basis for vibration tests of shipping containers.

MEASUREMENTS

Accelerations were recorded on four separate scheduled runs of tractor-trailers owned by a local truck firm. Three of these were intercity shipments and one was a "peddle run." Accelerometers were mounted at three vertical and two lateral positions in the trailer and the data recorded on magnetic tape. The frequency response of the system is 3dB down at 400 Hz.

13

ANALYSIS

Standard analyses of probability, root mean square, and power spectral density of the acceleration signals were performed. A VIBRAN plot was generated for comparison with other data. Peak acceleration of transients were measured. While the analysis procedure is rather routine to many engineers, it is foreign to most of the packaging industry.

RESULTS

RMS measurements showed that the lateral accelerations were roughly a factor of two smaller than the vertical accelerations. Generally, the rear vertical acceleration was the largest—on the order of 0.6 RMS. Increasing the speed from 45mph to 60mph raised the acceleration level only moderately.

Probability analysis of the rear vertical acceleration gave a somewhat sharper than Gaussian curve with peak values of slightly less than ± 2 G. The VIBRAN plot showed a dip at 12.5 Hz and showed lower vibration levels than reported by other researchers.

PSD analysis of rear vertical acceleration of one run discloses six sharp peaks in the 0-50 Hz range, a sharp peak at 70 Hz, and a broad peak at 160 Hz. All of the PSD levels are below 0.01 G^2/Hz. The other runs have PSD plots that are similar in character but not in detail. Increasing the speed of the truck raises the level of the PSD curve but does not change its shape significantly.

Analysis of the transients produced by railroad crossing, intersections, etc., show that the truck floor does not see a sharp pulse but rather an increase in the amplitude of low frequency vibration.

CONCLUSIONS

These preliminary data show that field data acquisition and analysis of the vibrations in common motor carriers is practical and reasonably efficient. The data presented can provide guidance for testing, but more measurements are needed to generate statistically reliable values. There are enough similarities in data recorded under various operating conditions that the development of a composite wideband test seems reasonable.

A NEW TRANSVERSE CALIBRATOR FOR ACCELEROMETERS

J. A. Macinante, N. H. Clark, B. H. P. Cresswell
Division of Applied Physics, National Standards Laboratory,
CSIRO, Chippendale, N.S.W. 2008, Australia

In methods of transverse calibration currently in use the test accelerometer is mounted on a fixture which, while being vibrated vertically for example, maintains the sensitive axis of the test accelerometer horizontal. The output of the accelerometer is measured with the accelerometer in a succession of angular positions about that horizontal axis.

A new method is presented in which the test accelerometer, with its sensitive axis vertical remains attached to a horizontal surface which is caused to oscillate with constant acceleration amplitude in any direction (θ) in its plane. The direction can be varied continuously to determine the transverse sensitivity ratio (TSR) as a function of θ, and specifically its maximum value (TSRmax) and the angular direction (θ(TSPmin)) that corresponds to minimum transverse sensitivity.

The transverse calibrator consists of a vertical cantilever beam of circular cross section clamped near its lower end. The test accelerometer is attached to the upper end of the beam with its sensitive axis coaxial with the beam. The beam is driven in transverse vibration by two small electromagnetic vibrators having their axes mutually perpendicular and in a horizontal plane a short distance above the clamp. The vibrators are operated in phase from a single oscillator which is adjusted to the transverse resonance frequency of the system. By varying the relative amplitudes of the two driving forces the test accelerometer can be subjected to transverse vibration in any direction in the plane of its mounting face.

The TSR is determined by measuring the output (E_z) of the test accelerometer when a known amplitude A of transverse acceleration is applied at successive values of θ. The magnitude A is determined by measuring its two orthogonal horizontal components, using a pair of monitoring accelerometers attached to flat surfaces ground on the beam near the test accelerometer. The outputs E_x and E_y of these accelerometers are connected to an oscilloscope so that an analogue of the transverse motion is displayed as a Lissajous figure.

In the prototype calibrator the beam is a 25 mm dia steel bar held in a clamp which forms part of a fabricated steel support bracket. The bracket also carries two small electromagnetic vibrators of force rating 8.5N, with their axes in a horizontal plane 0.1m above the upper face of the clamp.

The signal to the two vibrators is obtained through a two-channel amplifier from a common oscillator. Each channel has an amplitude control and a ± 90 deg phase shift control. The latter is necessary to compensate for the effects of small variations in the transverse mechanical stiffness of the system as the direction of vibration is altered; these variations cause elliptic instead of rectilinear transverse motion.

With the prototype system adjusted to a resonance frequency 100 Hz the free length of the beam is approximately 0.4m. Coarse mechanical adjustment is made by varying the free length, and fine adjustment by varying the axial position of a small (100 g) steel collar clamped on the beam.

The calibration procedure is as follows. The angular orientation of the test accelerometer is noted with reference to the axes of the monitoring accelerometers, making use of a suitable mark or feature on the accelerometer body. The phase and amplitude of one or both driving signals are adjusted to produce, on an oscilloscope screen carrying a polar co-ordinate scale, a straight line of length proportional to the desired acceleration amplitude A (typically 200 ms^{-2}) and inclined at a nominated angle θ. The magnitude and phase of the test accelerometer output E_z are observed on another oscilloscope. The outputs E_z, E_x and E_y of the test and monitoring accelerometers are also read on digital voltmeters. This prodecure is repeated at successive values of θ, e.g. 10 deg increments. A more rapid check can be make by scanning through θ until the minimum E_z is found. The values E_x and E_y are read and used to calculate θ (TSRmin). Then TSRmax is found by increasing or decreasing θ by 90 deg and again reading E_z, E_x and E_y

15

The transverse vibration is not exactly rectilinear; the test accelerometer is subjected to a radial component of acceleration a_r, along its sensitive axis, at double the transverse frequency. In the prototype $|a_r|$, which may be estimated and/or measured, was typically less than 0.1 percent of $|A|$.

Errors in calculating TSR and θ may arise from the transverse sensitivities of the monitoring accelerometers, but careful selection and thoughtful orientation of these accelerometers can reduce these errors to less than 0.2 percent and 0.1 deg respectively.

A more significant but calculable error in calculating TSR and θ can come from the unavoidable errors in the calibration factors (i.e. axial sensitivities S_z, S_x and S_y) of the three accelerometers. The relative values of S_x and S_y can be found precisely by back-to-back intercomparison, thus minimizing error in θ. By a similar intercomparison with the test accelerometer prior to transverse calibration, the error in TSR can also be minimized.

Experience to date in using the prototype to calibrate various piezoelectric accelerometers indicates that the new method is accurate, sensitive and easily applied. Further developments in progress will provide improved clamping of the beam and will extend the frequency range. Obviously, higher resonance frequencies can be attained by changing the length, material and cross section of the beam. Another and more interesting possibility is to operate a cantilever beam at resonance in its higher modes. Preliminary observations with the prototype system driven at its resonance frequency (600 Hz) in its second flexural mode have confirmed that the range can be extended in this manner.

DIRECT MEASUREMENT OF SHOCK EFFECTS IN METALS

C. Zaharia and P. Gershon
Mechanical Engineering Department,
University of the Negev, Israel

It was recently observed [1] that during metal deformation a transient e.m.f. is developed in the strain gradient field. Further, experiments indicate that the e.m.f. generated by the deformed metal is proportional to the applied stress within the elastic limit. In the plastic regime the e.m.f. generated is dependent upon the location within the strain-gradient field, i.e., the magnitude of e.m.f. generated decreases with increase of the distance between the point of nucleation of permanent deformation ("necking") and the point of measurement. The magnitude of the e.m.f. is also dependent upon the strain history of the sample, i.e., strain hardening and hardness. Repeated straining of the sample results in successively greater generated e.m.f.'s.

This generated e.m.f. is attributed to a charge carrier equilibrium perturbance. Therefore, the phenomenon is rapid and is comparable to the charge carrier relaxation time.

In view of the above factors it is believed that shock and vibration phenomena may be measured "in situ" by measuring the generated e.m.f. The primary advantage of this technique is the fact that the measurements are made directly on the test object without the use of models or surface sensitive devices. Consequently many of the uncertainties of accuracy of the model, test conditions, adhesion, and interface instrumentation error

16

are eliminated. The measurements involved and the technique of attaching probes are simple and present no problem for a large spectrum of shock and vibration measurements.

A series of shock tests have been performed on 1020 steel Charpy specimens in a 5 kgm. impact tester and the generated e.m.f. recorded. The results indicated:

1. The generated e.m.f. is dependent upon the strain history of the specimen.

2. The travel distance of the stress wave significantly effects the magnitude of the generated e.m.f.

The results are qualitative, showing the dependence of above parameters on the e.m.f. in different relevant cases for shock tests and vibration measurements.

REFERENCE

1. C. Zaharia, Strain-Electricity. Submitted to Journal of Applied Physics.

AN EXPERIMENTAL STUDY OF THE VISCOPLASTIC BENDING OF COPPER-NICKEL AND STEEL TUBING

Thomas M. Frick
Westinghouse Electric Corp., Waltz Mills, Pa.

and

V. H. Neubert
Pennsylvania State University, University Park, Pa.

This investigation is concerned with the experimental study of dynamically loaded viscoplastic beams with a tubular cross section where elastic strains are a significant part of the total strain. Two materials are considered: 1020 steel and 70 30 copper-nickel alloy. The results are significant in three respects. This work defines a successful experimental approach for obtaining dynamic data; the results can be used in defining failure for optimal design; and a demonstration of accurate analytical predictions of dynamic data is made.

Loading was accomplished on an Impac shock machine. Accelerometer and strain gauge signals were recorded and then used to determine the dynamic moment and curvature. Maximum curvature rates were 2.5 in.$^{-1}$ - sec.$^{-1}$ for the steel specimens and 5.6 in.$^{-1}$ - sec.$^{-1}$ for the copper-nickel specimens. These are equivalent to strain rates of 0.78 and 1.89 sec.$^{-1}$ respectively. Plots of results demonstrate the higher magnitude of moment in the plastic range of the moment-curvature curve and the increase in the yield moment generally found when comparing dynamic with static test results. A time delay between maximum moment and maximum curvature is also evident. This time delay is attributed to material damping.

Successful analytical representation of the dynamic response is made by considering two empirical constitutive relationships. It is shown that for the steel tubing a linear

17

equation is appropriate. For the copper-nickel tubing a non-linear form of the constitutive equation is best suited for describing the response. Parameters in both equations are evaluated using the data and predictions of dynamic curvature are made.

This work also supports the reported observations of other experimenters with regard to the results for steel beams.

DIGITAL FILTERS FOR SHOCK DATA EVALUATION

H. D. Carleton
U.S. Army Engineer Waterways Experiment Station
Vicksburg, Mississippi

A recent study at the U.S. Army Engineer Waterways Experiment Station (WES) has reduced complex but related earthquake accelerograms to simplified time histories which describe earthquake phenomena in the form of conventional shock pulses. This technique, which is based upon processing with filters in the time domain, should be generally applicable to other shock and vibration analyses.

A Wiener filter is a mathematical operator designed to convert a given waveform (the filter's input) into another waveform (the filter's output) which is as similar as possible, in the least squares sense, to a third waveform (the desired output). Where the fit of the Wiener filter's output to the desired output is close, the operator may be regarded as a measure of the difference between the filter's input and the desired output. The operator takes the form of a time history analogous to an electronic filter's impulse response.

Construction of a Wiener operator requires comparison of the input and desired output time histories by means of a time domain process called crosscorrelation, comparison of the input time history with itself by means of a time domain process called autocorrelation, and finally, solution of the Wiener normal equations using values determined by the correlations. The operator so produced is equivalent to the frequency domain transfer function, which results from the division of the desired output's amplitude spectrum by the input's amplitude spectrum, and subtraction of the input's phase spectrum from the desired output's phase spectrum. The time domain desired output/input crosscorrelation and input autocorrelation together furnish the required amplitude information to the Wiener construction, while the required phase information is contained in the values of the desired output/input crosscorrelation alone.

At this point an intriguing possibility arises. Could the difference between any chosen pair of waveforms be *characterized in a condensed form* by the single impulse response waveform which uniquely describes the transfer involved? Examples show that for certain idealized cases, such as those for calibration change, lag, integration, and differentiation, inpulse response forms do appear characteristic of the transfers involved. However, the usual data waveform pairs produce mathematical operators which appear extremely complex in nature, through these same operators usually perform any required transfers with precision. The key to waveform pair relationship characterization therefore lies in *use* of the operators produced to show the transfers involved in simpler forms. The operator which properly represents the difference between two complicated waveforms can be applied as a filter to a classical shock test pulse such as the half sine, with the output to be

18

evaluated in terms of overshoot, settling time, etc. Abutment and dam crest motion time histories from a recent California earthquake have been paired and processed at WES to produce sets of pulse response data which may be evaluated in shock test form.

The WES computer program used in this study constructs operators of up to 999 sample point length to define the differences between any two time history inputs from digital data tapes. Data inputs of up to 999 sample points are accepted by the program, which may then apply the constructed filter to as many extra data time histories as are available on a total of three tape reels. Filter construction is documented by a set of plots showing the original time history pair, the filter's impulse response, and a filter efficiency checkout plot. Extra plots are produced to document inputs and outputs where the constructed filter is used on extra time history inputs. Operation of the basic program may be preceded by a variety of raw data adjustments.

SHOCK I

DYNAMIC RESPONSE MEASURMENTS OF TRANSIENT SHOCK PHENOMENA

Jack G. Parks
U.S. Army Tank-Automotive Command, Warren, Mich.

The mechanical response of materials to shock type forces is a difficult phenomenon to quantitatively measure due to the transient nature of the processes involved. Quantities such as elastic moduli, viscosity coefficients, and general intrinsic rheological parameters are of particular importance in the study of the strength of materials. Little information is known, however, about the behavior of these parameters when the substance is subjected to high amplitude, short time duration forces as experienced during the propagation of shock waves. Measurements in this environment require considerable accuracy for subsequent application to the study of relaxation processes, deformation behavior, and fracture mechanisms.

Recent research at the U.S. Army Tank-Automotive Command has provided a new measurement technique for this realm of physical testing. It was initially recognized that the frequency spectrum of a system composed of two ultrasonic transducers bonded to opposite sides of a material specimen was largely determined by the electrical parameters of the transducer and the mechanical properties of the intervening material. Early experimentation disclosed that the application of steady state stress forces caused appreciable distortions in this spectrum and that these variations could be correlated to changes in the material through the use of simple mechanical models. When transient forces were applied, however, even the use of real time frequency analysis equipment did not permit adequate response times for the observation of relaxation phenomena and rheological behavior associated with shock type forces.

The new technique developed employs rapid frequency sweeping of the spectral region of interest. The signal supplied to one of the transducers is linearly frequency modulated through the resonant frequency of the system. An analog computer is then used to abstract from the output signal of the second transducer the spectral parameters required (e.g., maximum response, resonant frequency, bandwidth, spectral moments, etc.). The initial value of the frequency for each spectral scan must be selected to permit the decay of transient oscillations prior to encountering the system's resonant frequency. Frequency sweep rates of 10^6 Hertz/sec. have been achieved with no deterioration in measurement accuracy.

A technical difficulty was experienced and corrected during the development of this technique. The spectral response of all resonant systems when subjected to frequency modulated forcing functions exhibit amplitude and frquency distortions. Mathematical analysis of the behavior of such systems indicates that the final solution involves the error function with a complex argument. Although the evaluation of the spectral response for the case of relatively slow frequency sweep rates produce nearly intractable expressions, high sweep rates lead to final results which are mathematically simple. In order to

Preceding page blank

compensate for this phenomena, corrective circuits were programmed on the analog computer to modify the system's output and yield only those spectral changes resulting from the stress application.

The modeling aspects of the system consisted of a combination of mechanical analog elements which (a) satisfied the general properties of the material under investigation, (b) replicated the general ultrasonic wave properties exhibited in the steady state situation, and (c) permitted sufficient sensitivity for the determination of rheological parameters. Results of the analog computation are subsequently subjected to analysis compatible with the optimization of model parameters. The final perfection of this measurement method calls for the use of a hybrid analog/digital computer to condition the system's output signal and compute the variation of model parameters.

INDUCED SHOCK PULSE TESTING BY TRANSIENT WAVEFORM CONTROL

B. K. Kim
Jet Propulsion Laboratory
Pasadena, California

Induced environmental testing at JPL is primarily that of random noise, sinewave and shock excitation. Shock tests are performed on electrodynamic shaker systems, or on special purpose shock testing machines. Generating a shock pulse on an electrodynamic shaker can be controlled to a given shock spectrum using a shock pulse synthesizer and shock spectrum analyzer. The main concern with this method is the process of obtaining the meaningful shock spectrum specification. The single degree-of-freedom linear model assumption, proper Q assumption and damage potential with respect to the resonance behavior may be hard to justify for a given specimen. The other shock testing machines are controlled to a given time history, however they are limited to specific time profiles such as terminal peak sawtooth, half-sine, square wave, etc. The results of the test using these special machines can, of course, be displayed in the form of a shock spectrum or a time history.

With this much background, it became increasingly desirable to be able to deliver arbitrary shaped transient time pulse to a test specimen with good controllability and repeatability. With the advances of real time Fast Fourier Transform (FFT) processors, it seemed natural to combine existing shaker systems with FFT processors. In fact, recent experiments with digitally controlled random vibration testing have demonstrated the capabilities of coupling a FFT processor and a special purpose minicomputer with existing shaker-amplifier systems. The present work of transient waveform control (TWC) focuses on an electrodynamic shaker as the means of excitation, and controlling to a given time history waveform using a FFT processor and minicomputer system. The idea of waveform control is not new, however in the past it was performed with analog devices such as waveform synthesizers. This left the waveform control testing highly susceptible to human errors, poor controllability and poor repeatability. The first implementation of TWC using digital devices was proposed by Favour, LeBrun and Young of Boeing in 1969.

The purpose of this paper is to describe the first successful implementation of TWC at JPL, utilizing the JPL experimental digital vibration control system (Fourier processor, minicomputer and the environmental laboratory amplifier and shaker systems). The main

theory behind the TWC process is that of computing instantaneous transfer functions experimentally, assuming linearity of the system. It is most crucial to obtain a meaningful transfer function within the dynamic range of the digital equipment. In order to guarantee the full frequency response of wide bandwidth, a delta function can be chosen for the initial calibration pulse. The transfer function is computed by complex division of the Fourier transformed input and output calibration signals. Then the required waveform is synthesized for a given desired waveform compensated by the transfer function characteristics.

The TWC technique is demonstrated to be controllable to an arbitrary transient profile and repeatable to the JPL tolerances at least to the known limitations of the hardware. The main argument for this technique is that of better realism in the vibration testing, providing that a typical time history transient waveform can readily be defined for a physically transient phenomenon. This method of testing will compliment and improve the realism in a conventional shock spectrum testing, as well as sine sweep test specifications which are typically based on some transient phenomena.

COMPARISON OF SHOCK SPECTRUM TECHNIQUES AND
THE METHOD OF LEAST FAVORABLE RESPONSE

A. F. Witte and R. J. Wolf
Kaman Sciences Corporation
Colorado Springs, Colorado

The use of shock response spectra for defining dynamic loads and laboratory environmental test criteria to qualify hardware for field shock environments has within the past few years become very controversial. This controversy has been augmented by certain technological advances in digital calculation of the Fourier transform and in digital control of vibration exciters. Both advances make it possible to generate in the laboratory complex acceleration time histories which can be analytically expressed or represented as a series of time samples (1).

Methods of synthesizing field shock response spectra in the laboratory have been devised which utilize digital controlled exciters and oscillatory transients. These often better describe field environments than the normally used classical shock pulse which can be easily reproduced on conventional shock machines. However, the controversy over the applicability of shock response spectra still exists since calculational advances also make it possible to utilize the Fourier spectrum.

Critics of shock spectra cite the fact that its use necessarily requires the assumption that the system in question be accurately represented by a linear single degree-of-freedom system whose damping is independent of its resonance frequency. Shock response spectrum techniques are often applied to situations where the system in question is clearly not single degree-of-freedom in nature and damping is not independent of resonance frequencies. The conservatism of shock response spectra techniques for defining test criteria often depends on the method of laboratory synthesis, the biases applied to the field shock spectra to insure adequate conservatism in the laboratory, and the actual dynamic characteristics of the system to be tested.

23

Smallwood has suggested that a method proposed by Shinozuka for evaluating the effects of siesmic motions on structures has applicability in specifying worst case criteria for laboratory environment tests (2,3). The technique which is known as the method of "Least Favorable Response" (LFR) utilizes the envelope of the Fourier spectra moduli for the ensemble of all known field environments, $\underline{X}_e(\omega)$. It also uses the actual dynamic characteristics of the system in the form of the frequency response function, $H(\omega)$. The theory of LFR states that an input, $\ddot{x}(t)$, whose Fourier spectrum, $X(\omega)$, is defined by

$$X(\omega) = \frac{\overline{X}_e(\omega)\, H^*(\omega)}{|H(\omega)|} \quad \text{(a)}$$

will result in a response $\ddot{y}(t)$ whose absolute value is maximum for all possible inputs having Fourier spectra less than the field envelope, $\overline{X}_e(\omega)$. Thus, provided the field data adequately represents realistic situations, it insures that the laboratory test will result in a conservative and a worse case situation in the time domain. The method of LFR insures that adequate "simulation" in the frequency domain will also be accomplished.

Analytical and experimental studies have been performed by the authors to compare shock spectrum and LFR techniques. These studies utilized both single degree-of-freedom and multiple degree-of-freedom systems. Classical pulses and decaying periodics were used to match or synthesize ensembled field shock spectra and conservatively biased envelopes. The results were compared with those obtained using the method of LFR in the time, frequency, and response domains.

The results of the study indicate that the method of LFR produces a conservative response (an approximate factor of 2 was observed for the situations examined) and an adequate match of the field mean plus 3 standard deviation shock spectrum. The method of Least Favorable Response also insures that the system response will be adequately "simulated" in the frequency domain. The use of shock response spectra can result in an undertest and overtest depending on enveloping, biasing, and synthesizing criteria as well as system dynamic characteristics. The use of shock spectrum may not insure adequate "simulation" in the frequency domain.

This paper describes methods and criteria used to perform the study and presents the significant results in abbreviated form along with general conclusions derived from the study.

REFERENCES

1. LeBrun, Jay M., Favour, John, "Feasibility and Conceptual Design Study-Vibration Generator Transient Waveform Control System," Final Report prepared for NASA June 1969, Contract NAS 5-15171, Goddard Space Flight Center, Greenbelt, Maryland, by Aerospace Group, The Boeing Company, Kent, Washington. This report also released as Boeing Document D2-114438-1.

2. Smallwood, D. O., "A Transient Vibration Test Technique Using Least Favorable Responses," 43rd Shock and Vibration Symposium, December 1972. This report also released as Sandia Document SC-DR-61-0897.

(a)$H^*(\omega)$ denotes the negative conjugate of $H(\omega)$.

3.   Sinozuka, M., "Maximum Structural Response to Seismic Excitations," Journal of the Engineering Mechanics Division, Proceedings of the American Society of Civil Engineers (October 1970) pp. 729-738.

THE USE OF EXPONENTIALLY DECAYING SINUSOIDS
TO DUPLICATE SHOCK SPECTRA ON SHAKER SYSTEMS

D. O. Smallwood and A. R. Nord
Sandia Laboratories, Albuquerque, New Mexico

Present methods of simulating shocks in the laboratory are often inadequate. The usual method is to match the shock spectrum over a limited frequency band using classical pulses. Several methods (1,2) have been described for shaping shock spectra over a wider frequency band using oscillatory type pulses on shaker systems. The disadvantage of these techniques is that they frequently do not preserve the "character" of the field time histories. Exponentially decaying sinusoids are attractive for two reasons. First, there are physical reasons to believe that many field environments can be represented by sums of decaying sinusoids. For example, the response of a structure loaded impulsively (a truck hitting a pothole) will be the sum of several decaying sinusoids (one at each of the system's natural frquencies); and secondly, many field time histories resemble decaying sinusoids. The disadvantage of decaying sinusoids is that a nonzero displacement and velocity change are characteristic of these transients. Shaker systems can accurately reproduce only those transients which have a zero velocity and displacement change. (Strictly speaking, an electrohydraulic shaker system can have a limited displacement change.)

Decayed sinusoids have been used by other investigators to match shock spectra. However, if the velocity and displacement functions are not considered, the shaker will distort the waveform to produce a zero velocity change. The distortion implies that the velocity and displacement wave forms will not conform to pretest predictions. In addition to the undesirable distortion, it becomes difficult to predict the capabilities of a shaker to reproduce a given waveform, as the velocity and displacement limits of the shaker must be considered.

A method is described where the decayed sinusoids are slightly modified to reduce the velocity and displacement changes to zero. Basically, the method is to add a negative amplitude, highly damped ($\zeta \geq .5$), time shifted (see Figure 1)* decaying sinusoid. It is shown that the values of the amplitude (B) and delay (τ) can be used to control the change in velocity and displacement, respectively. The frequency (ω_m) can be used to control the low-frequency content of the waveform. The value chosen for the damping (ζ_m) is apparently not critical. Examples are shown to illustrate that the displacement waveforms can now be predicted.

A method is also described for picking the decayed sinusoid components to match a given shock spectrum. First, values are picked assuming each component acts independently from the others. Normalized shock spectrum curves can be used for this purpose. These values are used as the initial values for a computer routine which will then modify the magnitude (A_i's) of the components to match the spectrum.

---

*Figures have been eliminated to speed publication.

25

The resulting synthesized pulse can then be reproduced on a shaker using digital techniques.

REFERENCES

1.   D. O. Smallwood and A. F. Witte, "The Use of Shaker Optimized Periodic Transients in Matching Field Shock Spectra," Sandia Laboratories Report SC-DR-71-0911, May 1972.

2.   R. C. Yang and H. R. Saffell, "Development of a Waveform Synthesis Technique—A Supplement to Response Spectrum as a Definition of Shock Environment," Shock and Vibration Bulletin No. 42, Part 2, pp. 45-53.

A CASE FOR DAMPED OSCILLATORY EXCITATION AS A
NATURAL PYROTECHNIC SHOCK SIMULATION

Dennis B. Nelson and Peter H. Prasthofer
Sandia Laboratories, Livermore, CA

The objective of this paper is to develop a tractable simulation of the excitation experienced by a substructure when the parent structure is subjected to a pyrotechnic environment. To this end a rationale is established for using decaying oscillatory excitation and a methodology for specification suitable for use on electrodynamic exciters is developed. The specification is based on existing shock descriptors. A detailed illustration of these concepts is included.

The simulation is directed toward the low frequency region. Low frequency is defined in the sense that the substructure is sufficiently far away from the source of excitation that local stress fields have equilibrated and that the substructure is sufficiently buried in the parent structure that high frequency modal contributions are negligible. The substructure may include components which are of individual interest.

It is shown that the response of systems to impulsive inputs leads naturally to the selection of a superposition of damped oscillatory waveforms as a shock specification. In particular, if the system can be represented by a lightly damped, linear N degree-of-freedom, lumped element model, the impulsive response is a superposition of damped sinusoids. Significantly, waveforms of this nature are easily generated on electrodynamic exciters. It is recognized that a damped sinusoid in its pure mathematical form is not realizable on electrodynamic exicters. Therefore, a waveform which reasonably approximates the damped sine but has the properties that the residual velocity and displacement are zero is derived.

The specification of the component waveform is in terms of the amplitude, frequency, and decay rate of the individual components. These parameters may be obtained, in general, from the energy spectral density or the zero damped shock spectrum. Further insight into the relative importance of particular frequency components is obtained through the damped shock spectrum.

26

It is demonstrated that if the energy spectral density of the field environment is enveloped by the energy spectral density of the specified composite waveform, the energy imparted to each point in the structure is at least as great as that caused by the field environment. A heuristic argument is given that if the shock spectrum is enveloped in the "right" way, the peak response of each point in the structure should be at least as great as that caused by the field environment. Furthermore, if the decay rate of the test waveform is similar to the decay rate of the field excitation, an upper bound on the peak response is obtained. This bound is controllable and may be made to approximate the corresponding bound associated with the field environment.

A reasonably complex system consisting of nine masses and interconnecting elastic elements is used to illustrate the method. The structure is subjected to a simulated field environment and a shock specification for a three degree-of-freedom substructure is derived. The response of the substructure to the test is found to agree well with the response to the simulated field environment.

MINIATURE PYROTECHNIC SHOCK SIMULATORS

L. H. Albers and G. J. Milder
Jet Propulsion Laboratory
Pasadena, California

Pyrotechnic shock testing has developed in response to environments which have been induced in structures primarily as a result of the actuation of release and/or separation devices that use an explosive element as a prime mover.

In order to accomplish this testing, test equipment and facilities have been developed by a number of organizations using a variety of approaches to attempt to duplicate and envelope the environments produced by the various mission ordinance events. This includes the use of various test stands that actually use pyrotechnic devices, the simulation of pyrotechnic events on a vibration exciter, and an attempt by some to accomplish a test with the same damage potential as a pyrotechnic event on a conventional drop type shock machine. The above have met with varying degrees of success.

This paper presents an effort made by the Jet Propulsion Laboratory (JPL) in Pasadena, California, to develop a miniature pyrotechnic shock simulator. The thrust of this effort was not to develop a general purpose test machine, but rather a device which could be substituted on the Viking Orbiter 1975 Spacecraft Bus for the actual pyrotechnic device. Thus, the device had to be designed to fit in the same space and mount to the spacecraft in the same manner as the planned pyrotechnic device.

The actual device occupies a space on the spacecraft bus approximately 1.5 inches by 3.4 inches by 1.5 inches. This space is open only on one side. Eight of the devices are located on the spacecraft bus. Four are used to separate the spacecraft from the spacecraft adapter and four are used to separate the Aft Biosheild from the Viking Orbiter. Each device contains two squibs which are fired to effect the separation.

With the above in mind, the task at JPL was begun with several goals:

27

1. The simulator should be approximately the same size as the actual device.

2. The simulator should be able to reproduce the pyrotechnic shock spectrum within a specified scatter band (± 3 dB).

3. The device should be able to perform a simulated pyrotechnic firing with levels sufficiently higher than the actual device in order to constitute a margin test.

4. The simulator should produce a repeatable pulse, and the time to reconfigure the machine between pulses should not be excessive.

5. The simulator should be sturdy enough to produce a large number of pulses without suffering any degradation.

It was subsequently decided that high pressure gas would be used as the prime mover in the simulator to be developed. Among the problems encountered during the development were the following:

● Material selection was important as a consideration of the goal of obtaining reliability over a large number of tests.

● Gas dynamics were involved to the extent that it was desired to maintain gas flow subsonic and to prevent choking of gas flow at the inlet.

● Each of the four devices were required to actuate simultaneously as in the flight application.

● Actual measurement of simulator velocities had to be achieved for comparison with actual flight device velocities for design verification and shock repeatability.

Although this effort was not originally intended to produce a general purpose machine, the possibility of adaption for many types and levels of pyrotechnic shock would be relatively simple.

TIMEWISE OUTPUTS OF PYROTECHNIC BOLTS

V. H. Neubert
The Pennsylvania State University, University Park, Pa.

and

R. P. Parker
Uniroyal Research Center, Middlebury, Conn.

The paper describes experimental results of measurements of outputs of explosive bolts using a Hopkinson bar arrangement. It also presents an associated analysis, using the Love equation for the bar, to account for the wave dispersion which occurred in the bar.

It has been common to measure the acceleration response of structures near pyrotechnic devices and then to present the data in the form of shock spectra. While shock spectra are useful to show the rich frequency content of the pulses, they are of little use to a structural analyst when so many modes are excited. The purpose of the reported

study was to attempt to measure the foretime and moment-time output of explosive bolts, which create a severe shock loading of some components on space vehicles.

The explosive bolts were mounted on the end of a long Hopkinson bar. Strain gauges were located at various positions along the bar to trace the resulting wave. The bar was one inch in diameter and the pulse measured was less than 12 micro-seconds long. The wave dispersed as it travelled the length of the bar, and it was necessary to use Love's equation to trace the wave theoretically.

The paper describes the apparatus and shows a typical measured pulse from a 1/4″ diameter Holex explosive bolt. The detonations were found to be quite symmetrical, with a strong axial force but practically no bending applied by the bolt. Also presented is a normal mode solution for the bar for a 10 microsecond pulse according to the simple wave equation and also the Love equation, indicating the high number of modes required for convergence. It is also shown that the peak acceleration in the bar was greater than 200,000 g and that the equipment available at the time would probably not have measured acceleration accurately at the free end of the bar.

The measured force-time output could be used by analysts as a loading in order to predict timewise structural response.

STRUCTURAL ANALYSIS

PERFORMANCE OF STATISTICAL ENERGY ANALYSIS

R. F. Davis and D. E. Hines
McDonnell Douglas Astronautics Company
Huntington Beach, California

The increasing performance of aerospace vehicles has resulted in external acoustic fields and aerodynamic boundary layers that cause increasingly significant high-frequency random vibration environments. In general, these environments have been predicted using empirical scaling techniques; however, the advent of reusable space vehicles featuring new configurations with unique forcing fields requires extending these techniques beyond the configurations from which they were developed. These factors, together with a desire for optimal vehicle designs, have made the analytical prediction of high-frequency random vibration response in structures an important aspect of the design and development of such vehicles.

The classical modal analysis techniques for predicting dynamic response work well in the frequency range of the lower structural resonances. However, when these techniques are extended into the higher frequency range, the complexity and size of the model and the required solution time increase rapidly. Consequently, classical solutions in the high frequency range are well beyond the current state of the art for computer hardware.

Statistical energy analysis (SEA) techniques that can successfully circumvent the problems of classical determination of high frequency response were developed a decade ago. Although fundamentals were established, minimal effort was made to apply such methods to the complex structural systems that are typical of flight hardware.

The first SEA application to a complex vehicular structure was performed for the UpStage program*. The SEA effort on UpStage was directed to the scaling of data from an acoustic test specimen into design and component vibration test criteria for a flight design. Because of the specific interest in using SEA as a scaling technique, the approach was not evaluated in depth as a predictive technique.

This paper discusses a comprehensive evaluation of SEA applied to a complex system based on a study using experimental data from UpStage tests and supplemental tests on simple structural systems. The supplemental tests provided damping and coupling parameter values through the use of very simple test methods. A technique for introducing acoustic energy into the SEA model is utilized which gives good results with reverberant acoustic fields but requires further development before valid application to nonreverberant fields is indicated.

---

*Hines, D. C., Parker, G. R., and Hellweg, R. D.: Prediction of UpStage Random Environments Using A Statistical Energy Approach. 41st Shock and Vibration Bulletin, 1970.

This statistical structural analysis, in conjunction with the simple test methods, resulted in high-frequency vibration response predictions with an accuracy of ± 3 dB in comparison with test measurements. Frequency scaling methods are presented that may be used to evaluate the frequency range in which this accuracy can be expected for general structures. The complex structure considered in this paper is an elliptical cone excited with a range of acoustic configurations. In many respects, this represents a more complex analysis problem than that for typical vehicles. Considering the complexity of the structure examined in this study, together with the various types of acoustic input configurations, one can expect the results to be valid for a wide range of structural problems.

PREDICTION OF SHOCK ENVIRONMENTS BY
TRANSFER FUNCTION MEASUREMENT TECHNIQUES

G. Kao, J. Cantril, and G. Shipway
Wyle Laboratories, Scientific Services and Systems Group

and

M. Boyd
U.S. Army, Corps of Engineers

The vertical shock environment of three electrical power equipment cabinets supported by a shock isolated platform were estimated by means of an empirically determined transfer function. The mechanical impedances of the pendulum isolator system and the mobilities of the platform and equipment cabinets were measured and used to determine the transfer function of the whole system under five different preload conditions of the four isolators. An input shock spectrum and the system transfer function were then used to determine the vertical shock environments for each preload condition.

A set of load transferring points was assumed at the interface of each subsystem to define the load paths of the entire system. Each subsystem had a set of points which received the input motion and a set which transmitted the outgoing motion to the adjacent subsystem. Four input and four output points were used for the isolator subsystem corresponding respectively to the attachment points of the isolators to the ceiling and to the platform. Correspondingly four input points were used for the platform, ten output points of the platform were used for the interface of the platform with the equipment cabinets and ten corresponding points for the input motion to the cabinets.

To measure the necessary impedances and mobilities each subsystem was subjected to sinesweep forcing functions at each of its load transferring points with each forcing function and corresponding responses at all transfer points recorded on analog tape. The sinesweep frequency range was from 5 Hz to 500 Hz and forcing functions consisting of vertical forces, lateral forces, vertical moments, and lateral moments for the platform and equipment subsystems. Vertical forces only were used for the isolator subsystem.

The recorded analog data was played back through a computer drive A/D data acquisition system and the digitized data stored on magnetic computer tape for later reduction. The frequency range of the data was divided into a series of octaves based on frequencies at integral powers of 2 and a constant sampling rate was maintained in each octave giving at least 20 samples per cycle at the beginning of each octave and 10 samples per cycle at the end.

32

The raw digitized response data was then analyzed by computing the auto-correlation of the force channels and the cross-correlation functions between the four channels and the response channels yielding the force amplitude and the response acceleration amplitudes and the phase shifts between the force channels and response channels. After the data reduction acceleration impedances or mobilities were obtained by computing the appropriate ratios of force and response. Approximately 500 frequency intervals were used to define each impedance or mobility element. Computer plots were generated for each element as a function of frequency.

The response of the equipment cabinets to an input motion at the ceiling attachment points of the isolators was calculated as

$$G_3(\omega) = T_{13}(\omega)G_1(\omega)$$

where

$G_3(\omega)$ = Acceleration frequency response of the equipment cabinet,
$G_1(\omega)$ = Input acceleration at the ceiling attachment point of the isolator, and
$T_{13}(\omega)$ = Acceleration transfer function calculated from measured impedances and mobilities

Shock spectra for the equipment cabinets were determined using the above relation for each of the five preload conditions of the isolators. The results indicate an effective attenuation of input energy for frequencies between 5 Hz and 50 Hz and a moderate attenuation above this value.

DETERMINATION OF GUIDEWAY ROUGHNESS
FROM CONSTRUCTION TOLERANCES

B. J. Brock
Vought Systems Division, LTV Aerospace Corporation, Dallas, Texas

Ride quality has been identified as a prime consideration in the passenger acceptability of future mass transportation systems, and guideway roughness (or, if you prefer, smoothness) is a fundamental factor in the control of the ride quality of ground transportation vehicles. Total systems costs must be minimized if new transportation systems are to be economically feasible. Generally, the guideway construction and maintenance costs will increase with increased demands for accuracy, and a few dollars extra cost per mile of guideway adds up in a hurry. Therefore, construction and maintenance requirements must be established in a form compatible with surveying and construction practice so that guideway costs can be estimated and "traded-off" against vehicle suspension sophistication and cost.

The problem of maintaining satisfactory ride comfort becomes ever more difficult as vehicle speeds increase. Roughly, the root-mean-square of vehicle accelerations increases as the square root of the forward velocity. Some rail vehicles are already operating at speeds in excess of 200 mph, and target speeds are 300 mph +! So, the problem of guideway roughness/smoothness will become even more acute in the future.

33

This paper describes a technique for estimating the guideway roughness from construction tolerances. The current trend is to use power-spectral-density (PSD) techniques to evaluate the ride quality of transportation vehicles. This is a logical step because guideway roughness is basically random in nature, although there may also be discrete frequency components in the irregularities associated with joint spacings or the like. It has been shown that the general form of a roughness PSD can be approximated by $S(\Omega) = A/\Omega^2$, where $S(\Omega)$ is the roughness PSD with units of $ft^2/(rad/ft)$, Ω is the spatial frequency in rad/ft, and A is the guideway scale of roughness in feet.

Now, it is relatively easy to determine a maximum allowable guideway roughness PSD for operation of a given vehicle over a certain speed range. Unfortunately, surveyors and construction contractors are not accustomed to building to tolerances expressed in the form of allowable PSD of roughness. This paper describes a method by which allowable roughness PSD can be translated into construction tolerances.

A straight-forward approach capable of step-by-step intuitive checking was adopted for this first-cut analysis. Briefly, a composite PSD of guideway roughness was developed by calculating the PSD's of various components of the overall roughness and adding them together. The types of guideway irregularities considered and the magnitudes of the deviations were chosen based on:

- Association of American Highway Officials (AASHO) standard construction tolerances

- Various highway specifications and engineering texts

- Counsel of members of the academic community and construction contractors

The first step in the procedure is to generate a sample of guideway by mathematical simulation. This was accomplished by using a random number generator routine to produce random numbers with prescribed statistical properties which were used to establish the amplitudes of the various *types* of irregularities. Tabular data were then produced representing measurements of guideway deviations taken at regular intervals along the guideway. These data were then analyzed as though they were digitized, measured data. In this way power spectra were developed for each individual type of irregularity so that the contribution to the overall can be identified. This allows one to judge the relative importance of the various irregularities and to set the tolerances for each type.

SELECTED SYSTEM MODES USING THE DYNAMIC
TRANSFORMATION WITH MODAL SYNTHESIS

Edward J. Kuhar, Jr.
Spacecraft Dynamics Engineer
General Electric—Space Division, Valley Forge, Pa.

Modal synthesis methods have been developed to determine the low frequency modes of complex structures. These methods synthesize the vibration modes of the complete structure from substructure analyses where the size of the eigenvalue problem is reduced by truncating the high frequency substructure modes. A dynamic transformation method has been developed as a means of reducing the eigenvalue problem size. The method

not only reduces truncation errors for low mode solutions but also provides an exact solution for a selected system frequency or frequency range. The objective of this paper is to demonstrate the capability of the dynamic transformation to obtain system solutions for modes in a selected frequency range while providing criteria for assessing the accuracy of the solution.

The approach taken in this paper is to use a dynamic transformation method which includes the effects of modes not retained explicitly in the eigenvalue solution. A dynamic transformation that relates the unused coordinates to the retained coordinates at a selected system frequency is obtained from the complete equations of motion. This transformation is then used to reduce the mass and stiffness matrices while retaining those coordinates of primary interest. After solving the reduced eigenvalue problem, the solutions are revised using new transformations at the calculated eigenvalues. Comparison of the revised and initial reduced solutions are used to assess the accuracy of the modes. By examining the participation factors (component mode coefficients), one can determine whether or not the correct set of retained coordinates has been selected. If all of the modes of interest have not been obtained, the results are used to select a new set of retained coordinates and reduction transformation and then, the procedure is repeated. The transformation can be used with any of the basic modal synthesis methods. Because the transformation can be at any system frequency, the method is not restricted to low mode solutions but can be used for modes in any frequency range.

Under a NASA-MSFC study contract, the dynamic transformation was applied to three structural models using two methods of modal synthesis: a GE-SD stiffness coupling method and Craig and Bampton's method for coupling substructures. Three parameters were varied in the analyses: (1) the number of kept and/or reduced modal coordinates; (2) the reduction frequency, p; (3) the set of coordinates kept for the eigenvalue solution. The reduction frequency was selected between system modes to show general trends. The coordinates selected as the kept set were selected as a sequential group from the constraint modes and/or the frequency ordered component modes depending on the frequency range of interest.

The results of the analyses used eigenvalue and mode shape errors to evaluate the accuracy of the results. Eigenvalue errors were obtained by comparing the reduced solution eigenvalues to the corresponding system eigenvalues obtained from a complete solution of the problem. Mode shape errors were obtained for the corresponding eigenvalues by using the standard error of estimate of unit length vectors,

$$\left[\sum \frac{(X_{i_{exact}} - X_i)^2}{N} \right]^{1/2} .$$

In most analyses for the middle and high mode solutions, over half of the solution modes had frequency errors of less than .1% when the number of kept coordinates (eigenvalue size) were approximately 20% and 40% of the total structures' degrees of freedom. A sequential solution for one of the models was performed to indicate a possible approach to determining the system modes. All of the system modes were obtained in four eigenvalue solutions. Each solution was for 40% of the modes with the maximum frequency error in any mode of .04%. Sufficient overlap existed to assure that all the modes were obtained.

Several analyses were performed to determine if intermediate and high mode solutions could be obtained regardless of the kept set of coordinates. The results showed that, if the reduction frequency corresponds to a modal frequency, the vector errors were within computer accuracy regardless of the kept coordinates selected.

Participation factors were examined for solutions where large errors were observed for particular modes in the middle of a selected group. For the modes in question, the participation factors showed that the contributing modes were not included in the kept set, and indicated which modes should have been selected from the reduced set. Although the reduction frequency forces a system solution when it occurs near a real system frequency, the results indicate that a match with regard to the kept substructure modes and reduction frequency is needed to maximize the number of accurate system modes obtained from a solution.

The following conclusions are reached on the basis of this study: 1) selected system modes and frequencies can be obtained from the solution of a greatly reduced eigenvalue problem using the dynamic transformation method; and 2) the method provides error criteria which enable the accuracy of the solution to be assessed.

STRUCTURAL DYNAMICS COMPUTATIONS USING AN APPROXIMATE TRANSFORMATION

Clifford S. O'Hearne and John W. Shipley
Martin Marietta Corporation, Orlando, Florida

In performing structural dynamics analyses of flight or ground vehicles, it is frequently the case that mass distribution is varied but stiffness distribution is held constant. Payloads, releasable stores, or expendable fuels and propellants make negligible contributions to primary structural stiffness. The paper presents an approximation used in these cases for dynamic loads computations employing the normal mode method of Bisplinghoff and Biot. The approximation has value when the equations of motion of a large-order finite-element system have been reduced to low order for dynamical analysis. The ordinary sequence in such analysis is a Guyan reduction followed by selection of lower mode eigenvectors as a basis of the solution displacement space. The intuitive basis for the technique lies in the common observation that modal shapes in lower modes of motion are not very sensitive to mass distribution changes and thus all sets of eigenvectors may be expected to include a suitable analysis subspace within their span.

The approximation consists of computing a transformation which fits the eigenvector subspace corresponding to one weight condition to the other subspaces using a least square error criterion. This transformation is used to obtain approximate transformations from the physical applied forces to the solution force subspace and from the solutions back to the element loads or stresses of interest. In lieu of the approximation, exact computation of these lastmentioned transformations may be burdensome because of the large computer core size and input/output unit requirements of large structural analysis programs. These factors tend to increase computation cost, to reduce computer accessibility, and to increase turnaround time thereby increasing the duration and cost of the analysis period. The approximation may also be used in a converse fashion: When several weight conditions of the same elastostatic system have been treated using the exact transformations, the

approximate transformations provide an engineering check on the analyses. A substantial difference in exact and approximate transformations indicates that either too few modes were used or the model is very sensitive to mass change, or both.

Use of the approximation has been tested in engineering analysis of a multi-missile launcher with varying numbers of missile rounds. The launcher is loaded by air blast pressures. The computations are believed to be a severe test of the method and demonstrate its value.

PREDICTION OF COLLAPSE MODES IN CRASH-IMPACTED STRUCTURAL SYSTEMS

K. J. Saczalski
Office of Naval Research, Arlington, Virginia

and

K. C. Park
Lockheed Aircraft Corp., Burbank, California

Prediction of the mode of collapse would provide valuable insight into the energy absorbing capabilities and survivability potential of a given structural system. The magnitude of difficulties associated with this task become apparent when consideration is given to structural systems such as monocoque light aircraft. In view of the enormous complexities introduced by buckling, warping, large deformations, inelastic nonlinearities of structural materials and manufacturing imperfections, these problems do not lend themselves easily to a deterministic theoretical solution. In spite of this, however, some investigators have attempted, through the use of hybrid experimental-analytical techniques and finite element type numerical approaches, to develop analysis techniques for predicting the inelastic crash response of complex vehicular systems.

The difficulty with any hybrid approach is that the experimental work usually consists of catastrophic destructive testing of structural components and sub-systems for the purpose of obtaining nonlinear load-deformation information. The cost, time and magnitude of effort involved in this type of testing virtually eliminates the potential for employing hybrid techniques in the preliminary or early design stages. On the other hand, although the finite element type numerical simulation approaches appear to hold promise for predicting general structure crashworthiness in the early design stages, factors such as accuracy, efficiency, and economic considerations provide a practical limit on the number of elements and unknowns which may be handled by any simulation or finite element type modeling approach. The result of these limiting factors is that an a-priori estimate of the failure regions is made. This is somewhat like putting the cart before the horse and the danger of such an estimate should be evident. Obviously, a simplified analytical type technique to predict the most likely, or highly probable, regions and modes of failure would enable judicious modeling with a minimum number of elements and unknowns.

A quasi-statistical technique has been investigated as a feasible method for allowing the designer a means to predict failure modes and general crashworthiness of complex multi-degree of freedom structural systems, such as automotive and light aircraft vehicles, without the necessity of innumerable, costly destructive tests. The technique employs average internal reaction load density spectrums of structural elements as the mechanism for predicting collapse modes of the crash-impacted system containing large arbitrary-

shaped rigid bodies which are linked by structural elements, composed of nonlinear, rate-sensitive, materials. The average dynamic loads are combined with an empirically modified yield function so as to determine whether the average dynamic loads exceed a critical value dictated by the approximate yield function. Piecewise linear approximations account for the system nonlinearities and are coupled with the load density spectrums to provide a topology ot yield and establish the likelihood of failure modes associated with various regions of the complex structure.

The original system is modi: ed by failure mechanisms, such as plastic hinges, in the critical areas of indicated failure and a similar process is repeated to predict where the secondary or next most probable failure mechanisms will occur. If a constraint is violated, such as an engine block striking a firewall before the secondary failure mode has been reached, the secondary failure mode is adjusted accordingly. Segments of the system which appear to be in the elastic range are reduced, by a sub-structure approach, to linear couplings between the indicated locations of initial and secondary inelastic regions. The original complex system may now be considered as a nonlinear problem, of greatly reduced size, which incorporates all of the inertial and physical effects of the original system.

Some preliminary assumptions used in the technique are that the pulse width (in time) of the shock excitations are at least large enough to allow the predominant modes of the relatively stiff continuous system elements to respond. Work-hardening and strain-rate effects are accounted for in the empirically modified yield function. The term "relatively stiff" implies that the flexibility of the overall system, which includes large arbitrary-shaped rigid bodies, is higher than that of the individual continuous structural elements in the system. It is further assumed that during the initial phase of the shock excitation the complex system will respond as a linear elastic system until the maximum amount of elastic strain energy has been absorbed. This enables the use of the average internal load spectrum as a means for topologically identifying the locations of most probable initial failure.

By predicting where, and in what manner, failure is most likely to occur, the technique provides a simplified analytical type tool to aid in the crashworthy design of a broad class of shock excited structural configurations with general constraints. An outline of the technique, along with results of preliminary investigations are given. Relationships to the present state of knowledge in the field regarding analytical techniques for crashworthy design are also discussed.

LINEAR LUMPED MASS MODELING TECHNIQUES
FOR BLAST LOADED STRUCTURES

William J. Liss, Jr. and N. J. DeCapua
Bell Telephone Laboratories, Whippany, New Jersey

The determination of building motions in a nuclear blast environment is essential in assessing the shock mounting requirements for communications equipment in hardened installations. As a result of this, relatively simple linear lumped mass modeling techniques are developed that can accurately predict peak blast induced structural accelerations. Verification of the techniques is achieved by comparison to tests on actual full scale TNT blast loaded structures.

There are two basic components of structural response in a blast environment—rigid body soil structure interaction and flexural response of the various components of the structure. Test data indicating the nature and magnitude of the first of these, i.e., rigid body soil structure interaction was documented in TNT tests during Operation Snowball in Canada in 1964. Two $5' \times 5' \times 6'$ solid concrete blocks were buried in the ground and struck with a blast wave produced by a 500 ton TNT detonation. The first block was buried with its top flush with the ground while the second had a steel "sail" protruding 2 feet abovegrade. A simple lumped mass soil-structure model was developed and a modal analysis used to predict the acceleration response of various points on the block. The results indicated that peak predicted accelerations compared very well with measured values.

The technique for modeling a structure with combined rigid body and flexural motions is employed for an underground precast manhole. This structure was tested in a TNT blast environment at Event Dial Pack in Canada in 1970. A lumped mass two dimensional frame model of the structure was developed and a modal analysis was employed to predict the acceleration response of various locations in the structure. Some of the important conclusions and recommendations resulting from the study are as follows.

1. Soil mass need not be added to the mass of the structure in determining equivalent lumped masses.

2. For buried structures, horizontal blast loadings of 1/2 to 1 times the free field loading should be used for conservative predictions.

3. Due to high soil damping, structural elements of buried buildings can be accurately modeled with a one mass equivalent.

4. For aboveground buildings and interior elements of belowground buildings, more than one mass is necessary for accurate element modeling. A three mass model of beams and one way slabs, and a seven mass model of plates and two way slabs is necessary to predict actual peak acceleration responses to within 20% accuracy.

39

SHOCK II

POPPING MOTOR DOME SHOCK DURING FIRST STAGE
SEPARATION OF POSEIDON MISSILE FLIGHTS

Lane R. Pendleton and Ralph L. Henrikson
Lockheed Missiles & Space Company
Sunnyvale, California

Shocks as large as 33 g's peak-to-peak were measured in the reentry bodies during
first stage separation on Poseidon development flights. This shock occurred between 60
and 120 milliseconds after second stage ignition, and exicted the fundamental longitudinal
modes of the missile. The greatest problems resulting from this shock were large loads
on the reentry body support structure and severe shock environments for electronic and
hydraulic packages attached to the aft dome of the second stage motor.

An extensive effort was initiated to determine the cause of this shock in order to
effectuate a design change to eliminate or reduce the shock amplitude to acceptable levels.
The main clues were: one, the acceleration data measured in flight; two, the shock did
not occur during ground test firings of the second stage motor; and three, a large variation
in the amplitude from flight to flight. The amplitude varied from 2 g's to 33 g's for the
first ten Poseidon flights. The projected design load based on 100 flights was unacceptable.

Many theories were offered to explain this shock. Some of these theories were: one,
a piece of propellant passing through the nozzle; two, flow separation in the nozzle; three,
sudden shift in the choke plane; four, slippage in the missile frame joints; and five, popping
motor dome. The latter theory assumes that during the ignition process a seal develops
in the unbonded area between the propellant and the fiberglass aft dome of the second
stage motor. Then the seal suddenly releases during dome expansion, allowing gas to fill
the gap, thus resulting in a sudden redistribution of the chamber pressure forces.

The theories were screened by applying a calculated load for each theory to a math
model of the Poseidon missile and comparing the resulting calculated reentry body re-
sponse with the measured data at that location. The popping dome theory was the only
theory that matched the flight data and satisfied the clues. The theory was considered
sufficiently credible to justify a design change.

The chosen design change was to insert a polypropelene netting between the propel-
lant and the aft dome in order to vent this area and prevent the seal from forming. This
netting was included in the second stage motor for all Poseidon missiles beginning with the
twenty-first flight. Significantly lower shock levels resulted during flight beginning with
the twenty-first missile. Also, the variation from flight to flight was much smaller. The
mean amplitude for flights before the twenty-first was 14 g's compared to 5 g's for 35
flights beginning with the twenty-first. The fact that the shock amplitude was significantly
reduced by the netting indicates that popping dome was the cause of the "mystery shock."

Thus we were successful in reducing the shock. The loads and package environments based on the data measured on flights after the design change are acceptable for the Poseidon missile design.

Popping Dome shock is a potential problem for any missile which uses solid propellant motors. Motor cases are frequently made of fiberglass or similar material which experience large growth during motor ignition and pressurization. Motor dome growths of an inch or more are common. If the propellant is bonded to the dome, large bond stresses and large propellant strain results. One design solution which is used is to not bond the propellant to the dome thus allowing a gap between the dome and propellant when the motor is operating. This design solution can result in a 'popping dome" shock. This paper could make other manufacturers aware of this problem and offer a solution.

IMPACT TESTING WITH A 35-FOOT CENTRIFUGE

John V. Otts
Sandia Corporation, Albuquerque, New Mexico

An impact test technique, whereby the tangential velocity of the 35-foot centrifuge is used to create required impact environments, has been developed, proven and implemented. The accuracy, repeatability, low cost and efficiency offered by this technique make it highly competitive for future impact testing.

The 35-foot radius centrifuge is an outdoor facility. The basic function of this centrifuge is to provide normal acceleration environments up to a maximum of 250 G, which corresponds to 145 RPM at the maximum radius of 35.5 feet. The centrifuge structure can support a maximum test weight of 10,000 pounds and a dynamic test load of 450,000 G-pounds.

A test item or target restrained to the rotating centrifuge arm will experience a tangential velocity:

$$V = 0.1 \, R\omega \text{ ft/sec.}$$

where

R = radius of rotation (ft)
ω = angular velocity (RPM)

When the test item or target is unrestrained, it will "free fly" on a path tangent to the centrifuge orbital path with a velocity equal to that expressed above. Assuming that the test item is mounted on the centrifuge and the impact target is stationary, one has several options for testing:

1. Let the test item "free fly" into the target.

2. Extend test item radius during the last revolution to impact.

3. Insert target into test item orbital path during the last revolution to impact.

Obviously, the target and test item can be interchanged in the above options.

42

The technique reported herein consisted of throwing the test item into a 14,000 pound reaction mass. The test item was allowed to "free fly" to impact beyond the radial extension of the centrifuge arm.

The environment of the test item, restrained to the centrifuge arm traveling at ω RPM, includes a normal acceleration of:

$$G = 3.41 \times 10^{-4} R\omega^2$$

where

R = radius of test item rotation

Upon release from the centrifuge arm, the test item travels tangent to the orbital path at a velocity of 0.1 $R\omega$. During free flight, the test item continues to rotate about its CG at ω RPM, where ω is the rotational velocity of the centrifuge arm at the instant of release.

The fixture which adapts the test item to the centrifuge arm is simple, cheap and easily fabricated. Basic fixture requirements include:

1. Restraint of the test item at a static load of WG, where W is the weight of the test item and G is the normal acceleration prior to release.

2. Avoid interference of fixture with test item after release from the arm.

3. Provide adjustable release angle for the test item in order to compensate for test item rotation during free flight. The desired release angle is a function of impact angle, centrifuge speed and free flight distance to impact.

Briefly, an angle iron is used to cradle the test item and a steel cable restrains it prior to release. The angle iron is mounted to a steel plate which bolts to the centrifuge arm at any desired angle. Both the radius and release angle are adjustable by proper mounting of the steel plate.

Timely release of the test item is essential to accurate control of impact velocity, impact angle and impact location. This has been accomplished by a Holex guillotine cable cutter accurate to less than one millisecond. The cable cutter is activated by a micro-switch located on the non-rotating centrifuge base. The microswitch is closed by a rotating contact plate. The accuracy of the microswitch position allows precise control of all test parameters.

The weight, size, and complexity of the stationary target are unrestricted. However, one must insure that the target is free of the orbital path and that it does not interfere with the rotating arm as a result of the impact.

Impact data from transducers mounted on the test item are transmitted by trailing cables between the test item and centrifuge arm. Signal conditioners and amplifiers are located at the center of the arm and transmit the data to tape recorders via slip rings. One distinct advantage of this test technique is that long lengths of trailing cable are not required since the distance between impact point and the centrifuge arm is normally less than 5 feet. Therefore, cable breakage prior to completion of the impact pulse is not a serious problem.

43

The test capabilities of the "free flight" technique include:

Impact Velocity	10 to 500 ft/sec (± 1%)
Test Weight*	10,000 pounds max.
Max. Arm Load	450,000 G pounds
Target	Optional
Impact Angle	Optional
Free Flight Distance	Optional

ADVANTAGES

1. Accurate and repeatable impact velocity (± 1%).

2. Velocity control in the range of 10 to 500 ft/sec.

3. Accurate and repeatable impact location on target.

4. Accurate and repeatable impact angle with target.

5. Negligible tangential acceleration ($<$ 1.0 g) prior to impact.

6. High confidence in obtaining data as a result of a minimum of trailing wire.

7. Inexpensive cabling due to short trailing wire.

8. Inexpensive fixturing.

9. Fast setup and turnaround time.

10. Minimal test personnel requirements (two people).

11. Sequential or simultaneous firing or multitest item arrays.

DISADVANTAGES

1. Test item undergoes high radial acceleration.

2. Test item undergoes rotation ω during free flight.

3. Coriolis acceleration during free flight and impact.

4. Rebound of test item must be treated with caution.

To date, about 150 impact tests have been conducted using this technique. The accuracy, flexibility, low cost and reliability have proven this technique highly competitive for future impact test series.

---

*One must stay within the 450,000 G pound limitation.

SHOCK SPECTRA, RESIDUAL, INITIAL AND MAXIMAX
AS CRITERIA OF SHOCK SEVERITY

Charles T. Morrow
Advanced Technology Center, Inc.
Dallas, Texas

When a shock test severity is specified by a shock spectrum without further qualification, the spectrum is by definition a maximax spectrum, in other words either initial or residual, *whichever is greater*. The residual spectrum can be shown to be a measure of spectral energy at any frequency, whereas the initial, while useful information for some problems (e.g. rattle space of an isolator) reduces at high frequencies merely to the peak value of the acceleration pulse. Consequently, the loosely stated requirement can sometimes have no more control over spectral energy than a prescription of the peak acceleration of the pulse.

The maximax spectrum is a useful means for description of the severity of a shock to be simulated, and a conservative means of doing so—it will be at least as large as the residual. However, the latter undamped spectrum, or alternately the Fourier spectrum to which it is simply related, is the more fundamental tool for specification of environmental test severity. For this purpose, initial and maximax spectra are preferably regarded as useful supplementary information, along with finite Q spectra and other variations that yield more detail on the response of a simple resonator but may have misleading implications about responses of multiple degree of freedom systems.

One of the recognized advantages of a spectral prescription of shock severity is that it can permit testing on a vibration table without transfer to a drop tower. Because of limited excursion, the usual standard acceleration pulse shapes can not be used. The residual and maximax spectra are definitely defined, but the initial may not be separable from the maximax. One beneficial way of prescribing the spectra is to put a lower limit on the residual, but an upper limit on the maximax to avoid overtest.

Whether one performs a shock test by means of a shaker or a drop tower, there is usually a tacit assumption that any steady acceleration occurring at the same time as the shock to be simulated is negligible or can be ignored. If, alternately, one wishes to simulate the combined effect, it may become possible to modify standard pulse shapes to accomplish this. The environmental specification would appropriately contain a lower limit on the *initial oscillatory* spectrum, and upper limits on the residual and maximax to avoid overtest.

To facilitate the application of the results, all derivations are deferred to appendices. These appendices include treatments of energy spectral density, Fourier and Laplace transforms, the Heaviside expansion theorem, and responses of multiple degree of freedom systems (with definitions of higher order shock spectra), and excerpts from an ICBM airborne equipment specification prepared some seventeen years ago primarily by the author. These excerpts are criticized and evaluated in the main body of the text in the light of recent trends.

A simple relationship has long been recognized between the undamped residual shock spectrum and the Fourier transform or spectrum. By the Heaviside expansion theorem, it is shown that there is a relationship between the damped residual shock spectrum and the Laplace transform.

SCALING OF WATER IMPACT DATA FOR SPACE SHUTTLE SOLID ROCKET BOOSTER

Richard Madden
Bolt Beranek and Newman, Inc.
Cambridge, Massachusetts

and

Dennis A. Kross
NASA—Marshall Space Flight Center
Huntsville, Alabama

The space shuttle vehicle concept was developed to provide an efficient and cost effective means for delivering men and materials to earth orbit and beyond. One of the chief cost-saving features of the design is the fact that the major components may be used for a number of missions. For the components to be reusable, of course, they must be designed to withstand the varicus loading environments without damage. This study is ccn. cerned with the effects of water impact on the solid rocket booster (SRB) which, following its firing, reenters, is decelerated by parachutes and finally lands in water. Preliminary investigations of these water impact loads indicate that they should be a controlling factor in the mechanical design of the booster.

To perform water impact tests on a full-scale vehicle is not feasible due to the costs and time involved in both constructing and testing a full-scale structure. The most feasible approach is to investigate existing theories for water entry and then to perform a rumber of tests on scale-model SRB's and thereby establish appropriate scaling rela:.ionships. The loads on the full-scale vehicle may then he estimated by extrapolating the data from the scale-model tests.

The present paper discusses the comhined analytical and experimental program which was performed to analyze the water impact loading environment and, in particular, to assess the effects of model flexibility on resultant loads. The analytical studies identified the parameters which are the principal contrihutors to the loading of the vehicle and provided techniques for extrapolation from small scale models to full size vehicles. The principal nondimensional parameters in addition to the usual geometric scaling parameters are:

Froude number	V^2/gD
Strouhal numher	$\omega D/V$
Pressure scaling parameter	$P/\rho gD$

where V is impact velocity, g is acceleration due to gravity, D is the geometric scaling parameter, ω is a frequency of vibration, P is the ambient pressure at which the test is

conducted and ρ is the density of water. Froude number scaling is typical of rigid body water impact testing. The Strouhal number scaling considers the effects of flexibility. Note that equality of the pressure scaling parameter requires that small scale tests be conducted in a partial vacuum. The experimental program was conducted to verify the analysis and to point out those parameters which are not amenable to scaling.

Tests were conducted on a 6-inch diameter rigid model and on a 12-inch diameter rigid and flexible models. The tests consisted of dropping the models in a tail first configuration at various impact velocities. The testing was done without pressure scaling. The results of these tests were analyzed to determine axial and pitch acceleration, penetration depth, and slapdown pressure as a function of impact velocity during the various phases of water impact from initial impact to final slapdown.

Some of the principal conclusions of the study are summarized below.

1. Changes in entry angle are much more significant to slapdown pressures and to penetration depth than are changes in velocity.

2. Pitch acceleration is virtually independent of impact velocity for the rigid models and has highest values near the nose cone.

3. Flexibility effects are not evident in the results for axial acceleration and penetration depths. Although there were wide scatter bands, more flexible models appear to experience significantly less pitch acceleration during slapdown and rebound.

FRAGMENT VELOCITIES FROM EXPLODING LIQUID PROPELLANT TANKS

R. L. Bessey and P. A. Cox
Southwest Research Institute
San Antonio, Texas

Hazards produced by exploding liquid propellant tanks include those associated with the blast waves, those associated with thermal effects, and those associated with the missiles produced by fragmentation of the tank. In a recent study, the authors have had the opportunity to investigate some of the phenomena associated with fragmentation. Specifically, the proposed paper will present the results of our efforts to measure fragment velocities from tests of exploding propellant tanks and to develop a method for predicting maximum fragment velocities from such explosions. These efforts were part of a larger program which included a substantial amount of data gathering related to the fragmentation hazards of bursting liquid propellant tanks, an investigation of blast yield, a somewhat extensive statistical analysis of missile maps, and the fragment velocity data discussed in this paper.

Fragment velocities were measured from films taken during Project PYRO tests of liquid propellant tank explosions. These tests were well documented so that fragment velocities obtained from film data could be correlated with other test conditions. This permitted us to make comparisons between measured fragment velocities and those predicted from the mathematical model.

The mathematical model was developed to predict the maximum fragment velocities attained in the explosion of a liquid fuel rocket. The problem is idealized by considering a spherical volume of fuel and oxidizer of radius, R, mixed in the stoichiometric ratio, which is entirely converted to a "hot gas" volume of the same radius at the instant of explosion. The "hot gas" of the explosion by-products is characterized by κ, M_0, V_0, P_{00}, at time $\tau = 0$, where κ is the ratio of specific heats, M_0 is its mass, V_0 the occupied volume, and P_{00} initial pressure. The fragmenting container is characterized by n, M_t, U_f, where n is the number of fragments, M_t is its total mass, and U_f is the velocity of a fragment.

The fragment velocity is obtained by an extension of the techniques described by D. E. Taylor and C. F. Price (1), and G. L. Grodzonski and F. A. Kukanov (2) in their papers on bursting gas reservoirs. The explosion products forming the "hot gas" are assumed to behave like an adiabatic ideal gas reservoir. As the container wall fragments with radial symmetry, gas is lost to the external sphere region through cracks

$$\frac{dc(\tau)}{d\tau} = -k\rho_* a_* \Pi W \tag{1}$$

where the derivative is the rate of change in mass of the confined explosion products, ρ_* and a_* are the critical gas density and velocity as gas escapes through the cracks, Π is the crack perimeter or length, W is the crack width, and k is a discharge coefficient. From this equation, the equation of motion for a fragment, the state equations for the gas, and one-dimensional flow equations, the following differential equations in normalized coordinates were obtained for fragment motion

$$g'' = nP_* \left[1 - \frac{g'^2}{(P_*)^{\frac{\kappa - 1}{\kappa}}} \right]^{\kappa/(\kappa - 1)}$$

$$g^3 \frac{P'_*}{P_*} = [-\alpha g^2 + \alpha\beta] P_*^{(\kappa - 1)/2\kappa} - 3kg^2 g' \tag{2}$$

where g is a normalized fragment displacement, P_* is the normalized pressure of the confined gas, α and β are coefficients depending on initial constants, and the primes denote derivations with respect to normalized time.

Equations (2) were solved numerically, using the Runge-Kutta method, for the initial conditions in which fragment velocity was zero, fragment displacement was R, and the confined gas pressure was P_{00}. The maximum fragment velocity was obtained as the fragment acceleration went to zero (i.e., drag effects were not considered).

It was found that maximum fragment velocity was not affected by n except for very low n. Plots of maximum fragment velocity as a function of κ and mass ratio M_0/M_t were obtained. Our model predicted results which compared favorably with those of Taylor and Price for the examples cited in their paper. Our model predicted maximum fragment velocities which compared favorably with data from a NOLTR study of bursting high pressure tanks (3). With reasonable assumptions made about conditions occurring during Project PYRO tests of liquid rocket explosions, our model predicts initial fragment velocities comparable to those measurable in the high speed films of some of these events.

48

REFERENCES

1. D. B. Taylor and C. F. Price, "Velocities of Fragment From Bursting Gas Reservoirs," *ASME Transactions, Journal of Engineering for Industry*, Nov. 1971.

2. G. L. Grodzovski and F. A. Kukanov, "Motion of Fragments of a Vessel Bursting in a Vacuum," *Soviet Engineering Journal*, Mar./Apr. 1965.

3. J. F. Pittman, "Blast and Fragment Hazards From Bursting High Pressure Tanks," NOLTR 72-102, May 1972.

ANALYSIS OF OPEN CELL POLYURETHANE FOAM
UNDER IMPACT LOADING

Valentin Sepcenko
Boeing Aerospace Company
Seattle, Washington

This article presents the theory and the analytical technique used to represent the dynamic behavior of polyurethane foam blocks and shaped ethylenepropylenedienemonomer elastomeric springs that are incorporated in a new Minuteman missile suspension system.

Two kinds of tests are needed to define the parameters used in the analytical models for these elements. Static compression loading-unloading tests are used to determine the upper limit of strain amplitudes. Dynamic compression tests conducted with an initial impact velocity of a few hundred ips are needed to determine the model parameters associated with strain rates. The range of strains and strain rates for which the analytical models are valid is governed by the range of these items achieved in the tests.

The response of an open cell prismatic foam block when compressed to large strains, up to 70% in these tests, is two fold. A part of the response can be described in terms of nonlinear visco-elasticity, independent of the size of the block. The stress σ at any time t can be written in the form of a convolution integral

$$\sigma(t) = \int_0^t E(\epsilon, t - \tau) \frac{\partial \epsilon}{\partial \tau} d\tau \qquad (1)$$

where $E(\epsilon, t)$ is both strain and time dependent relaxation function defined for foam in compression.

Another part of response is associated with the air flow in and out of the block during loading and unloading. This part of response depends upon the size and shape of the block, and is approximated in the model by an pneumatic element consisting of a chamber with an air-tight piston, a strain dependent variable area orifice, and a semi-analytical air friction function determined from available pressure gradient tests.

The resulting equation for the pneumatic element derived for adiabatic conditions is

$$\sigma(t) = \alpha\gamma p(0) \left\{ \left[\frac{\gamma - \Delta V/V}{\gamma - \epsilon} \right]^n - 1 \right\} \tag{2}$$

with

$$\frac{\Delta V}{V} = B \int_0^t (\gamma - \epsilon)^3 \left[\frac{\sigma(t)}{1 - \gamma + \epsilon} \right]^{-1/2} dt \tag{3}$$

where
  γ = initial porosity of the foam block
  $p(0)$ = atmospheric pressure
  α and B are constant determined from dynamic tests
  n = 1.38 for adiabatic case

Although the system of equations (2) and (3) may appear cumbersome, the developed algorithm for numerical solution is simple. It is assumed that visco-elastic effects and air flow effects are independent and may be superimposed.

The test program indicated a simplification of Eq. (1) is possible. Tests strongly hinted that nonlinear visco-elastic effects are essentially independent from strain rates. Thus, all nonlinearities can be found from static type tests. Dynamic effects are linear and may be superimposed over the static. Accordingly Eq. (1) takes the form:

$$\sigma(t) = \sigma_s(\epsilon) + \int_0^t G(t - \tau) \frac{\partial \epsilon}{\partial \tau} d\tau \tag{4}$$

$\sigma_s(\epsilon)$ is a double-valued function of strain with separate loading and unloading branches. For a particular strain amplitude it coincides with static test data for this amplitude. While the loading branch depends only upon the instant value of strain, the unloading branch depends on the maximum value of strain reached before the unloading begins. An algorithm was developed which utilizes static test stress-strain curve obtained for maximum test amplitude from which it derives unloading branch for any intermediate amplitude.

The linear visco-elastic dynamic effects given by the convolution integral in Eq. (4) can be approximately by a number of discrete Maxwell elements each associated with a rigidity modulus G_i and relaxation time τ_i. From the analysis of continuous relaxation spectra of various elastomers and from considerations arising from the substitution of long time relaxation effects by $\sigma_s(\epsilon)$, the shape of discrete spectrum G_i verus τ_i can be obtained, which reduces the number of independent parameters for the series of Maxwell elements. Two visco-elastic parameters were found to be sufficient for matching of test data of all investigated foams.

Visco-elastic model, Eq. (4), was also successfully used to calculate response of shaped elastomeric springs.

MEASUREMENT OF PEAK PRESSURES PRODUCED AT THE GROUND
SURFACE BY SHALLOW BURIED EXPLOSIVE CHARGES

Bruce L. Morris
U.S. Army Mobility Equipment Research and Development Center
Fort Belvoir, Virginia

An experimental program was conducted to measure the peak pressures produced at the ground surface by the detonation of shallow buried explosive charges. Pressures were measured in both C-7 epoxy and soda-lime glass targets, and predictions of peak stresses in both steel and aluminum targets were made. Experimental results were compared with hydrodynamic computer code calculations.

The explosive charges were cast 50/50 Pentolite weighing 1.5 pounds. Both spherical and cylindrical (with a height to diameter ratio of 1:3) geometries were used. Burial depths to the top of the charge were .85, 2.55, and 5.10 inches, corresponding to depths of 2, 6, and 12 inches for a 20-pound prototype charge. All charges were centrally initiated. The soil was in a nominally "dry" condition.

Pressures were measured using manganin wire gages embedded in both C-7 epoxy (initial density of 1.18 gr/cm^3 and sonic speed of .265 $cm/\mu sec$) and soda-lime glass (initial density of 2.52 gr/cm^3 and sonic speed of approximately .58 $cm/\mu sec$) matrix materials (1). The manganin wire measures the pressure in the surrounding matrix material, and the use of two materials with widely separated acoustic impedances (.3127 gr/cm^2-μsec and 1.4616 gr/cm^2-μsec for C-7 and soda-lime glass respectively) permits estimation of peak pressures in different target materials.

For each burial depth tested, the peak pressures ranked, qualitatively, as follows:

1. Glass gage—cylindrical charge
2. C-7 gage—cylindrical charge
3. Glass gage—spherical charge
4. C-7 gage—spherical charge.

It was expected, from impedance matching considerations, that the pressures in the glass gages would be higher than those of the C-7 epoxy. The increase in pressure from the cylindrical over the spherical charge is also expected (the scaled distance, defined as distance from the center of the charge in feet divided by the cube root of the charge weight in pounds, is less for the cylinder than for the sphere for a given burial depth to top of charge) and has been experimentally observed elsewhere in similar type tests (2). Pressures measured here ranged from 72.5 Kbar for the glass gage—cylinder charge at a burial depth of .85 inches to a low of 6.5 Kbar for the C-7 gage—spherical charge at a burial depth of 5.10 inches.

The impedance match concept was used to estimate the peak stresses that steel or aluminum targets would be subjected to. For a given charge configuration and burial depth, the equation expressing shock transmission from medium 1 to medium 2, i.e.,

$$P_{Trans} = \frac{2Z_2}{Z_1 + Z_2} P_{Incident} ,$$

was used to generate two simultaneous equations from the data for the C-7 and glass gages. In each of these equations, P_{Trans} is the measured pressure, Z_2 is the acoustic impedance of the gage, Z_1 is the "effective" impedance of the soil (unknown) which is a function of the charge configuration and burial depth, and $P_{Incident}$ is the pressure in the soil (unknown) at the soil/gage interface. These unknowns were determined, then the impedances of steel or aluminum were substituted for the gage properties and P_{Trans}, now the stress to be transmitted to the new target, was calculated. This process gives estimates of from 77.1 Kbar for a steel target and a cylindrical charge with .85 inches burial to 7.2 Kbar for an aluminum target and a spherical charge with 5.10 inches burial.

The TOODY-3 hydrodynamic computer code was used to simulate the test conditions with a simple elastic-plastic-hydrodynamic equation of state to model the soil. Agreement between the calculated and experimental values was good, especially for the smaller burial depths where inaccuracies in the soil modeling, due to compressibility, locking, hysteresis, etc., are less pronounced.

REFERENCES

1. Keough, D. D., Procedure for Fabrication and Operation of Manganin Shock Pressure Gages, Stanford Research Institute, AFWL-TR-68-57, August 1968.

2. Wenzel, A. B. and Esparza, E. D., Measurement of Pressures and Impulses at Close Distances from Explosive Charges Buried and in Air, AD 903534L, 21 August 1972.

ENVIRONMENTS AND THEIR SIMULATION*

NON-LINEAR SHOCK ISOLATION OF RE-ENTRY VEHICLE COMPONENTS TO HIGH SHOCK GROUND TEST SIMULATING HOSTILE FLIGHT ENVIRONMENTS

C. G. Parks, Jr.
General Electric Reentry Systems Division
Philadelphia, Pa.

The primary concern of this type ground test is to evaluate the performance of components in a nuclear environment. Accompanying this environment is a high energy ground shock which must be accounted for. The shock environment can affect the performance of the component, therefore the isolation of components to this environment is of equal importance to assure safe levels.

The particular program which gave rise to the design of a non-linear shock isolation was due to severe displacement limitations imposed on the components/support fixtures-referred to hereinafter as the cassette. The input shock has a duration of 15 milliseconds, peaking at 136 g's in the critical region. This level had to be reduced to 100 g's simultaneously limiting displacements to a maximum of 1 inch. A preliminary analysis was undertaken using a linear isolation system. Results of this study limited acceleration to 100 g's, but yielded displacements on the order of 3 inches. In light of this fact a non-linear energy absorbing system was dictated.

The system analyzed is basically a mass supported by two sets of springs in the horizontal direction and a single set of springs in the vertical direction with center of gravity removed from the mass. The springs are mathematical simulations of an aerospace grade aluminum honeycomb 1/4-5052-. - .004. The springs are referred to in sets because of the fact that the honeycomb is only able to absorb compressive forces, therefore to account for plus and minus displacements a single spring was used in each direction. The force deflection curve for this material is characterized by a linear increase overshooting the crush strength followed by a decaying oscillation about the crust strength with increasing deflection. The region of maximum over and undershoot (approximately one cycle in duration) was eliminated by pre-crushing the material by 2 inches before installation. The effect on the force deflection curve was to give a linear rise in force until it reached the crush strength then flat response for increasing deflection. A compression test was performed to verify, and the results were in total agreement.

It was then determined that this approach would yield results within specification and the subsequent test was successful.

---

*Secret papers -- Unclassified Titles and Summaries.

A VIBRO-SHOCK TEST SYSTEM
FOR TESTING LARGE EQUIPMENT ITEMS

J. Carden
General Electric, Syracuse, New York

T. K. DeClue
Wyle Laboratories, Huntsville, Alabama

and

P. A. Koen
Bell Laboratories, Whippany, New Jersey

The test facility discussed herein was built to test large (both in size and weight) SAFE-GUARD Perimeter Acquisition Radar (PAR) equipment items to the shock and vibration induced by a nuclear weapon while equipment is exercised electrically. The PAR building is above ground and as a result, the radar equipment is subjected to shock and vibration environments induced by both the air blast and ground motion effects produced by a nuclear event. These tests represent a portion of the hardness verification program being employed to insure that the radar equipment contained in the PAR building will maintain its operational integrity both during and after experiencing the dynamic environment.

The shock and vibration test which the equipment was subjected to was a "synthesized waveform" type of test. In particular, the desired synthesized waveform consisted of a linear combination of damped sinusoids, i.e.,

$$a(t) = \sum_{i=1}^{n} A_i e^{-0.05t} \sin (w_i t + \phi_i)$$

where:

- $a(t)$ = Acceleration on the test table
- w_i = Frequency of each damped sinusoid
- A_i = Amplitude of each damped sinusoid
- ϕ_i = Arbitrary phase angle of each damped sinusoid

This particular type of synthesized waveform was chosen since it was both achievable in the laboratory and yielded an accurate simulation of the motion of the interior floors of the PAR. To insure that this particular type of waveform was developed by the vibration test system, a set of predistorted inputs were used. The particular characteristics of the predistorted inputs were selected from single damped sinusoid calibration tests and synthesized waveform response spectra at various values of analysis damping (0%, 1%, 3%, 10%).

Proper use of the predistorted inputs provided a technique for controlling and shaping the vibration test table waveform characteristics at the frequency of the actuator oil column resonance and above. The success of controlling and shaping the test waveform frequency characteristics will be discussed in the paper in terms of damped and undamped response spectra evaluated from 2 to 1,000 Hz. In addition, the response spectra of the cross-axes excitations for each of the three test directions (i.e., vertical, longitudinal and lateral) will also be reviewed.

54

The test system consists of a test table restraint system which provides single degree of freedom motion in each of the three orthogonal test axes (i.e., longitudinal, lateral and vertical) while providing restraint in all other directions (i.e., pitch, yaw and roll as well as the two axes which are orthogonal to the prime test axis).

The test table geometry (i.e., overall dimensions) was optimized in order to minimize its weight and insure that the first natural frequency of the system was above 100 Hertz. The test system was driven by two electrohydraulic exciters where each exciter requires a peak flow of 525 gpm, and a peak pressure of 3,000 psi. (The flow requirements were met by supplementing an existing 480 gpm, 3.000 psi hydraulic power supply with precharged accumulator banks.)

Due to various design constraints, such as thermal loading, high natural frequency in six degrees of freedom, large overturning moments, large specimen weight, and out-of-phase displacements (which were always less than .125 in. during the tests) it was necessary to make numerous design tradeoffs. The final design used only a 25% safety margin on the expected loadings on the bearings and actuator. Extensive strain gage monitoring was used during initial setup to insure that the 25% safety margin was not ever encroached upon in practice.

The paper will provide detailed information as to the control and analysis system, the hydraulic system, the test fixture and restraint system, test methodology, the synthesized waveform test technique employed, the test results achieved and test anomalies.

SHOCK AND VIBRATION HARDNESS VERIFICATION OF A RACK-MOUNTED, TRANSIENT CRITICAL SAFEGUARD SYSTEM MEMORY UNIT

J. Frederick Stevenson
Bell Laboratories
Whippany, New Jersey

and

J. L. Parker, Jr.
Bell Laboratories
Greensboro, North Carolina

The SAFEGUARD System data processor makes use of an EMI (Electronic Memories Incorporated) memory unit. This unit consists largely of printed circuit cards that are fully enclosed in a metal container which is mounted in standard digital and analog racks. The unit is transient critical in that it must not only survive the weapon effects-induced building shock and vibration environments prescribed for the SAFEGUARD System, but also must not experience transient malfunctions during the excitations implied by such environments.

This paper reports on an analytical-experimental program that was undertaken to verify the shock and vibration hardness of the EMI memory for use in standard SAFE-GUARD System digital racks. In order to estimate the in-rack excitations experienced by the memory unit, dynamic response analyses of a planar model of the digital rack were performed using the MacNeal Schwendler Corporation's Version 3.0 of NASTRAN. The

finite element model of the rack consists of ninety (90) bar elements, thirty eight (38) quadrilateral plane stress elements and ten (10) triangular plane stress elements. This model gives rise to 247 independent degrees of freedom and this number was not reduced for the eigenvalue analyses that preceded the response analyses. Motion time-histories of the model were computed using as input a motion time-history representative of the floor motions previously predicted for the PAR (Perimeter Acquisition Radar) building. Up to fifteen modes (i.e., all modes having frequency less than or equal to 500 Hz) were carried in some of these response computations. From a subset of the model motion time-histories response spectra corresponding to the digital rack-EMI memory interface were computed and criteria spectra $S_R(\omega)$ were established for use in the test portion of the verification program.

The shock and vibration hardness of the EMI memory was subsequently verified by showing that an electrically monitored memory unit would not experience malfunctions when subjected to transient excitations that simulate the analytically predicted in-rack environments. The simulation was carried out on an electrodynamic shaker having the capability of imparting to the test specimen an acceleration time-history composed of ten (10) damped sine wave components. This waveform was porportioned to simulate the analytically predicted in-rack environments in two senses:

(1) $\tau_T \stackrel{\sim}{=} \tau_R$

    where τ_T is the duration of the test exictation

        τ_R is the duration of the predicted response at the digital rack-EMI memory interface

(2) $S_T(\omega) \geqslant S_R(\omega)$ $15\,\mathrm{Hz} \leqslant \omega \leqslant 500\,\mathrm{Hz}$

    where $S_T(\omega)$ denotes the response spectra of the test excitation

        $S_R(\omega)$ denotes the criteria spectra corresponding to the digital rack-EMI interface

Waveforms satisfying these criteria were independently applied to three axes of the test specimen corresponding to side-to-side, front-to-back and vertical motions of a rack-mounted unit.

To detect the occurrence of an electrical malfunction, the test specimen was monitored with a specially designed mobile test set capable of storing and retrieving information to and from the memory during the test excitation. In the absence of malfunctions under test conditions, the memory unit was certified hard to the prescribed environments.

56

MEASUREMENT AND CORRELATION OF NUCLEAR
X-RAY INDUCED SHOCK ENVIRONMENT

K. C. Kalbfleisch and T. R. Szabo
McDonnell Douglass Corp., Huntington Beach, Calif.

An anti-ballistic missile system is required to perform during and after exposure to a nuclear burst environment. One aspect of the nuclear environment considered was the x-ray energy imparted to the missile when it is out of the atmosphere. This x-ray energy causes instantaneous heating of the surface material resulting in very rapid spallation and vaporization of the outside layer. The very rapid material blow-off results in an impulse load imparted to the exposed missile surface. In response to this impulse load, a high intensity high frequency shock environment is transmitted throughout the missile.

This paper reviews the nuclear underground test that was performed on the missile with emphasis on describing the shock environments. The objective is to describe the shock data acquisition system, specimen and resulting data. Correlation of the nuclear shock data with data from contact explosive tests and predictions is presented. Specimen structural characteristics and the impulse forcing function are defined to enable the reader to scale the presented data for other applications.

In a recent underground nuclear test, three missile specimens were subjected to an x-ray environment. Each specimen had a different position in the test tunnel so that they were subjected to different impulse levels. The achieved impulse ranged from 1400-2400 taps at the low impulse position to 4900-11000 taps at the high impulse position. At each position the noted impulse variation results from the different surface materials used on various missile sections.

The shock instrumentation system used in this test was developed utilizing the experienced gained from the system performance on a previous underground test. The data acquisition system used previously is summarized to define the problems encountered and the changes incorporated for this test. Electrical shielding and accelerometer mounting is discussed.

Thirty-eight accelerometers were mounted in the three specimens. Twenty-seven of these were installed in the low impulse specimen, and 6 in the intermediate impulse specimen, with the remaining 5 in the high impulse specimen. Of these, 6 accelerometers were control units, being nonresponsive to mechanical shock so as to define the induced electrical transients. The accelerometers were located at subsystem mounting points to define the input shock environment and in free skin locations. These free skin positions were selected to minimize the influence of dynamic interaction from the subsystems in order to provide fundamental data on shock response to a nuclear impulse load.

Valid shock data were recovered from 19 of the 32 active accelerometers. The primary cause of data loss was mechanical failure of the accelerometers due to overstressing by the shock environment. All accelerometers that failed were located along the onside ray, indicating that the initial impulse exceeded their capability. Accelerometer failures and the other data acquisition problems encountered are discussed.

Data reduction consisted of removing the superimposed electrical noise from the acceleration history and calculating shock response spectra. Signals from the control

accelerometers defined the electrical transient characteristics so they could be distinguished from the acceleration component. Shock response spectra were digitally computed using a MDAC program. Data were digitized at an effective sampling rate of 200,000 samples per second.

Shock data are compared with analytical predictions and generally show favorable results. The best correlation is from the free skin data where the influences of subsystem dynamic response are minimized. Results from two prediction methods are compared (1) response computed using a finite element shell model of the specimen and (2) response using a Green's Function technique.

Shock data are also normalized and compared with data from other tests; a previous underground nuclear test and a series of contact explosive tests. The data from these various tests were normalized to a unit surface weight of the structure in the region of the measurement and a unit impulse to remove test differences. These comparisons generally show good agreements. This indicates that once the shock environment from an x-ray source is known, contact explosive testing is an acceptable alternative to underground testing.

The paper concludes with observations and recommendations for measuring the shock environment during an underground nuclear test. This test series has demonstrated that it is feasible to instrument and measure the shock environments. Proper choice of accelerometers, their shielding and location must be considered. Measurement of the on-side shock is beyond current accelerometer capability without some type of isolation to mitigate the very high frequency ($>50,000$ Hz) loads on the accelerometer.

FLIGHT QUALIFICATION OF SPECIAL INSTRUMENTATION

Jerome Pearson and Roger E. Thaller,
Air Force Flight Dynamics Laboratory
Wright-Patterson AFB, Ohio

A common procedure in qualifying a new payload for the expected aircraft flight vibration environment is to analyze the design to predict the structural vibration modes and frequencies, to vibrate the completed prototype with shakers to define the actual modes, and finally to fly the payload on the aircraft to measure flight vibration levels. The flight vibration test is thus the crucial proof of the project. The results of the flight vibration test may also point out deficiencies in the design or analysis and show unexpected dynamic effects. This paper describes the results of such a flight vibration test, compares them with the analytical prediction and the ground vibration tests, assesses the accuracy of the analysis, and recommends improvements for future programs.

The program involved the analysis, vibration testing, and flight testing of special instrumentation to be flown aboard a C-135 aircraft. The analysis and vibration testing were performed under Air Force contract, and the flight test vibration measurements were performed by the Air Force Flight Dynamics Laboratory. The analysis consisted of a finite-element representation of the complete structural system of the special instrumentation, mount and floor. The first twenty elastic modes of the system were obtained and were used to predict the overall system response at the mounting points to the expected

random vibration environment. These analytical results showed a high vibration amplif:-
cation factor which would degrade the performance of the special instrumentation if the
aircraft flight vibration were as severe as previous measurements indicated. The ground
vibration test revealed resonances somewhat lower in frequency than the predicted values.
Because of these differences in frequency, and because of the difficulty in predicting the
flight vibration environment of the aircraft, which was extensively modified, a flight vibra-
tion test was conducted to encompass measurements over the entire flight regime.

The flight vibration test showed several low-frequency resonances which differed in
frequency from both the finite-element analysis and the ground vibration test. These res-
onances would have caused difficulties but for the fact that the observed excitation of
the floor during flight was lower than expected. The results of the flight test are pre-
sented as a set of envelopes of acceleration spectral density versus frequency for vibration
test qualification of the special instrumentation. These curves are relatively low, allowing
the special instrumentation to operate satisfactorily even though its low-frequency ampli-
fication factors are higher than expected. The lower-than-expected floor vibrations are
attributed in part to the mass effect of the added weight of the special instrumentation
and mount on the aircraft. The effect of this mass on the analysis is examined and sug-
gestions are made for improving future analyses for airborne systems.

OPERATION MIXED COMPANY

Lt Col J. Choromokos
Air Force Systems Command, Andrews AFB, Md.

and

Mr. J. R. Kelso
Defense Nuclear Agency, Washington, D.C.

Since the Limited Nuclear Test Ban Treaty of 1963, which prohibited atmospheric
detonations of nuclear devices, simulation techniques have been used to obtain needed in-
formation concerning the blast and shock effects on military weapon systems and to fur-
ther understand the phenomena associated with such explosions. Shock tubes, as well as
a variety of blast load generators, have been used as small scale simulation devices.

Simultaneously, the U.S., under the sponsorship of the Defense Nuclear Agency
(DNA), formerly the Defense Atomic Support Agency, has participated in Canada in a
series of high explosive test programs beginning with a 5-ton TNT shot in 1959, followed
by 20-, 100-, and 500-ton TNT tests in 1960, 19 and 1964. In 1965, three 500-ton
TNT charges were detonated on the island of Kahoolawe, Hawaii, and two additional 500-
ton TNT tests were conducted in Canada in 1968 and 1970. All of these tests were de-
signed to obtain data on basic blast and shock phenomena as well as to obtain target
response information on military weapon systems, equipments and structures.

In this continuing program of non-nuclear field testing in the atmosphere, another
large-scale high explosive experiment called Operation MIXED COMPANY (MC) has been
completed under the sponsorship of DNA. The primary objective for MC was to provide
a simulated 1.8 KT airblast environment for target response experiments for the military

59

services and defense agencies; to obtain cratering and ground shock information in a layered media (partially cemented silty sand over sandstone) not previously tested, and to confirm empirical predictions and theoretical calculations for cratering, ground shock and response of military structures, equipment, and weapon systems. A 500-ton spherical TNT charge, resting on the surface, was chosen to meet these objectives.

The main event (1,000,000 pounds) consisted of 30,600 blocks of TNT with a diameter of 27 feet. Forty U.S. projects, with two from the United Kingdom and four from Canada, were divided into four programs. The airblast program involved the measurement of various airblast parameters as well as the structural response of aboveground structures and military equipment. Military equipment exposed to the airblast wave included such items as model nose cones, full scale aircraft shelters and doors, helicopters inside revetments, tactical antennas and electronic shelters and various U.S. Army weapons. The ground motion program consisted of detailed measurements of the crater, ground shock, ejecta, and the response of underground structures. Airblast induced and direct ground shock measures were taken in two separate gage lines and some of the targets tested were model silos, underground electronic systems and personnel shelters. In the biomedical program, anthropomorphic dummies were placed in open personnel shelters and two man fighting bunkers at different pressure levels. Lastly, in the photographic program, high speed cameras recording at rates up to 25,000 frames per second were located at three camera stations to record the early shock wave formation and fireball growth. The 1,000,000 pounds spherical charge of TNT was successfully detonated on 13 Nov. 1972.

This paper will consist of showing the official DNA documentary film which reviews briefly the participating projects, the detonation, high speed photography and some of the results of the individual projects. Since the film is unclassified, a short briefing will be given on some of the classified projects that participated in MC. The entire presentation will be classified secret and will last 45 minutes.

ISOLATION AND DAMPING

DESIGN OF CONSTRAINED LAYER DAMPING FOR BROAD TEMPERATURE CAPABILITY

David I. G. Jones
Air Force Materials Laboratory
Wright-Patterson. AFB, Ohio

A significant fraction of the noise and vibration problems occurring day by day in aerospace and non-aerospace transportation systems and industrial plants is due to clearly identifiable resonances of parts of the structure, which in turn radiate noise. In many cases, significant contributions can be made toward solution of the overall problem by using properly optimized damping treatments. One such application, described in another paper being offered for the 44th Shock and Vibration Symposium (1) involved the use of a multiple constrained layer damping treatment to reduce interior cabin noise levels in a large helicopter.

Many prior investigations have demonstrated the merits of constrained layer, or shear, damping treatments for resonant vibration control, and have considered the effects of wavelengths, frequency, structure geometry for simple cases, and even temperature and the use of more than one damping material. However, points at which most prior analysis agree include the difficulty with which the work can be applied to more practical structures with any degree of accuracy and the difficulty of applying the complicated mathematics for any kind of simple design procedure.

However, if one confines attention to multiple layer constained damping treatments, many of these difficulties are minimized because the treatment can be represented by an equivalent homogeneous, free-layer, treatment with complex Young's modulus depending on semi-wavelength, modal aspect ratio, and several other parameters. Such treatments can be then applied, one upon the other with different damping materials in each, to extend the temperature range over which important amounts of damping might be achieved.

In this paper, therefore, use will be made of prior work (2) defining the effect of relevant parameters such as damping material complex moduli, treatment dimensions, semi-wavelength etc., on the equivalent complex treatment moduli in order to predict the effect of multiple built-up treatments using several damping materials on response and modal damping of structures. Use will be made of simple Euler-Bernoulli beam and plate theory, including the effects of free-layer damping treatments, and results will be compared with experimental measurements.

REFERENCES

1. J. P. Henderson and A. D. Nashif, "Reduction of interior cabin noise levels in a helicopter through additive damping" submitted for 44th Shock and Vibration Symposium, 1973.

2.   D. I. G. Jones, A. D. Nashif and M. L. Parin, "Parametric study of multiple layer damping treatments on beams," Journal of Sound and Vibration, 29, 3, 1973.

REDUCTION OF INTERIOR CABIN NOISE LEVELS IN A
HELICOPTER THROUGH ADDITIVE DAMPING

John P. Henderson
Air Force Materials Laboratory
Wright-Patterson AFB, Ohio

and

Ahid D. Nashif*
University of Dayton, Research Institute
Dayton, Ohio

In any large helicopter, a significant fraction of the high noise level inside the cabin is due to clearly identifiable resonances of the hull structure, the supporting frames, the transmission oil-pan cover and housing and so forth. This particular investigation is concerned with an effort to (a) delineate the role of these resonant sources of secondary sound radiation in a USAF MAC HH-53 helicopter as regards internal cabin noise level (b) determine the possible reduction in cabin noise level which might be achieved by use of optimized damping treatments by reducing important resonances contributing to the noise, and (c) demonstrate the feasibility of using such damping treatments in a number of helicopter applications where cabin noise reductions are really needed. The investigation was conducted as part of a joint effort between Air Force Materials Laboratory, the University of Dayton, the Air Force Flight Dynamics Laboratory, the HH-53 SPO and USAF Military Airlift Command (MAC) at Hill AFB, Ogden, Utah, and the University of Dayton. Only Air Force Materials Laboratory and University of Dayton efforts will be reported in detail in this report.

The approach adopted was (1) to use artificial excitation tests with a small shaker to determine structural response and modal behavior on the ground, (2) to remove a small section of the acoustic blankets between two frame stations, under the transmission, and apply an appropriate constrained layer damping treatment to every skin panel, (3) conduct further artificial excitation tests on the damped structure to determine the increase in modal damping, (4) conduct several in-flight vibration and acoustic tests under various conditions to measure internal noise levels and panel response behavior, at several locations, for the acoustically untreated helicopter, the acoustically treated helicopter and a partially damped/partially acoustically treated helicopter and (5) conduct narrow band analysis to determine effects of various parameter changes on the noise and vibration spectra.

As a result of the tests, it was found that overall cabin noise levels were reduced by as much as 5-11 db and acceleration levels by as much as 15 db. Changes in the treatment needed to ensure greater useful temperature ranges are described briefly, along with relevant discussions of analytical investigations of structural response behavior, investigations of damping material behavior, the role of tuned damping devices and recommendations for future efforts.

*Currently at Structural Dynamics Research Corporation, Cincinnati, Ohio.

CONTROLLING VIBRATION OF VIKING LANDER
ELECTRONIC PACKAGES

William H. McCandliss
Martin-Marietta Corporation
Denver, Colorado

and

Clyde V. Stahle
General Electric Company
Valley Forge, Pennsylvania

In order to assure reliable operation of Viking Lander Electronic equipment after exposure to the rigors of the launch vibration environment, it is necessary to control the vibration levels experienced by the electronic parts. This requires packaging designs that provide both stiffness and damping to limit deflections and accelerations of the components within the package to acceptable levels. Although the stiffness of the package is amenable to analysis and can readily be varied, damping is difficult to predict and incorporate into the design. Because the results of early development tests indicated high resonant magnifications within the packages, an extensive experimental program was undertaken to develop effective methods of incorporating damping in the designs.

Initial tests of the DAPU indicated that GE-SMRD 100 viscoelastic epoxy damping material could be used to limit the resonant response of printed circuit boards within a package. The DAPU consists of a series of metal picture frame "slices" each containing two large PC boards bolted together through the four corners and at intermediate points along the edges. Tests were performed with various PC board damping treatments including conformal coating on one set of boards and SMRD 100F90 damping strips between an adjacent set of boards. The transmissibility was measured for the center of the two boards. The test of the damping materials was not controlled in that box resonances, etc., create high frequency vibration. However, the fundamental board resonance between 200 and 300 Hertz was evident. The amplification at the fundamental resonance was reduced from 60 for the conformally coated boards to 2 for the SMRD damped boards. At higher frequencies, resonances of the box structure make the damping somewhat less effective, but the damping still limits the amplification to approximately 8 as compared to 25 for the higher modes of the conformally coated board. These results demonstrated that the epoxy material could be used effectively and sparked additional experimental evaluations of other configurations.

One dimensional single board tests were used to evaluate various candidate materials and optimize a damping strip configuration. A 2 inch by 6-1/2 inch board was supported at its corners and a single damping strip applied along the center. Epoxy glass of varying thickness was used as a constraining layer. The maximum resonant amplification measured at the center was obtained for a number of damping treatments. The amplification was reduced to approximately 3 with the epoxy materials. The epoxy materials were found to provide both stiffness and damping to the board. The results were used to determine the optimum thickness of the damping layer and the constraining layer and included variations in the PC board thickness and the mass loading of the board.

One dimensional double board tests were used to evaluate various materials, partial lengths, and various methods of connection. The best results were obtained for a full

63

length bonded strip which provided an order of magnitude reduction in resonant magnification in addition to a significant stiffening.

Tests of the damping strip configurations at various temperatures showed that the damping treatments were tailored to the launch environment. Different materials provide high damping over varying temperature ranges. The temperature range for which the dynamic magnification is less than 10 is approximately $75^\circ F$. The results show the materials to be ideally suited to the temperature range of launch vibration.

Using these results as a guide, damping treatments for the electronic packages were developed for each application. By using salt migration studies and other experimental data, damping strips were strategically located to provide acceptable vibration levels. In many instances, it was found that the damping strips could be applied without significantly affecting the areas containing the printed circuit. Edge damping strips were both effective and practical.

VIBRATION DAMPING AND ISOLATION WITH
ENERGY ABSORBING COMPOSITES

J. Nunes
Brunswick Corporation
Skokie, Illinois

Most vibrating systems are designed to include some sort of damping to control the undesirable amplification effects encountered at resonant frequencies. This paper concerns the use of material damping (also called hysteretic damping) for vibration control utilizing composites, particularly metallic composites, that are designed to convert mechanical energy into heat energy due to the plastic deformation of one of the composite's components. (Other damping mechanisms, e.g., viscous and frictional as well as other types of material damping; e.g., viscoelastic and magnetoelastic are not covered here.) Because of their relatively high strengths and elastic stiffnesses, these composites can also be fabricated into resilient structural forms for use as vibration isolators and shock absorbers; e.g., as helical spring mounts.

A simple model system was initially conceived toward describing and predicting the behavior of energy absorbing composites by taking into account the component materials mechanical properties and the relative volume fractions of metal needed to optimize damping. Damping is obtained by yielding and plastically deforming one of the metal components during cyclic deformation of the composite. This damping behavior is characterized by a hysteresis loop whose enclosed area is proportional to the amount of energy dissipated in the form of heat. Some assumptions made are:

1. The composite experiences a uniform stress field that may be either tension, compression or shear.

2. The ductile plastic component has zero work hardening and is isotropic.

3. The elastic component yields at a strain at least twice that of the plastic component.

64

The region where little or no damping occurs is where both components deform elastically and is called the primary modulus region. Another region, called the secondary modulus, is reached once yielding occurs in one of the components. It is in the secondary modulus region where a closed hysteresis loop develops during cyclic deformation because of the plastic flow occurring in the lower yield strength component.

Some of the more significant developments and observations that have resulted are as follows:

1. A uniformly stressed composite model system has been formulated to facilitate the design and analysis of potentially high damping capacity combinations of materials. Using this type of analysis, energy absorbing composite materials capable of damping up to 40 percent of input mechanical energy have been developed.

2. Superior damping characteristics have been retained for test temperatures up to approximately 550°F. This coupled with the naturally high load bearing capacities of metallic composite materials makes them competitive with conventional elastomeric materials.

3. Fatigue lives of up to 7.5 million cycles have been measured on energy absorbing composite materials, where relatively low strains and damping (15 percent) capacities were experienced. At resonant frequencies (which is the most severe fatigue condition) cyclic lives of 100,000 cycles have been obtained with damping capacities up to 40 percent.

4. Using energy absorbing composite materials, helical spring isolators have been designed and developed with resonant frequency transmissibilities as low as 3 for an input displacement of 0.1 inches double amplitude.

SUPPRESSION OF TORSIONAL VIBRATION WITH
ZERO TORSIONAL STIFFNESS COUPLINGS

J. M. Vance
University of Florida
Gainesville, Florida

and

R. A. Brown
Dupont
Wilmington, Delaware

Power transmission drive trains and other types of rotating machinery are often subjected to exciting forces which set up torsional vibrations throughout the system. For systems with many different exciting frequencies or many degrees of freedom, the design requirement to avoid excitation at the resonant frequencies may be difficult, or even impossible to meet. Critical design parameters such as strength, weight, material, and size often dictate the mass distribution of rotors and shafts. Required gear reduction ratios often put practical limitations on effective shaft stiffnesses which can be obtained. Thus

the resonant or critical frequencies of the system may not be subject to selective control by the design engineer if they are determined solely by shaft stiffness and mass distribution.

The objective of this paper is to describe the effect of zero torsional stiffness shaft couplings on the torsional vibration response of such a system.

Zero torsional stiffness couplings (henceforth ZTS couplings) are not new (1,2), but the authors have introduced several design innovations which broaden the range of potential applications.

A ZTS coupling transmits torque which is non-linearly dependent on the angle of twist across the coupling. The coupling can be designed so that the slope of the torque vs. twist angle curve (i.e., the torsional stiffness) is zero at a preselected condition of design speed and transmitted torque. The non-linear characteristic allows a ZTS coupling to transmit large amounts of torque without the requirement of extremely large angles of twist. This is in contrast to a low stiffness linear elastic torsional coupling, which for very low stiffness would require several complete turns of twist across the coupling to produce a significant level of torque, and which can never transmit torque at zero stiffness.

The unique properties of ZTS couplings are obtained by utilizing the centrifugal force of masses rotating with the coupling to act through pinned linkages or deformable links to produce the torque transfer from the driving to the driven flange. The patented designs by Chapman (1) employ both pinned rigid links and deformable links, depending on the application. One of these designs is presently in use to suppress torsional resonance in diesel marine drives.

A study was performed to determine the feasibility of designing a ZTS coupling suitable for use in a turboshaft powered helicopter drive train, and which would suppress torsional resonance and vibration.

The sources of torsional excitation in a helicopter drive train are basically two-fold:

1. External excitation, primarily from oscillating air loads at the rotary-wing, and

2. Self-excited, due to feedback instability produced by the automatic speed governor.

Due to length limitations of this paper, and since an analysis of the instability problem ((2) above) is largely concerned with the dynamics of the fuel control system, this paper will be limited to a consideration of response to external excitation for the open-loop system. Analysis of the torsional stability problem will be presented in a future paper.

The open-loop (no feedback control) dynamic system model is formulated using Lagrangian dynamics, for a helicopter drive train with and without a zero torsional stiffness coupling. A numerical simulation is performed on a digital computer, using first order equations derived directly from Hamilton's principle by a new method (3).

Curves of frequency and time response to external excitation are presented to demonstrate the areas of coupling effectiveness. A beneficial effect of the ZTS coupling is to effectively isolate the engine inertia from the rest of the system, resulting in a reduction

66

of the engine speed variation about the normal operating speed. For the helicopter studies, the engine speed and torque are virtually unaffected by exciting torques at the rotary wing for all frequencies about 5 Hz, when a ZTS coupling is employed. This particular system without a ZTS coupling has a natural frequency at 6 Hz.

REFERENCES

1. Chapman, C. W., "Zero (Or Low) Torsional Stiffness Couplings," *Journal Mechanical Engineering Science*, Vol. II, No. 1, Feb. 1969, pp. 76-87.

2. Balzhi, M. F. and Esing, G. D., "Flexible Metallic Couplings With Dynamic Links," *The Engineers Digest*, April, 1960.

3. Vance, J. M. and Stitchin, A., "Derivation of First-Order Difference Equations for Dynamical Systems by Direct Application of Hamilton's Principle," *Journal of Applied Mechanics*, June 1970, pp. 276-278.

FRICTIONAL EFFECTS IN HELICOPTER VIBRATION ISOLATION SYSTEMS

K. L. Lawrence
University of Texas
Arlington, Tex

and

R. W. Blake
Bell Helicopter Company
Dallas, Texas

The need for vibration isolation in helicopter pylon systems is brought about by the large low frequency loadings which exist at the rotor and may, in the absence of isolation, be transmitted to the fuselage and its occupants. The focal pylon-nodal beam mechanism provides a simple but effective means of establishing isolation while at the same time sustaining large steady loads without excessive relative deflections between the pylon and fuselage. Conceptually the focal pylon may be idealized as a mechanism which provides a virtual pivot between the fuselage and pylon at a point other than the actual points connecting the two bodies, and proper location of this virtual hinge can cause the pylon to act as a vibration absorber.

During the design process, determination of the mechanism geometry which provides optimum fuselage response is accomplished using analyses which disregard bearing frictional effects that may in fact be present in the final hardware. Friction in absorber systems can defeat the purpose of the design if it causes the absorber mechanism to lock and cease to perform its function. Because of characteristic nonlinearity, frictional effects may thus cause various behavior modes over a range of input force amplitude which might possibly limit the usefulness of the device. On the other hand, a certain amount of friction damping is both unavoidable and desirable. Otherwise, external transient disturbances would cause persistent low frequency natural mode vibrations.

In order to more fully understand these effects, an analytical and experimental program was undertaken in which bearing frictional moments in the focal pylon mechanism were specifically isolated for study. The analytical study was made with the aid of a hybrid computer. Mechanism link lengths and bearing breakout and dynamic moments were included as parameters. The experimental phase involved vibration testing of full scale hardware. The results of the investigation give clear guidelines for design under circumstances where friction may become an important factor.

PYROTECHNIC SHOCK REDUCTION

S. N. Prescott
Jet Propulsion Laboratory
Pasadena, California

The pyrotechnic shock output from electro-explosive release devices has been reduced by changes in the separation mechanism designs. State-of-the-art hard point release devices were tested on an instrumented simulated spacecraft structure. The accelerometer data were reduced by computer analyses to shock spectra. Comparisons were made between shock spectra and actual degradation or damage to spacecraft equipment. Theories of shock generation mechanism were propounded. Devices were designed and fabricated to incorporate shock mitigation features suggested by theory. These devices were fired on the instrumented structure and the shock spectra obtained were compared with those taken from the previous devices. Significant reduction in shock output was noted.

To keep the investigation within manageable limits, it was restricted to hard point release devices installed with an axial preload of 10,000 pounds. The mounting provisions were kept as similar as possible. The stored energy in the structure external to the release device itself thus remained constant. The spacecraft structure was of semimonocoque construction with longerons and shear web skin. There were simulated electronic chassis "black boxes" attached in the same manner that would be used on the actual space vehicle. Relays and other circuit components mounted in these boxes were electrically monitored for shock effects. High frequency crystal shock accelerometers were mounted at twelve points on the structure and chassis. Therefore, data were obtained, both on nearby shock effects and on the shock transmitted through realistic structural paths.

The reduction of analog data from the accelerometer to shock spectra was accomplished by digitizing the data in the selected time interval, and transforming the data from the acceleration-vs-time domain to the acceleration-vs-frequency domain by a Fortran program on the Univac 1108 computer. The transformation is assigned a Q value representative of the structure. The shock spectrum of a transient at a point on the structure is taken to be the maximum response of a massless oscillator placed at that point where the transient is applied to the transducer. Both "primary" and "residual" shock spectra were obtained.

Modified and redesigned devices were made in-house and were submitted for test by outside manufacturers. These designs incorporated provisions for reducing the internally stored mechanical energy, eliminating the impact of moving internal parts, and reducing the rates of release of stored preload energy.

The preliminary results have been encouraging. Further analysis of the test data and comparisons with prospective tests of actual spacecraft equipment should be performed. Theories of shock generation should be refined. Improved explosive release devices should be designed and fabricated to test these theories.

Based on the information generated by these experiments, the phenomenon of pyrotechnic shock is amenable to mitigation by mechanical design changes in the devices.

SPECIAL PROBLEMS

PIPING DESIGN FOR HYDRAULIC TRANSIENT PRESSURE

Charles C. Huang and Richard J. Bradshaw, Jr.
U.S. Army Corps of Engineers
Huntsville, Alabama

and

Howard H. Yen
Sperry Rand Corporation
Huntsville, Alabama

When a sudden change in flow velocity (relative to pipe) occurs in a fluid filled piping system, hydraulic transient pressure is generated. Audible knocks commonly known as water-hammer manifest this phenomenon as the flow is suddenly obstructed by closing a valve. Similarly, hydraulic transient pressures can be generated by shaking a pipe with strong motions, e.g., earthquakes or detonation of weapons. Severe hydraulic transient pressure is a potential danger to the critical equipment in a piping system and has been one of the concerns of piping designs for earthquakes or weapons effects.

This paper presents the recent development of a computer program (HYTRAN) to aid in the design of piping systems which are required to withstand strong base motions. With given excitations, it computes the magnitude of transient pressures, identifies the location where the pressure exceeds the allowable and column separation occurs, and prints flow velocity and pressure time histories which can be used as a basis for the design of pressure attenuators. HYTRAN is capable of analyzing three-dimensional complex systems containing up to 800 pipe segments and 800 connections between segments. Large piping systems often extend from the ground floor to the ceiling of a building. To account for the different motions experienced by pipes supported at various locations, HYTRAN accepts up to 12 different motion excitation functions. It has been successfully used for the design of large prototype piping systems in several protective structures.

The mathematical formulation of the physical phenomenon used in the development of the computer program is presented in detail. Particular emphasis is given to the boundary conditions for all the piping components normally used in pipe systems, e.g., three-pipe joints, two-pipe joints, deadend, reservoir, various types of pumps, and pressure attenuators. Modeling techniques for transforming physical systems to mathematical ones for HYTRAN application are discussed and guidelines provided. The comparison of HYTRAN results with the experimentally measured data of an actual system for validation purposes is also summarized.

There are three subprograms of HYTRAN:

HYTRAN—I calculates steady state flow conditions of the piping system; its output provides the initial conditions for subsequent transient analysis.

HYTRAN—A calculates hydraulic transient pressure in a piping system subject to strong base motions and identifies the locations where column separation occur.

HYPLOT prints and plots variations of flow velocity and pressure as a function of time at selected locations.

The capabilities and limitations and salient features of each subprogram are discussed complete with illustrative examples.

SPACECRAFT VIBRATION TEST LEVEL OPTIMIZATION

Joseph P. Young
NASA, Goddard Space Flight Center
Greenbelt, Maryland

When performing any "not to destruction" test designed to demonstrate the acceptability of flight design hardware, a common question arises regarding the proper magnitude of the test level. This question is prompted by the desire to set the test level at a point that is high enough to provide a high level of confidence in the strength of the design but not too high so as to cause unreasonable test failures. Due to the complex statistical nature of the problem and the unique characteristics associated with each testing situation, little progress has been made toward defining a universal "optimum" test level. Therefore, the objective of this investigation was to study the possibility of establishing optimum vibration test levels that would be compatible with the test philosophy and program management at Goddard Space Flight Center.

The basis for this investigation was a cost model and test level optimization study done by Piersol & Maurer (1). Most specifically, this effort has dealt only with the cost model and test level optimization results from Reference 1 that pertain directly to the proto-flight program case. A proto-flight program by definition is a program where a specific spacecraft article will serve both as a prototype and a flight model. In addition, all the random variables were assumed to be normally distributed.

The cost model from Reference 1 is derived from the cost of error viewpoint. That is, the model is the sum of the expected cost resulting from an overtest and the expected cost resulting from an undertest. This cost model is

$$C = P_1 C_{RT} + P_2 C_f \tag{1}$$

where

    C = total expected cost for both overtesting and undertesting

    C_{RT} = cost resulting from a test failure

    C_f = cost resulting from a service failure

    P_1 = probability of experiencing an overtest

    P_2 = probability of experiencing a service failure (undertest).

In Reference 1, the above cost model was minimized with respect to the test level. This resulted in an optimum test level expressed in terms of the percentile of the environment statistical distribution. The general expression for the optimum test level percentile was derived to be

$$X_0 = \frac{100}{1 + C_{RT}/C_f} \qquad (2)$$

It is to be noted that, although the expected cost expression in Equation (1) is a function of both the strength and environment distributions and the relative spread between the two; the derived optimal test level is a function of only the environment distribution.

The individual minimized overtest and undertest cost relations are functions of both distributions and their separation, but when added, the strength distribution is a common term that is eliminated. A possible physical explanation of this independence can be presented by considering two limiting cases of expected hardware strength. Assume an "optimum" test level had been determined for a condition where the strength distribution had a very minimal separation from the environment distribution (i.e., marginal strength). Then consider how this "optimum" level might change if the strength distribution was changed to have a very large separation from the environment (i.e., considerably overstrength). From one viewpoint, one could surmise that the "optimum" level could be *increased* without overdue risk of overtesting, while reducing the probability of flight failure. But conversely, one could argue that the "optimum" level could be *decreased* without overdue risk of experiencing a flight failure, while reducing the probability of a test failure. This kind of reasoning would suggest that the two opposing arguments cancel one another leaving the result that the optimum test level is in fact independent of the strength.

Since the practice for establishing qualification environmental test levels at Goddard Space Flight Center is to multiply the maximum expected flight levels (95% percentile or mean plus 2σ) by a test factor (typically 1.5), the need was felt to study the optimum test level in terms of this test factor procedure. Additionally, it was considered to be of value to investigate the sensitivity of the optimum test level and the expected cost to parameter variations. This report presents the details of how this study was performed and a discussion of the results. The results indicated that the limits for an optimum vibration test factor can range between slightly less than 1.0 to slightly more than 1.5.

REFERENCE

1. Piersol, A. G. and Maurer, J. R., "Investigation of Statistical Techniques to Select Optimal Test Levels for Spacecraft Vibration Tests," Digitek Corporation Report 10909801–FC, NASA CR-115778, May 1971.

DYNAMIC ENVIRONMENT TESTING OF THE SKYLAB
ORBITAL WORKSHOP SOLAR ARRAY SYSTEM

R. V. Mendoza
TRW Systems Group
Redondo Beach, California

This paper presents a discussion of the Dynamic Environment test program performed on the Solar Array System (SAS) for the Skylab Orbital Workshop (OWS). A full-scale wing assembly including fairing structures, deployment mechanisms, solar cell panel wing assemblies, and actuating ordnance devices were subjected to launch and boost vibration environments and the vehicle stage separation shock event.

The SAS consists of two structural wings that attach to the OWS and house solar array panel assemblies which provide solar-energy conversion for generation of electrical power for the OWS during mission operations. Each SAS wing assembly weighs approximately 2300 pounds and is 35 feet long by 48 inches wide by 13.5 inches high. The wing assembly is constructed of two primary structural sections: a forward fairing box section, tapered at one end, which is designed to distribute loads to the OWS structure, and a beam fairing assembly, constructed of honeycomb panel/torque box sections. The beam fairing is compartmentized into three bays which house the solar array panel assemblies that are stowed in "accordion" fashion inside the beam fairing until the solar panels are deployed in space to a fully extended 25 x 30 foot square array wing. The forward fairing is permanently attached to the OWS. The beam fairing is secured to the forward fairing with two structural hinge fittings that are used during beam fairing deployments, and the entire structure is secured to the OWS at ten locations, six of which are ordnance actuated frangible structural attachments.

Test requirements included performing sinusoidal and random vibration exposures in each of three axes and performing a simulated stage separation shock event. Vibration requirements were unusual in that vibration inputs were required to be applied to the wing assembly at the forward and aft attachment locations which are separated by a nominal distance of 25 feet. Additionally, random vibration levels of different spectrum shapes were required to be simultaneously applied to the forward and aft ends of the SAS. Because of the unusual geometry and weight of the SAS, a number of practical problems were encountered in performing laboratory dynamic tests. Some of these problems in the area of vibration included resolving the following items:

- What special considerations are necessary in the design of vibration fixtures to mechanically couple a relative large area of the test specimen to the small area of a vibration shaker?

- What techniques are necessary to install the test specimen on two separate vibration systems including accurate mechanical alignments and adjustments during installation?

- How do we install the vibration exciters in order to avoid "walking" of the shakers during test and possibly damaging the test specimen?

- What techniques do we utilize for performance of the vibration tests?

Initial efforts were focused on the type of fixturing necessary to properly couple vibration energy into the test specimen and consideration of the types of vibration exciters which might be utilized for test. It was learned through engineering analysis that all the primary vibration modes of the SAS occurred in the 5 to 20 Hz frequency region. Additionally, a significant amount of modal displacement occurred at the attachment locations with the flexibility of the OWS backup support structure included in the analysis. It was finally decided that, for test, a 6 foot square section of the OWS structure would be used to simulate the backup structure flexibility in order to minimize modal distortion at low frequencies. Fixtures for the vertical axis of the test proved to be the most difficult to design since it was necessary to transition from a 6 foot square area to a 30 inch diameter shaker head. Weight was of prime consideration in design of these fixtures since the combined weight of the fixtures and test specimen indicated that some levels of test might not be achievable with existing shaker capabilities. Final design of the vertical axis fixtures was based on a concept previously used by McDonnell Douglas Astronautics Company. The fixtures were of multiple-cell construction and pyramid in shape. Magnesium plates, 1/16 inch x 9 inches x 9 inches in size were welded together to buildup the structural configuration. The cell void areas were filled with polyurethane foam which provided necessary damping to minimize structural fatigue of the magnesium plates due to vibration. Additional problems encountered with fixtures and test setups will be described in detail.

Two MB C220 shakers together with two MB 5140, 140 KVA, power amplifiers were used for the vibration tests. A combination of single point and multiple point control techniques were employed for sinusoidal sweeps. Random vibration tests were performed utilizing multiple point averaging and separate vibration control for the forward and aft ends of the SAS wing assembly. Problems were initially encountered equalizing some of the required spectrum shapes above 1500 Hz due to mechanical decoupling between the OWS backup structures and the vibration exciters. A considerable amount of margin was available in the derived test environments which allowed reasonable modification of the test spectrum in this frequency region. The entire dynamic testing program was successfully completed without encountering any structural failures of the wing assembly. Results of these tests will be described in detail.

APPLICATION OF LEAST FAVORABLE RESPONSE TECHNIQUES INCORPORATING FIELD DATA FOURIER TRANSFORM PHASE ANGLE

R. J. Wolf and A. F. Witte
Kaman Sciences Corporation
Colorado Springs, Colorado

The method of Least Favorable Response (LFR) is a technique for computing the absolute maximum response of a system having a known frequency response function and subjected to a number of given input time histories. It also provides a means for computing the input time history which results in this maximum response. Smallwood [1] has proposed this technique to establish laboratory test criteria.

Witte and Wolf [2] have made a study comparing the method of Least Favorable Response to classical shock spectrum techniques. The results of this study indicate that for

a class of input field time histories which are decaying periodics, the least favorable response is approximately twice the field response experienced for a single degree of freedom system. In some cases this may be considered as overly conservative and would result in unrealistic cost/weight/performance penalties. It has been suggested by Smallwood (3) that utilizing field data Fourier transform phase angle information as well as the envelope of the modulus will result in lower response amplitudes than those obtained using least favorable response analysis. If the established bounds on the field data Fourier transform phase angle are carried through the least favorable response analysis, the problem reduces to that of determining the absolute maximum response for any input time history whose Fourier transform moduli is less than or equal to the envelope of the field moduli *and whose Fourier transform phase angle is within the bounds established.*

A formulation of the least favorable response analysis including phase angle has been done analytically by Smallwood (3) in terms of delay functions. A slightly different formulation more suited to digital techniques is presented in this paper.

A phase function $U(\omega)$ is defined by

$$U(\omega) = \cos\{\theta(\omega)\} \tag{1}$$

where $\theta(\omega)$ is the phase angle of the Fourier transform of the field dtaa. The least favorable response for a given Fourier transform moduli envelope $\bar{X}_e(\omega)$ and allowable band of phase functions $U(\omega)_{max}$ and $U(\omega)_{min}$ is then given by:

$$y(t)_{max} = \frac{1}{2\pi} \int_{-\infty}^{\infty} \bar{X}_e(\omega)|H(\omega)|$$

$$\times \left\{ U(\omega)_{max} C_1(\omega, t) - (\pm)\sqrt{1 - U(\omega)_{min}^2}\, C_2(\omega, t)\right\} d\omega \tag{2}$$

where

$X_e(\omega)$ = Envelope of moduli of field data Fourier transforms,
$|H(\omega)|$ = Magnitude of the system's frequency response function,
$C_1(\omega, t)$ = $\cos(\theta_H(\omega) + \omega t)$,
$C_2(\omega, t)$ = $\sin(\theta_H(\omega) + \omega t)$, and
$\theta_H(\omega)$ = the phase angle of the frequency response function.

The corresponding least favorable input is given by

$$x(t)_{LFI} = F^{-1}\left[\frac{F[y(t)_{max}]}{H(\omega)}\right] \tag{3}$$

where F^{-1} and F^{-1} are the Fourier transform and inverse transform respectively.

Least favorable input and response calculations including bounds of allowable phase angle have been performed numerically and compared with the usual least favorable inputs and responses, and with shock spectrum results of Witte and Wolf (2).

It is seen that for the class of input time histories considered, decaying periodics, the typical conservatism factor of 2 can be reduced to typically 1.3 by including field data established bounds on allowable phase angles.

REFERENCES

1. Smallwood, D. O., "A Transient Vibration Test Technique Using Least Favorable
    Responses," SC-DR-71-0897 (February 1972), Sandia Laboratories, Albuquerque,
    New Mexico.

2. Witte, A. F., and Wolf, R. J., "Comparison of Shock Spectrum Techniques and the
    Method of Least Favorable Response," to be presented at the 44th Shock and Vi-
    bration Symposium, Houston, Texas, 4-7 December 1973.

3. Smallwood, D. O., "An Extension of a Transient Vibration Technique Using Least
    Favorable Responses," SC-RR-73-0735 (November 1972), Sandia Laboratories,
    Albuquerque, New Mexico.

DEVELOPMENT OF A PYROTECHNIC SHOCK TEST FACILITY

Dan R. Powers
McDonnell Douglas Astronautics Company
Santa Monica, California

Qualification of equipment that must survive a pyrotechnic shock environment has
long been a problem. Producing flight environments by performing ground tests utilizing
flight separation hardware has two main disadvantages: cost and the inability to obtain
qualification margins. Electrodynamic shakers controlled by shock synthesizers have been
used successfully to qualify equipment for service in some of the less severe shock environ-
ments; inherent shaker limitations in acceleration obtainable, frequency response, and
weight restrictions have prevented their use in simulating environments whose shock
spectra specifications exceed 5,000 g's or 10,000 Hz.

Fixtures and apparatus developed to meet specifications beyond these limits include
barrel testers, short separation cylinders, flower pots, and large discs or rectangular plates
with charge holders mounted on their surfaces. In general, these fixtures are designed to
produce one particular shock environment. Some latitude in acceleration levels is possible
by positioning the equipment to be tested at various distances from the explosive or by
mounting the equipment on backup structure.

This paper describes a test facility that has been developed to produce a wide range
of pyrotechnic shocks. Spectra levels can be varied from 5,000 g's to 100,000 g's (5%
damping). In conjunction with the development of the facility, a parametric study was
conducted. Some of the parameters that were varied included: charge size, charge type,
material thickness cut, material type, transducer mountings, transducer type, mass loading
and size and type of the response plate.

Twenty-four firings were made and the outputs from 14 accelerometers were recorded
for each firing. The results presented in this paper substantiate or disprove many findings
of past experimenters, and answer many questions which have been posed.

The fixtures used in this facility were designed by incorporating desirable features
from several types of existing fixtures. One of these features was the re-usable joint

concept presently used on barrel testers which has proven to be very successful. In order to achieve high accelerations and greater versatility, a thick flat plate was chosen for the response member rather than a thin cylindrical section typical of barrel testers.

Two flat plates were used. Both measured four feet by eight feet. One was 1/2 inch thick steel and the other was 1/4 inch thick aluminum. At each end of both plates, a high strength steel ordnance housing was attached. Different size cavities in the housings allowed for a wide selection of charge sizes to be used. Separation sheets of various thicknesses were bolted to the top of the ordnance housing. Shocks were generated by detonating flexible linear shaped charge inserted in the ordnance housing and severing the separation sheet. Combinations of charge sizes, ranging from 7 grains/foot to 50 grains/foot and separation sheets ranging in thickness from .030 inches to .250 inches were used to generate a broad range of accelerations. Advantages of this approach has been proven by its predictability, repeatability, and low cost per firing.

Because of the numerous firings required to develop this facility, an excellent opportunity was provided to investigate some of the problems associated with the pyrotechnic shock phenomenon. Results are presented which can be used as a basis to answer some of the typical questions arising in the prediction of shock levels and in the conduct of shock tests. Topics discussed are:

- Relationship between separation sheet thickness and shock spectra levels.

- Relationship between charge size and type, and shock spectra levels.

- Effect of changing the material hardness of the separation sheets.

- Differences in acceleration outputs of two popular types of shock transducers.

- Effect of mass loading.

- Effect of acoustic overpressure on accelerometer response.

- Attenuation due to placing dielectric spacers under transducers.

OPTIMAL CONTROL LAWS FOR SUPPRESSING RESPONSES OF HIGH SPEED TRACKED AIR-CUSHION VEHICLES

Walton E. Williamson and Ronald O. Stearman
The University of Texas
Austin, Texas

A promising future means of transportation is the tracked air cushion vehicle. Vehicles of this type are capable of achieving speeds of 300 miles per hour. This makes them an attractive means of transportation between cities. One of the basic questions concerning the vehicle is whether or not good ride quality can be maintained at these speeds. Both guideway irregularities and wind gusts will cause the vehicle to experience substantial accelerations. Some method of reducing the accelerations experienced by the passengers must be developed. Passive suspension systems are not adequate to produce good

78

ride quality (1). An active suspension, however, such as the one proposed in **Ref. 2**, does appear to be capable of producing good ride quality. The approach suggested in this reference is to attach small aerodynamic control surfaces near the front and rear of the vehicle. The control surfaces are used to interact with the air and thus produce a smooth ride in the vehicle. At high speeds the control obtained from the fins is substantial and should be adequate to produce the desired ride quality. The basic question is to determine control laws for the fins that will produce the desired ride quality. In order to determine the effects of the fins on the ride quality, Ref. 2 considers a six degree of freedom model for the vehicle. Thus only the longitudinal (heave and pitch) motion of the vehicle is considered. The control laws derived for the fins were obtained by simply monitoring the response of the vehicle for many different assumed control laws. Thus a trial and error approach was used to produce the control law shown. The purpose of this paper is to present the results of applying optimal control principles to the problem of determining control laws which will produce good ride quality for the vehicle.

The model for the vehicle can be written in the standard first order form as

$$\dot{x} = Ax + Bu$$

$$x(0) = 1$$

(1)

where x is the state vector (14 variables), u is the control vector, and A and B are constant matrices. Here the control is taken as the moments applied to the airfoils and is thus a two component vector. This is essentially the model used in Ref. 2 except here it is written in first order form. At this point, the impulse response of the system is obtained and the general response due to guideway and/or gusts determined by means of the Duhamel principle. The state x represents deviations away from a nominal path. The problem then is to find u in order to keep acceleration experienced by the vehicle at a minimum. An approach for doing this was developed by Kalman (3). It essentially produces a linear feedback control law for the system which causes x to go toward zero as time becomes large. This is accomplished by defining an associated optimization problem. The performance index or quantity to be minimized is chosen to be of the forms

$$I = \frac{1}{2} \int_{t_0}^{t_f} \left\{ x^T F x + u^T G u \right\} dt$$

Here F is a 14 × 14 positive semi-definite matrix and G is a 2 × 2 positive definite matrix. Both F and G are weighting matrices which are selected in order to produce the desired ride quality.

One F and G have been selected, a regulator or steady state solution may be obtained by solving the algebraic Riccati equation

$$SB(G^T)^{-1} B^T S - SA - A^T S - F = 0$$

for S. Here S is a 14 × 14 matrix of variables determined by the Riccati equation. Once S is obtained, then the linear regulator solution is

$$u = -(G^T)^{-1} B^T S x.$$

79

Thus a linear feedback constant coefficient control law is obtained from the optimal control problem.

This control law is then applied to the problem of producing good ride quality. The Riccati matrix is calculated numerically using Potter's method (4). This involves calculating eigenvalues and eigenvectors of a 28 x 28 matrix associated with the two point boundary value problem describing the optimization problem. The computations are performed on a Control Data Corporation 6600 computer. Approximately six seconds of computing time are required to produce a control law. Thus it is possible to vary F and G and generate several control laws very rapidly.

In order to simulate the behavior of the vehicle, a model for the disturbances must be developed. Here only the guideway irregularities are considered. A sinusoidal forcing term is used to simulate the guideway. Plots of frequency versus amplitude for reasonable guideways are shown in Ref. 5. The response of the vehicle can be calculated for several frequencies spread over the representative frequency range. This allows the determination of whether or not the control law can produce good ride quality over representative guideways.

The procedure outlined above is used to compute control laws for the vehicle. Several control laws are calculated for the vehicle. The results of the study indicate that the control laws produced by the approach outlined above can be used to produce good ride quality.

REFERENCES

1. Hanks, B. R. and J. D. Leatherwood, Dynamics and Noise Research Related to Tracked Air-Cushion Vehicles, (ASME Paper) Joint Transportation Engineering Conference, October 11-14, 1970.

2. Nolte, E. P., R. O. Stearman, and P. E. Russell, A Simple Active Aerodynamic Suspension System for High-Speed Tracked Air Cushion Vehicles, AIAA Dynamics Specialists Conference paper No. 73-321, Williamsburg, Virginia, March 19-20, 1973.

3. Kalman, R. E., Contribution to the Theory of Optimal Control, Bol. de Soc. Math. Mexicana (1960) p. 102.

4. Potter, J. E., Matrix Quadratic Solutions, *SIAM Journal on Applied Math*, Vol. 14, 1966, pp. 496-501.

5. Calcatterra, Peter C., Richard D. Cavanaugh, and Dale W. Schubert, Study of Active Vibration Isolation Systems for Severe Ground Transportation Environments, (NASA CR-1545). Watertown, Massachusetts: Barry Wright Corporation, November 1969.

DEVELOPMENT OF SAM-D MISSILE RANDOM VIBRATION
RESPONSE LOADS

Paul G. Hahn
Martin Marietta Aerospace
Orlando, Florida

An investigation was performed to obtain the random vibration response loads for inclusion in the design of the SAM-D ED flight vehicle. The response loads are assumed to be the summation of the individual responses of the lightly damped lateral bending vibration modes of the vehicle when the vehicle is subjected to the excitation of the random aerodynamic pressures generated in flight.

Design loads acting within the primary structure of the vehicle are a function of the vehicle translational load factors and angular accelerations plus the loads resulting from transient excitation of the vehicle by fluctuating aerodynamic pressure generated by vehicle boundary layer, base and cross flow, and control surface motion.

Vehicle loads generated are limited to the lateral bending moment and shear force distributions resulting in the vehicle in response to random loading of the vehicle by the fluctuating aerodynamic pressures. The effect of aerodynamic control surface motion is included by assuming the vehicle to have an airload distribution including a control surface rotation consistent with the maximum angle of attack obtainable by the vehicle in its burnout flight condition. The associated random vibration lateral acceleration distribution is also generated. The characteristic lateral bending vibration modes are a function of the vehicle structural stiffness and mass distribution. The higher lateral response accelerations occur for the lighter mass condition, and hence the burnout condition was assumed for the principal investigation. Eleven modes having characteristic frequencies up to 500 Hertz were included in the evaluation of the random loads.

Estimation of the random aerodynamic excitation force must be made with three aspects of the force in mind. An evaluation of the maximum amplitude of the applied force is required as well as the frequency spectrum distribution of the applied force and the mode participation factors apportioning the total load to drive each of the normal lateral bending modes. An evaluation was made to determine the airload distribution which would tend to maximize the excitation of the structural modes.

The excitation force associated with the random aerodynamic pressure distribution acting on the external surface of the vehicle in flight was evaluated from data obtained during flight tests of the SAM-D CTV flight vehicle. This external force was assumed to have an amplitude versus frequency spectral distribution similar and proportional to measurement distributions obtained from several accelerometers on each flight test vehicle. The energy contained in the measured lateral acceleration frequency band of 0 to 2000 Hertz was assumed to be effective within a reduced frequency band of 0 to 1000 Hertz thereby developing a conservative magnitude for this external force input to determine the random response of the structural modes. The aerodynamic force magnitude was not extrapolated beyond that associated with the maximum dynamic pressure flight of the CTV. For flight at higher dynamic pressure conditions the frequency content of the random force excitation would shift upwards such that much more of the energy would appear at frequencies above 2000 Hertz and hence would be less effective in the generation of primary structural bending moments, shear forces and modal accelerations. This higher

81

frequency content would affect such things as insulation bond and joint fatigue life which is not a product of this random loads analysis.

Using the flight vehicle characteristic and aerodynamic force data described above, the random response loads acting in the vehicle structure were obtained. Consideration was also given to the possibility of higher random loadings occurring coincident with the maximum lateral loading during the flight vehicle boost phase.

Random vibration loads estimated in this analysis for the flight vehicle burnout condition can be considered the maximum attained throughout the ED flight vehicle operational range. Computations were performed to yield the root-mean-square magnitudes of the response loads acting in the vehicle primary structure. These magnitudes were then multiplied by a factor of three to obtain the expected peak magnitudes. These loads are incremental loads and are to be added to the basic structural design loads.

ASYMMETRIC DYNAMIC BUCKLING OF RING STIFFENED CYLINDRICAL SHELLS UNDER LATERAL PRESSURE

T. Tsui and C. Lakshmikantham
Army Materials and Mechanics Research Center
Watertown, Mass.

BACKGROUND

This paper forms part of a study recently initiated at the Army Materials and Mechanics Research Center on the dynamic buckling of imperfect stiffened shells under various types of loading and reports the results for ring-stiffened cylinders under lateral step loads. In the first phase of the program, dealing with axially stiffened cylinders under axial step loads, it was demonstrated that structures which are imperfection-sensitive under static loads remain so under (dynamic) step loads. Ref. (1) also showed that the eccentricity effects which are pronounced in the case of perfect cylinders are not so important when imperfections are taken into account.

Ring-stiffened cylinders, with which we are concerned here, are even more fascinating in some ways than the axially stiffened cylinders. During the course of the investigation of Ref. 1, it was found that the eccentricity of stiffeners not only affected the buckling load but also profoundly changed the buckling modes. Thus for instance, a ring-stiffened cylinder of certain stiffening geometry would buckle axisymmetrically if the stiffeners are located outside the shell surface; whereas if the stiffeners were inside, the mode changes to an asymmetric one; even more importantly, external rings of certain size would cause asymmetric buckling. This modal behavior, summarized in Ref. 2, plays an important role in the imperfection-sensitivity study. In this connection it may be remarked that the axisymmetric post buckling of either ring-stiffened or unstiffened cylindrical shells with or without geometric imperfections, in general has not been of particular concern of the researchers. This is due to the fact that the governing differential equations based on a nonlinear Donnell type formulation reduce to a linear system which yields a dynamic buckling load equal to the corresponding static buckling load. As a result it is found that pure axisymmetric buckling cannot be influenced by geometric imperfections. Therefore

82

it can be concluded that asymmetric post buckling configurations must be assumed in order to examine the imperfection sensitivity.

With the preceding arguments clearly stated, we are concerned in the present paper with the asymmetric post buckling behavior of imperfect ring-stiffend cylindrical shells under lateral step loads. Our goal is to determine the influence of imperfections and the location of the stiffeners on the dynamic buckling load.

APPROACH

Basing on the nonlinear Donnell type strain-displacement and stress-strain relationships, we obtain a set of three nonlinear equations of motion through the application of Hamilton's principle. Instead of attempting to solve the governing equations directly, the normal displacements of the shell are represented by a four-parameter deflection function which depicts the diamond shaped buckles familiar in the static stability analyses. Making use of an assumed stress function, we obtain a single equation in the normal displacements. This is then solved by using a Galenkin type procedure. The result is a set of four ordinary nonlinear differential equations expressed in terms of the four parameters.

For a given set of input parameters such as, loading, geometries of the shell and stiffeners and initial conditions, the four ordinary differential equations are integrated numerically to obtain the four parameters as functions of time. In the present study a Runge-Kutta scheme is used for numerical integration and the convergence of the solution is verified by altering the time-step size.

The buckling criterion employed in this study is based on the one proposed by Budiansky and Roth (Ref. 3) and it is based on the jump in the peak amplitude of the normal displacements.

HIGHLIGHTS OF RESULTS

Dynamic buckling loads for asymmetric buckling of ring-stiffened cylindrical shells under a suddenly applied uniform lateral loads have been obtained. The effect of the locations of the stiffeners and the geometric imperfections on the buckling loads have been determined.

It is found that as in Ref. (1), that the ring stiffened shells are also imperfection sensitive and there is considerable reduction of the buckling loads by taking initial imperfections into account. Rings on the inside of the shell yield higher buckling loads than that those obtained with identical rings on the outside. It may be concluded that it is more efficient to place the ring stiffeners on the inside of the shell. This is similar to the findings reported in Ref. 4, though the authors there were only concerned with linear static stability.

REFERENCES

1. Lakshmikantham, C. and T. Tsui, "Dynamic Stability of Axially Stiffened Imperfect Cylindrical Shells Under Axial Step Loads," to appear in AIAA journal.

2. Lakshmikantham, C. and T. Tsui, "Linear Stability of Eccentrically Stiffened Cylindrical Shells Under Axial Compression: A Second Look," to appear

3. Budianski, B. and R. S. Roth, "Axisymmetric Dynamic Buckling of Clamped Shallow Spherical Shells," TND-1510, 1962, NASA.

4. Baruch, M. and J. Singer, "Effect of Eccentricity of Stiffeners on the General Instability of Stiffened Cylindrical Shells Under Hydrostatic Pressure," Journal of Mechanical Engineering Scie ce, Vol. 5, No. 1, March 1963.

IDENTIFICATION OF AN OPTIMUM SET OF TRANSIENT SWEEP PARAMETERS FOR GENERATING SPECIFIED RESPONSE SPECTRA

R. C. Rountree
The Aerospace Corporation
El Segundo, California

and

C. R. Freberg
University of Southern California
Los Angeles, California

A globally optimum set of transient sweep excitation parameters are identified for generating response (shock) spectra that match shock spectra specifications. The parameter identification is accomplished by an algorithm that applies a general purpose optimization technique known as the deflected gradient method. The algorithm generation of these optimum transient sweep parameters is functionally described in terms of overall equations in block diagram form and also portrayed by a simple programming flow chart. The particular equations are described that are used in the algorithm to define the specified response spectra, the transient sweep excitation, and the response spectra resulting from this excitation. The performance of the algorithm is shown by means of results from three demonstration cases.

The computer algorithm represents a practical nonlinear application of the deflected gradient method since the specified response spectra are indicative of actual vibration test conditions. The optimization involves minimizing an error criterion function that expresses a weighted squared difference between the specified response spectra and those generated by the transient sweep excitation. The specified spectra are expressed as logarithmic linear magnitude-versus-frequency test envelopes of arbitrary slope. Two shock spectra are specified in order to control both the magnitude and duration of the transient sweep excitation. The excitation is expressed in terms of four parameters that are iteratively adjusted within the algorithm until their optimum values are attained. The excitation is chosen from a class of time domain functions $g(t) = A(t) \sin \theta(t)$ which represent a wide range of real environments. The system being excited is modeled by the classical collection of tuned oscillators (i.e., single degree-of-freedom systems) inherent in the definition of shock spectra.

Shock spectra specifications, which are generally presented in graphical form, are translated into an equation form in order to be amenable to the algorithm. These

84

specifications are generally presented utilizing logarithmic scales for both the ordinate and abscissa. The particular specifications of interest in this paper are those corresponding to two straight line log-log plots representing either two shock spectra (i.e., one for each of two damping factors) or a shock spectrum for a given damping factor and its ratio to a second shock spectrum for another damping factor.

The general class of excitations functions $\{g(t) = A(t) \sin \theta(t)\}$ is also reduced to an equation set form for incorporation into the algorithm. This is accomplished by means of a vector containing four adjustable parameters. The elements constitute extensions of classical forms of the time varying sweep amplitude, $A(t)$, and time varying sweep argument, $\theta(t)$. Both generalized and restricted forms of the equation set are presented. The restrictions pertain to reducing the general form to the classical special case forms.

A mathematical representation is assigned to the particular form of shock spectra and ratio used in this paper. Determination of the oscillator response requires solution of the assigned differential equation for acceleration by means of integration. The integrand involved is a function of the oscillator frequency and the frequency associated with the transient sweep (the latter inherently covers a broad range of frequencies). For numerical integration it is desirable to have the integration step size independent of the oscillator frequency. An integration algorithm to achieve this independency is described such that the integration step sizes vary only with sweep frequency.

A specific error criterion function and gradient vector are also identified that are required for use of the deflected gradient method. Mathematical formulations are presented for both the error criterion function and the gradient vector.

Three demonstration cases are used to exhibit algorithm performance and show that the algorithm generates optimum transient sweep parameters. The three cases represent increasing generality. The description and purpose of each demonstration case are provided, including a brief description of the algorithm input and output. Criteria are presented in graphical form for estimating initial numerical values of the adjustable parameters. The overall results of these runs are provided as well as an evaluation of sweep duration characteristics.

A practical and pertinent conclusion of the tabulated results is that the set of optimum parameters, in conjunction with the sweep duration, constitute a complete description of the transient sweep excitation. A vibration test machine may be programmed with the optimum parameter vector and sweep duration to satisfy the particular shock spectra specification.

REDUCTION OF HULL NOISE AND VIBRATION BY
CENTER OF PERCUSSION ROADARM DESIGN

Daniel D. Ustick
U.S. Army Tank—Automotive Command
Warren, Michigan

The study investigates a method for reducing roadwheel noise and shock loads into the vehicle hull of a track-laying vehicle. This reduction is theoretically possible by

designing the center of percussion of the roadarm to coincide with the roadwheel spindle axis. In this manner dynamic forces applied at the spindle, normal to the roadarm length, will not be transmitted as shock to the center of arm rotation, i.e., the point of assembly to the vehicle hull.

The design constraint is given as a function for application in the design of future roadwheel and roadarm assemblies. It is modified for application of design changes to existing assemblies. A brief discussion about the potential magnitude of impulse energy input is followed by an application of design principle to the M551, Sheridan.

It is concluded that by application of the "center-of-percussion principle" to the design of roadwheel and roadarm assemblies, components of impulse normal to the roadarm length will transmit energy into the vehicle suspension system rather than directly to the vehicle hull.

Future design implications are briefly discussed.

SYNCHRONIZATION AND PHASE ANGLE OF TWO
UNBALANCED ROTORS

Mario Paz
University of Louisville

and

Preston Schrader and Robert Blackmon
Rexnord, Inc.
Louisville, Kentucky

Rectilinear vibration required in some types of mechanical equipment such as vibrating feeders and conveyors may be produced by two synchronized motors having eccentric weights rotating in opposite directions. The condition for self-synchronization, as well as the phase angle maintained by the rotors, has been investigated for simplified cases by Blekham (1) for one directional motion, and by Paz (2) for two directional motion. These developments gave solutions prescribing the conditions for self-synchronization but could not analytically predict the stable phase angle or the resultant direction of motion.

The purpose of this paper is to extend the scope of the previous work to include the general case of plane motion of any mechanical system subjected to the driving action of two unbalanced rotors. With this extension it is possible to analytically predict the stable phase angle and the direction of the resultant force of any two rotors with parallel axes of rotation. Development of the general solution for plane motion of two unbalanced rotors permits further extension of the scope of the theory to incorporate the following factors:

1. Systems with more than two unbalanced rotors.

2. Systems with rotors in any orientation in space.

3. Effect of dissipative forces (damping) in the synchronization of rotors and stability of the phase angle.

These extensions have applications in mechanical vibrators used for packing, screening, conveying materials, and similar operations. Ability to analytically determine the conditions for self-synchronization of large mechanical systems would produce more efficient designs. Furthermore, the possibilities for extensions of rotors to military applications appears patent. Helicopters and small military craft, such as torpedoes, constructed with two or more rotors are subjected to the principle of self-synchronization. Rotating parts of these crafts, when built, contain small imperfections which produce mass eccentricity and hence act as unbalanced rotors.

The method presented in this paper is general and applicable to any mechanical system acted upon by the unbalanced rotors. It is shown that the use of Hamilton's Principle permits the determination of the magnitude of the phase angle of two self-synchronized unbalanced rotors as well as the necessary condition of a stable solution.

A brief outline of the mathematical development follows.

The differential equations of motion for the mechanical system are obtained in terms of the generalized coordinates and transformed to principal coordinates. These equations are functions of the phase angle maintained by the rotors. The Lagrangian function in terms of the principal coordinates is given by

$$L = \sum \frac{1}{2} M_n \dot{Y}_n^2 - \sum \frac{1}{2} K_n Y_n^2 \tag{1}$$

where M_n, K_n, Y_n, and $\dot{Y}_n$ are respectively the mass, stiffness, displacement, and velocity corresponding to the nth mode.

Hamilton's principle states that a conservative system moves in such a way that the integral of the Lagrangian function

$$I = \int_{t_1}^{t_2} L \, dt \tag{2}$$

has a stationary value which is a minimum for a stable solution. This condition is expressed mathematically as

$$\delta I = \int_{t_1}^{t_2} \delta L \, dt = 0 \tag{3}$$

Substituting the Lagrangian function from equation (1) into equation (3) and taking the variation during a cycle with respect to the parameter θ (the phase angle) results in

$$\delta I = \int_0^{2\pi/\omega} \left(\sum M_n \dot{Y}_n \frac{\delta \dot{Y}_n}{\delta \theta} \delta\theta - \sum K_n Y_n \frac{\delta Y_n}{\delta \theta} \delta\theta \right) dt \tag{4}$$

Finally, substituting in equation (4) Y_n and $\dot{Y}_n$ from the solution of the modal equations and performing the integration indicated results in an explicit expression for the trigonometric tangent of the phase angle of synchronization. To ascertain the stable

87

solution among the two resulting roots given by the tangent function, it is necessary to examine the second variation obtained from equation (4).

The paper gives a general and detailed mathematical development of the method. The theoretical results for the self-synchronization of two unbalanced rotors are applied to a system for the whole range of pertinent parameters. Also it is reported in this paper the experimental results conducted on a test unit in the study of this problem which corroborates the analytical conclusions of the analysis.

REFERENCES

1. Blekham, I. I., "Rotation of an Unbalanced Rotor Produced by the Harmonic Oscillation of the Axis," Bulletin of Academy of Sciences, USSR, Division of Technical Sciences, No. 8, 1954.

2. Paz, Mario, "Self-synchronization of Two Eccentric Rotors on a Body in Plane Motion."

DEVELOPMENT AND CORRELATION, VIKING ORBITER ANALYTICAL DYNAMIC MODEL WITH MODAL TEST

Ben K. Wada, John A. Garba, and Jay C. Chen
Jet Propulsion Laboratory
Pasadena, California

The Jet Propulsion Laboratory is responsible for the Viking Orbiter System which is part of the overall Viking Project managed by the Viking Project Office at Langley Research Center for NASA. The Spacecraft will be launched on a Titan IIIE/Centaur Launch Vehicle in August 1975.

The Viking Orbiter (VO) design and flight loads for the primary structure are established by Load Analysis. Load Analysis is a procedure for obtaining VO member loads from the dynamic response of a complex finite element model of the complete Booster System (includes the VO) subjected to Booster Engine transients. Load Analysis requires modal coupling of the various Booster System structural subsystems to allow a solution with present computer capabilities.

The dynamic mathematical model of the VO was continually updated as the design evolved and as the test data became available since the design loads are dependent on the model. The design loads were reiterated during the design. The establishment of the final flight loads to qualify the primary structure are to be based on a Load Analysis with a VO model verified by test.

Analytical models are required because the flight configuration differs from the test configuration. Differences include the use of referee fluid during test, different quantities of fuel for the two Viking Missions, and exclusion of selected hardware for the test.

The paper describes three general activities resulting in the VO analytical dynamic model which has been updated and verified by test data during the Project.

- The overall plan for Load Analysis, analytical dynamic model, and development test.

- The VO subsystem static and modal tests.

- The VO system modal test.

The overall plan for Load Analysis, approach to develop an analytical dynamic model, and development must be integrated to assure orderly development of a mathematical model that will be verified by the VO system modal test. The task is complicated by the interfaces created because the VO is between the Viking Lander Capsule (VLC) on top and the Centaur Adapters on the bottom. Although the interactions with organizations external to JPL were minimized, the VO system modal test configuration included a rigid mass simulation of the VLC, major components of the VO, and the Centaur Adapters. The VLC and the Centaur Adapters are designed by MMA and GD/CA. The configuration is consistent with the modal coupling plan for Load Analysis.

The overall plan includes the coordination of the VO math model subsystem modal coupling approach with the availability of the subsystems for static and modal tests. The mathematical model of the VO are updated during the Project using subsystem mathematical models modified to match test data whenever possible. Until the final VO modal test, the model used to update design loads consisted of a mixture of subsystem models and parameters either verified or not verified by test. In specific cases, constraint modes and effective fluid mass are experimentally determined. The modal corrections on the subsystems are simplified since the number of parameters are less than on the system.

The VO system modal test has been established as the verification of the mathematical model for use in Load Analysis to obtain flight member loads for the qualification of the structure. The correlation of the analysis and test is reasonably good. The analysis procedure is briefly defined with the major emphasis on the methods and techniques used to correlate the mathematical model to the modal test results.

The VO data are presented to illustrate the general approach and the relative success achieved. The information will be of value to help plan a modal test program for future Projects. Projects like Shuttle would benefit because of its interfaces and need for good dynamic models using modal coupling concepts.

EXPERIMENTAL INVESTIGATION OF THE DYNAMIC RESPONSE
OF CANTILEVER ANISOTROPIC PLATES

R. L. Sierakowski
University of Florida
Gainesville, Florida

and

C. T. Sun
Iowa State University
Ames, Iowa

The continued widespread use of filamentary composite materials as structural sub-systems and components has required an understanding of the response characteristics of such materials to a wide spectrum of loading conditions. One technologically important area being considered for introduction of such types of laminated structural composites is for the inlet fan stages of air breathing propulsion systems. In order to establish guidelines for examining the vibratory response of composite fan blades, information dealing with the influence of various material parameters on dynamic characterization are necessary.

Some previously reported studies on the vibratory response of anisotropic plates have been discussed in Reference (1-4). In these studies, analytical techniques for predicting frequencies and mode shapes of composite plates using energy methods have been compared with experimental data generated for particular plate boundary conditions, specifically fully clamped plate configurations.

In the present study, an experimental investigation of the natural frequencies and mode shapes of cantilever composite plates with one edge clamped and three free edges is reported on. The plates have been tested over a frequency range of forty to 1000 Hz using a 1200 lb. dynamic shaker. Plate excitation was generated using a controlled sweep oscillator with signal amplification; and response monitored on an oscilloscope. Frequency response was checked using a graphic level recorder synchronized with the sweep oscillator. A minaturized accelerometer with piezoelectric sensing element was positioned on the plate specimens to locate nodes and antinodes for the various mode shapes recorded.

Included in the current studies are such parameters as variable ply orientations (0°, $\pm 15^\circ$, $\pm 30^\circ$, $\pm 45^\circ$), number of plies (m = 4, 8, 16) and several plate aspect ratios. For the initial studies, controlled S-glass type 1002 resin matrix composites have been tested. Analytically predicted frequencies and mode shapes using an updated version of the codes discussed in (1) experimental studies on spanwise tapered cantilever plates fabricated from graphite—epoxy have been examined.

REFERENCES

1. Ashton, J. E. and J. D. Anderson, "The Natural Modes of Vibration of Boron-Epoxy Plates," Shock and Vibration Bulletin, Vol. 39, Part 4, pp 81-91, 1969.

2. Ashton, J. E., "Natural Modes of Free-Free Anisotropic Plates," Shock and Vibration Bulletin, Vol. 39, Part 4, pp 93-97, 1969.

3. Bert, C. W. and B. L. Mayberry, "Free Vibrations of Unsymmetrical Laminated Anisotropic Plates with Clamped Edges," Journal of Composite Materials, Vol. 3, pp 282-293, 1969.

4. Mohan, D. and H. B. Kingsbury, "Free Vibrations of Generally Orthotropic Plates," Journal of Acoustical Society of America, Vol. 50, pp 266-269, 1971.

UNDERWATER PROBLEMS II*

SHOCK RESPONSE OF SUBMERGED STRUCTURES

Thomas L. Geers
Lockheed Palo Alto Research Laboratory
Palo Alto, California

Summary not printed for security reasons.

THE SMMS STRUCTUREBORNE NOISE MONITORING PROGRAM

W. H. Barnes, III
Naval Ship Research and Development Center
Annapolis, Md.

Since November 1971, the Structureborne Noise Branch (Code 1927) of the Naval Ship Research and Development Center has conducted a pilot program of structureborne noise measurements for the Shipsystem Maintenance and Monitoring Support Office (SMMSO) of the Naval Ship Engineering Center. Periodic acceleration measurements on selected machinery provide the data base for evaluating machinery condition. Recommendations are made to fleet units for corrective action to machinery when the analyzed data so indicate. Progress in the vibration monitoring program and recommendations for its future use in aiding the fleet in machinery maintenance is discussed.

WORTH OF SHOCK HARDENING OF SHIPS

P. Roger Gillette
Stanford Research Institute
Menlo Park, California

and

Robert Belsheim
Naval Research Laboratory
Washington, D.C.

This proposed paper is taken from an NRL report now in publication.

Preceding page blank

The purpose of the study was to provide a basis for determining how far above the ship shock hardness level required for normal (non-combat) naval operations one should go in designing naval ships to withstand combat stresses.

By the nature of warfare, all naval vehicles, whether designed for offensive combat, defensive combat, or combat support operations, are subject to attack by hostile forces. Hence all naval vehicles must be provided with appropriate defenses. These defenses may be in the form of protective screens, active self-defense capabilities and or passive self-defense capabilities. The defenses may act against hostile sensors, to hinder detection, identification, and localization; or against hostile weapons, to limit damage to the vehicle's structure, equipment, and personnel. Planning of the development and deployment of any type of naval vehicle should include careful delineation of the various defensive measures that may be feasible for that type of vehicle, and comparison of such measures with respect to effectiveness and cost.

This study was concerned with the worth of ship shock hardening. More specifically, it is concerned with the role that strengthening and isolating a ship's internal equipment can and should play as one element of the ship's defensive capability.

The relative importance of such shock hardening obviously depends upon the relative probability of hostile actions in which the ship is detected, identified, and localized, weapons are launched against it, the weapons explode underwater, and the resulting shock level is sufficient to lethally damage the internal equipment but not the hull. For example, if the weapons a hostile force may be expected to use against a ship are of sufficient yield and accurary to achieve a very high single-shot probability of hull rupture, strengthening the ship's internal equipment will not be worth while.

Considerably less progress has been made in operations analysis than in engineering analysis of ship shock hardness. Some idea of the quantitative relationship between ship hardness is obtainable from engineering analysis and design studies of various projected ship types. Much less information is currently available on the quantitative relationship between the combat effectiveness of a naval force and the shock hardness of its ships. Hence the basis for quantitative determination of optimum levels for ship shock hardness is far from adequate. The promulgation of hardness level requirements have therefore of necessity been based primarily on qualitative judgement rather than quantitative analysis.

The study was constrained in scope not only by the limited availability of information on ship equipment criticality, hardness, and hardening costs but also by the even more limited availability of information on possible future missions and threats. Because of these constraints, the main emphases in the study have been on the development of a method for identifying critical equipments and the development of a method for comparing the combat effectiveness of increased ship hardness with that of increased ship numbers using minimum information on missions and threats. The several constraints dictate the development of a method of analysis that requires a minimum amount of information collecting and processing effort. Simulation techniques involving Monte Carlo sampling are excluded by this requirement, and so are any analytical techniques that necessitate the use of electronic data-processing machines.

The method that has been developed is based upon a very simple, general scenario to which Lanchester's Square Law is applicable. An optimality condition for ship shock hardness level has been derived from Lanchester's Square Law and presented in graphical form. If a relation between ship cost and ship shock hardness can be established for a

94

given projected ship design, and if values of two parameters (an effective single-shot ship survival probability and an effective force survival or attrition ratio) can be established for the combat conditions in which the projected ship may be expected to operate, the optimum hardness level for the ship can be determined by inspection of the graph.

A relatively simple analytical technique has been developed. The primary tool utilized in this technique is a "contour map" of a surface representing the basic condition that a ship designer must satisfy to achieve an optimum level of ship shock hardness. The designer enters this map with values of three parameters, derived for a design he has formulated, and determines by inspecting the map whether the hardness of the design he has formulated is at, above, or below the optimum. The values of the three parameters (effective ship single-shot survival probability against expected hostile weapons, acceptable force survival ratio against expected hostile forces, and the rate of change of total ship cost with respect to ship shock hardness) may be obtained by processes ranging from rough estimation to fairly detailed analysis, depending upon the accuracy required and the availability of information and computation resources.

A few applications of this approach have shown it's value in setting fairly broad limits on desireable amounts of shock-hardening, as compared with one other alternate way to spend available money. The method can be used for many comparisons, and is believed useful.

A HARDNESS VERIFICATION PROGRAM FOR
ELECTRONIC EQUIPMENT HOUSED IN PROTECTIVE STRUCTURES

P. A. Koen and G. C. Stocker
Bell Laboratories, Whippany, New Jersey

ABSTRACT

The methodology and significant test findings of a shock and vibration test program to verify the survivability of over 65 different electronic cabinet designs is presented. The survivability of these equipment items to the shock and vibration environment induced by a nuclear weapon is essential to perserving the operational integrity of the Perimeter Acquisition Radar (one of the major elements of the SAFEGUARD Antiballistic Defense System). All radar equipment is verified by one of three methods: (1) vibration tests of complete equipment cabinets, (2) vibration tests of unique subassemblies and selected components and (3) similarity determination of equipment items to the ones covered in two latter groups. Decision matrices which systematize the process of selecting the method of verification were formulated and are applicable to other verification programs. Computerized documentation of all electronic items in the radar are used to insure complete coverage of all equipment while simultaneously avoiding duplication of test items.

SUMMARY

One requirement of the SAFEGUARD Radar System dictates that the system remain operational during and after the shock and vibration environment caused by a nuclear event. The Perimeter Acquisition Radar (PAR) equipment, is housed in a five story, above

ground building. As a result it is subjected to severe shock and vibration environments induced by the air blast and ground motion produced by the nuclear event.

An ideal verification program would require that all equipment in the radar system be subjected to the prescribed shock and vibration environment. The testing of all equipment items (over 950 cabinets) is not being done since it was determined to be more cost effective to make use of equipment modularity, and of similarity among the various modular design groups, to reduce the number of operational tests and test items to a minimum. The verification program that evolved incorporates:

(1) Full scale vibration tests of unique cabinet designs (i.e., very large units, units with equipment mounted in an unusual fashion or unusual electrical designs).

(2) Full scale vibration tests of hybrid cabinets (i.e., specially assembled for this verification program) which are made up of unique subassemblies from different radar system cabinets.

(3) Subassembly and component tests.

(4) Similarity (both mechanical and electrical similarity) of equipment items to the ones covered in the three previous groups.

Factors which were considered in assigning the cabinets, subassemblies and/or components to the particular verification method above included (a) criticality of the items to the radar operation, (b) equipment vulnerability to the shock and vibration environment, (c) the confidence level which the particular method of verification would yield and (d) the extent of electrical monitoring required. It should be noted that during shock and vibration tests discussed above, the equipment is powered, operationally exercised and electrically monitored both during and after the shock and vibration tests. Details concerning the operational tests and the selection procedure will be discussed in the complete version of the paper. The selection procedure will be discussed in terms of systematic decision matrices which should be applicable to other programs.

A computerized procedure is used to document the decision path taken for each equipment, subassembly and component in the over sixty-five different radar equipment cabinet designs. The computerized procedure also ensured that all radar items were verified and served as a basis for numerous similarity studies. The evolution and usage of the above procedure will also be discussed in more detail in the paper.

In summary, this paper reviews the methods employed to verify the shock and vibration survivability of over 65 different radar equipment designs contained in the PAR radar. Details concerning the verification methods, decision paths, the operational tests, the documentation procedures, and the major test results will be discussed.

MEANS OF CONTROLLING THE DYNAMIC MOTION OF BOTTOM MOORED MINE CASES EXPOSED TO HIGH CURRENT

John J. O'Neill, Jacob Berezow and J. Goeller
Naval Ordnance Laboratory, Silver Spring, Maryland

Summary not printed for security reasons.

VIBRATIONAL SIGNATURE PHENOMENA

Bruce G. Wrenn and Dalton D. Walters
Lockheed Missiles and Space Company
Sunnyvale, California

Summary not printed for security reasons.

SHOCK ANALYSIS OF SERIES I SSTV TESTS

W. W. Wassmann
Naval Ordnance Laboratory
Silver Spring, Maryland

A series of tests was conducted in the Chesapeake Bay during June 1970 on a Submarine Shock Test Vehicle (SSTV) with a pressure hull and structural arrangement identical to the missile compartment of the USS LAFAYETTE (SSN-616) class submarine. Test Series I consisted of four tests in which the standoff distance from the SSTV was decreased successively to obtain increasing shock severity. Each test employed an HBX-1 charge positioned on the horizontal perpendicular bisector of the longitudinal axis of the vehicle, on the starboard side.

Machinery and equipment representative of selected systems within the engineroom space of the USS STURGEON (SSN-637) class submarine were installed in the SSTV. Specifically, a portion of the main seawater system, auxiliary cooling system, the main steam loop, ship service turbogenerator, associated pumps, motors and masses simulating the propulsion unit were installed. The locations selected for analysis were chosen as being representative of existing or potential locations for mounting or storing ordnance or auxiliary devices. The general locations determined to be of interest were: (1) on or rigidly connected to the hull frame, (2) on an internal bulkhead, (3) on the starboard box girder and (4) at the input to the base of heavy machinery to determine how the input shock is affected by the weight of the item undergoing shock. The frequency range of the data was limited by the velocity gages on the low end of the spectrum by the 4 Hz natural frequency of the gages, and on the high end of the spectrum by the coil form resonant frequency at about 2500 Hz. The total linear range of the velocity gages was 2.75 inches.

Velocity gage data from Test Series I of the SSTV are analyzed for application toward the establishment of environmental criteria for submarine-carried ordnance. The analysis includes the computation of peak velocity values, peak acceleration values and shock spectrum analysis. The velocity records were digitized and differentiated digitally to obtain acceleration vs. time records. These data were then filtered to enhance the signal to noise ratio which had been degraded at high frequencies by the differentiation process. The acceleration records were then analyzed for shock spectrum response over the frequency range of 1 Hz to 5000 Hz, using 10 oscillators per decade and a 2% damping ratio. The maximum velocity change was 39.7 fps, the maximum acceleration was 2400 g and the maximum shock spectrum response was 9500 g at 398 Hz on the pressure hull. The shape of the shock spectra over certain frequency ranges of interest classifies the response of certain locations in the vehicle as mass-like where other locations are found to be spring-like.

Comparison of the analyses for the two different shock levels gives an indication of the linearity of the test series with respect to shock intensity. The analysis indicates that the test vehicle is relatively linear with respect to shock intensity in the direction of the shock up to the highest level tested.

VIBRATION TESTING AND ANALYSIS

VEHICLE SUSPENSION EVALUATION USING A ROAD SIMULATOR

James W. Grant
U.S. Army Tank-Automotive Command
Warren, Michigan

TACOM's Road Simulator was developed as a tool to study suspension and frame dynamics under controlled laboratory conditions. The Road Simulator places the total vehicle system in a vibrational environment similar to that which the vehicle encounters during field operation. It is the purpose of this paper to describe the Road Simulator system, show advantages over field testing, point out limitations, and describe results obtained from this type of testing.

The advantages of road simulation testing when compared with field testing are many:

1. Downtime during costly field testing is reduced. A laboratory simulation ideally is performed on a prototype vehicle prior to developmental field tests. This results in vehicles on which major frame and suspension deficiencies have been corrected; thus, a major portion of downtime during field testing is eliminated. This is particularly significant where more than one prototype is field tested.

2. Better determination of causes of failure can be made. A failure generally does not occur without some form of warning. It is very desireable from the standpoint of failure mode determination and correction to observe the propagation of a failure from its inception. The "clean" environment and ease of observing the test specimen during laboratory simulation testing lead to ideal conditions in detecting and following failure progression.

3. Quantitative information on the test specimen is improved. In order to obtain the best quantitative data on a vehicle, it must be instrumented. Field testing presents problems in transducer location in hazardous areas, space allocation for recording equipment, and a necessity to utilize telemetry equipment in some instances. Laboratory simulation testing eliminates all of these problems and allows direct data acquisition.

4. Road simulation testing offers absolute repeatability between test samples. One of the problems with field testing is the incalculable effects of the environment, course variation and driver variation. Road simulation can be conducted on a pilot vehicle and repeated any time in the future on a prototype or production vehicle, with confidence that all tests were subjected to the same vibrational environments.

5. Road simulation testing offers significant cost savings over equivalent field testing. This results not only from the decreased cost of testing in a controlled environment under

ideal conditions, but also from an ability to eliminate the "dead time" of dynamically non-significant inputs to the vehicle.

The limitations of Road Simulator testing fall into three categories:

1. They almost never provide absolute simulation of the field dynamics. The complexity of the road simulator system grows as more inputs are added. To maintain a feasible and cost effective system, many simulators excite the vehicle only in one or two axis (almost always vertically and sometimes longitudinally). This results in arbitrary elimination of some dynamic factors.

2. The Road Simulator does not test the total vehicle system. The engine and drive train components are not tested on the Road Simulator, with the exception of Vibratory inputs. This results in neglecting both the effects of the power train on the vehicle and evaluation of the components themselves. Simulation methodology development at TACOM in the future will address the addition of a programmed load cycle on the drive train during road simulation testing.

3. The Road Simulator ignores the effects of environmental conditions such as wind, rain, dust and temperature.

To date, two vehicle systems have completed tests on the TACOM Road Simulator. Computer modeling techniques were evaluated at an elementary level and the laboratory test data were correlated with available field data. Preliminary steps were taken to analyze strain data on one prototype vehicle frame to assess its life expectancy when subjected to the test terrain.

STUDY OF AN EXPERIMENTAL TECHNIQUE FOR
APPLICATION TO STRUCTURAL DYNAMIC PROBLEMS

Richard F. Snell
McDonnell Douglas Astronautics Company
Huntington Beach, California

A program is described that investigated the feasibility of using a new experimental technique for the determination of the dynamic response of proposed aerospace vehicles when subjected to pyrotechnic shock loading. This technique can be divided into three areas, that of the loading device, that of a model of the proposed vehicle, and that of instrumentation for determination of the response of the model to the loading. The loading device employs the energy stored in a high-energy, high-voltage capacitor bank to produce uniform impulsive loads that simulate shock loads from the detonation of pyrotechnic devices. The test specimen models proposed vehicle configurations and is made of Lexan polycarbonate plastic. Lexan, a photoelastic material, allows the determination of the states of strain in the model by use of a dynamic polariscope. The model can also be instrumented with strain-gages and low-mass accelerometers to further characterize the model response. As a final step in this technique, the dynamic response of the model must be related to the dynamic response of an actual prototype by the use of appropriate similitude relationships.

In this program, performed under the sponsorship of NASA—Lyndon B. Johnson Space Center, McDonnell Douglas Astronautics Company (MDAC) investigated the feasibility of such a technique, using the available MDAC stress-wave generator to conduct three test series on two configurations (without a cutout and with a cutout) of a simple monocoque cylinder of Lexan. In these tests the generator loaded the cylinder in the axial direction around the circumference of the cylinder such that a compressive stress wave propageted in the axial direction of the cylinder. The stress wave had a sine-squared shape with a duration of approximately 25 microseconds and produced a peak, strain in the cylinder of approximately 5500 μ in./in. A dynamic photoelastic polariscope and strain gages were used to determine the states of strain in the cylinder and accelerometers were also used to obtain data for correlation with the photoelastic and strain-gage data. As the thickness of the walls of the model were inadequate to allow the installation of the accelerometers directly to the model, the accelerometers were attached to a Lexan block which, in turn, was attached to the walls of the cylinder. The experimental data was analyzed to determine dynamic response of the model (acceleration and shock spectra) and finally a study was conducted to investigate problems associated with the scaling of model results in the determination of the dynamic response of an actual prototype.

Reduction of the data indicated excellent correlation between the strain-gage and accelerometer results (4 percent difference) and good correlation between the photoelastic and accelerometer results (14 percent difference). For both comparisons accelerometer data were compensated to account for the effects of the accelerometer mounting block. The scaling study showed that, for models and prototypes made of linear elastic materials and loaded in the elastic range at load rates below 10^3 in./in./sec., all required scaling relationships can be satisfied with the exceptions of the relationships involving body forces and the relationships involving Poisson's ratio. Body forces can in all likelihood be neglected but the effects of incompatibility of Poisson's ratio must be assessed with analytical and experimental means. In the event such effects are unacceptable and uncompensatible, models must be constructed from the same materials as the prototype. Scaling relationships were also developed for two classes of visoelastic materials. The scaling study showed that the relationships of one of these classes can be satisfied even at load rates greater than 10^3 in./in./sec. The results of the scaling study in conjunction with the excellent data correlations show that the modeling techniques investigated in this program may indeed be feasible for predicting the response of full-scale prototypes to pyrotechnic shock loads.

EVALUATION OF BLOCKED PRESSURE ON STIFFENED
CYLINDRICAL SHELLS

V. M. Conticelli
Aeritalia S.p.A., Naples, Itaiy

and

G. C. Kao
Wyle Laboratories
Huntsville, Alabama

Integrity and performance of critical and expensive components packages mounted inside rocket vehicles must be assured for the entire flight mission. These packages, which

are subjected to dynamic loads caused by random acoustic excitations and transmitted by the external shroud through the connecting structural members, must therefore be tested on the ground with simulated in-flight environments.

Recently a new technique has been suggested which allows the testing of each component instead of the entire vehicle. With such a technique, which represents a very realistic approach, interaction forces between a component and its support structure are first determined and then the component is tested under the force controlled environments.

The interaction forces (force spectra) are predicted by a one-dimensional equation which utilizes four types of data measured at equipment mounting locations. These data consist of: Input impedance of support structure; Acoustic mobility of support structure; Input impedance of component package; and Blocked pressure spectrum.

Analytical methods are described in this paper for computing blocked pressure spectra relative to cylindrical structures. These methods can be used when the far-field pressure or the pressure on the surface of a flexible structure is known.

Also, an experimental program which was used to assess the accuracy of the analytical methods is discussed in this paper. During these experiments, a stiffened aluminum cylinder with the dimensions of 3 ft (diameter) x 3 ft (height) x 0.02 in. (skin thickness) and a rigid dummy concrete cylinder with the same diameter were employed. The aluminum cylinder was used in acquiring input impedances and acoustic mobilities and the concrete cylinder was used for measuring the block pressure spectra.

Comparisons between theory and experiments indicate that, for the structure considered in this study, the maximum deviation in data is within 1 dB. A comparison is also made between pressure measurements obtained with flush mounted and external mounted microphones. No significant differences are detected between these two types of measurements and this leads to the conclusion that both mounting configurations are acceptable.

THE USE OF LISSAJOUS FIGURES
IN VIBRATION TESTING

John D. Ray
Memphis State University
Memphis, Tennessee

and

Charles W. Bert
University of Oklahoma
Norman, Oklahoma

Lissajous figures have been used quite extensively by engineers to study the relationship between two electrical signals. With the advent of electronic instrumentation the vibration engineer has been using the Lissajous pattern to study the resonance frequencies and phase relationship between two input signals. Introduced in this paper is an extension to the information that can be obtained from the Lissajous pattern. A method is described for obtaining the spring constant and damping factor for a single-degree-of-freedom

system and extended to specific multi-degree-of-freedom systems. Simple single-degree-of-freedom experimental results for harmonic excitation are presented to exemplify the method described.

STRUCTURAL DYNAMIC RESPONSE ANALYSIS OF ROCKET TEST SLEDS

Terry N. Gardner
Mechanics Research, Incorporated
Los Angeles, California

BACKGROUND

A variety of rocket propelled test sleds are run on the track at Holloman Air Force Base. Duel rail sleds run at speeds between Mach .4 and Mach 2.5 and weigh up to 30,000 pounds. Monorail sleds use only one of the tracks and generally weigh less than 1000 pounds. Their speeds have approached Mach 9.0.

Sleds ride the rails on steel slippers with replaceable liners. Reasonable life of the liners requires that a gap be left between them and the rail surface. A standard value of .125 inches is used for all size sleds.

Structural design of the Holloman sleds has been a success in that over the years, structural failures have been rare. The absence of failures points up the possibility that the design procedures have been overly conservative. This is especially true with regard to dynamic excitation about which a minimal amount of data has been available. The practice has been to design to a high-steady-state G level, the amplitude dependent upon the design velocity of the sled, without regard to the dynamic nature of the excitation.

Higher performance sleds could be designed if structural weight could be reduced without loss of integrity. Dynamic isolation of sensitive pay-loads could also be accomplished more efficiently with better understanding of the dynamic environment. A mathematical simulation which would correlate with available test data was needed for such understanding.

APPROACH

MRI performed a study of the available test data which consisted of strain gage data from the slippers of various test sleds and rail height measurements made every 10 inches over a 400 foot section of track. The results of MRI's work showed that the bumpiness of the rail was the principal sources of dynamic excitation and was especially severe at high velocities. Oscillating aerodynamic loads and transient behavior of the rocket motors amplified the excitation. The philosophy was adopted that if a simulation could be developed which would reproduce the response to rail roughness which was seen in the data, design factors could be used to account for the amplification caused by oscillating aerodynamics and motor transients.

There were two primary difficulties in developing the simulation. First, only a short stretch of track had been surveyed. Second, the presence of the slipper gap, which seemed to be an important part of the dynamic behavior, precluded the direct application of linear

finite-element, modal response, and random analysis and frequency domain techniques. Time domain simulation was selected as the only reliable approach.

The problem of generating a rail height profile of indefinite length was solved with a random approach. First the slope and mean height were removed from the data by a least square fit. Next, the 400 foot section was divided into 10 segments so that the first and last value of height in each segment was zero. A random integer generator was used to generate a sequence and the corresponding segments of track laid one after the other to produce as much rail as necessary. A power spectral density analysis of the rail height data showed that this generation method left its frequency properties unchanged.

The slipper gap of the high speed sled is a problem similar to the recontact problem occurring during staging of rocket launch vehicles. In both cases, complex structure requires detailed finite element representation with subsequent reduction of degrees of freedom by a modal method. In the solution of the launch vehicle problem, several sets of modes are used depending on whether the stages are in contact or not. Such an approach in impossible with the rapidly bouncing sled. The method developed for simulation of the sleds involves only one set of modal functions. Ground restraints are applied to the mathematical model of the sled at points near the slipper contact with the rail. The stiffness from the restraint point to the rail contact point is calculated and enters into the equations. It has been shown that the method accurately represents the modal characteristics of the sled structure for all boundary conditions, i.e., when the slippers are either in contact or in the gap.

IMPLEMENTATION AND COMPARISON WITH TEST DATA

The random rail generation scheme and the nonlinear coupled equations of motion were implemented in a digital computer program using an Adams-Moulton predictor-corrector integration scheme. Program results, in terms of peak dynamic slipper loads, have been compared with test track data. Correlation is good for coast phase, i.e., when there is no excitation from motor burning. Comparisons were made for both high speed monorail sleds and slower, heavier, dual rail sleds.

The computer program, called SLEDYNE, has been developed into a design tool by incorporation of searches for maximum stresses and displacements at critical points in the structure. Amplification factors are included to account for the excitation of motor burning and oscillating aerodynamic loads. SLEDYNE is used by MRI and at the Holloman test track for design analysis of test sleds.

104

CONSIDERATIONS OF THE RESPONSE OF
A SLED BORNE MISSILE

Alva Roy Glaser
Rockwell International
Columbus, Ohio

and

Larry Mixon
A.F. Special Weapons Center
Holloman AFB, New Mexico

A program has been recently completed which demonstrated the feasibility of performing captive tests of ramjet engines at realistic supersonic flight conditions aboard rocket sleds. The track tests were tailored toward simulation of low level flight in the Mach 2.5 regime and provided duplication of both Mach number and Reynolds number for a full size missile at $0°$ and $-4°$ angle of attack.

The program required that an existing flight test missile be structurally modified and adapted to an outrigger rocket sled. The layout of the rocket sled/ramjet was controlled by the necessity that the ramjet's aft mounted inlet be unaffected by reflected shock waves and other interference effects. In compliance with these stringent configuration requirements, ten (10) feet of the missile was cantilevered forward of the sled structure. This cantilevered arrangement and the relatively high induced loads associated with testing the system on a test track directed the extensive use of mathematical models and environmental test techniques.

The multi-degree-of-freedom system response was derived based on random forcing functions applied to the guide surfaces. The predicted system response, coupled with the trajectory associated forces, were then used to perform the detail design of structural modifications to the missile and rocket sled. Preceding the track tests, a laboratory modal survey was conducted of the complete system, and iterations of the mathematical model were performed until the first six (6) modes of vibration were adequately modeled.

A unique facet of the design was the incorporation of force transducers between the missile and the sled structure which provided invaluable information concerning the forcing functions applied to the relatively large cantilevered payload. These transducers provided measurements of the vertical forces, lateral forces, and roll moments subjected to each of the two missile support structures. In addition to these force measurements, several strain gage bending circuits with appropriate force calibrations and accelerometers were mounted to the missile.

This instrumentation was continuously monitored during several track tests. Each successive track test involved changes in the missile configuration and/or increases in maximum test velocity until the program objectives were achieved. A series of random data analysis computer programs were used to format the forementioned measurements for correlation with the predicted responses following each track test. Measured and predicted data were determined as functions of time and velocity, and the resultant system response was studied both from the design requirements and the analysis viewpoints.

The result of this experimental/analysis approach was the establishment of an analysis method which provided meaningful comparison between predicted and measured payload response in both the amplitude and frequency domains. This correlation afforded the means for not only satisfying this particular program objectives, but also provided a method to determine design requirements for other flight test missiles adapted for carriage on high speed rocket sleds. Based on the resulting analysis method and experimental data, design requirements were determined for future missile systems where the projected goal is to air launch the missile after propulsion systems have properly functioned.

MODAL TEST RESULTS OF THE
VIKING ORBITER

L. Leppert, R. Miyakawa, and B. Wada
Jet Propulsion Laboratory
Pasadena, California

The Jet Propulsion Laboratory is responsible for the Viking Orbiter System which is part of the overall Viking Project managed by the Viking Project Office at Langley Research Center for NASA. The Spacecraft will be launched on a Titan IIIE/Centaur Launch Vehicle System in August 1975.

The Viking Orbiter (VO) Project elected to establish the design and flight loads for the primary structure by Load Analysis. Load Analysis is defined as a procedure to obtain VO member loads as a result of subjecting a complex finite element model of the complete Booster system to Booster Engine transients. The dynamic solution requires modal coupling of the various structural subsystems of the Booster System to allow a solution with present computers.

Since the design loads are dependent on the dynamic characteristics of the VO, they were updated as the design progressed. The flight loads needed to qualify the structure will be based upon Load Analysis using a VO mathematical model which had been verified by test.

The test performed to verify the mathematical model of VO is a modal survey. The test configuration compatible with the mathematical model was used for modal coupling. Since the VO is between the Viking Lander Capsule (VLC) on top and the Centaur on the bottom, hardware representing VLC built by MMA and Centaur built by GD/CA were included. The configuration selected was a rigid VLC with representation of its inertia properties, the major components of the VO, and Centaur Adapters below the VO. Selected subsystems of the VO were removed to simplify the test and to allow the verification of those mathematical models that most required verification.

Modal tests were also performed on selected subsystems prior to the system test. The subsystem tests influenced the system modal test configuration. Questions such as the potential influence of internal pressure or ullage in the tanks were resolved. Subsystems not included in the final modal test were modally tested separately.

The paper will present the overall plan to coordinate the modal tests and modal coupling analysis for the VO. A summary of the VO modal test results will be presented

106

along with analyses, data reduction, and test methods to help perform the test. Analyses to support the test included analytical mode shape and frequency predictions, mode shape plots, residual weight, modal force transformations, modal kinetic energy distribution, and strain energy distribution. Data reduction methods include the calculation of the analysis parameters using test data; factors to establish maximum force limits; comparison of the modal force, accelerometer, strain energy, and kinetic energy data; and orthogonality data. Special tests were conducted to perform the system modal survey on the VO. The modal predictions and data evaluation during the test helped detect strain gage, accelerometer, and input data errors which were corrected prior to the completion of the test.

Approximately 20 modes from 4.6 cps to 50 cps were obtained with off-diagonal of the orthogonality matrix generally less than 5%. Many modes were run at several levels to establish the non-linearity of the modal characteristics, especially damping, with amplitude.

A successful modal test has been completed on a complex structure with a large fuel mass. The success is attributed to the coordination of the modal test configuration, analyses predictions, and data analysis during the test program. The modal test results are directly of value since the test configuration was coordinated with the modal coupling analysis procedure established for the Load Analysis. The paper will be of value to engineers planning a modal test program to support a flight project.